Electronic Journal of Differential Equations, Vol. 2023 (2023), No. 83, pp. 1–57.
ISSN: 1072-6691. URL: https://ejde.math.txstate.edu, https://ejde.math.unt.edu
DOI: 10.58997/ejde.2023.83

GLOBAL ANALYSIS ON A CONTINUOUS PLANAR PIECEWISE LINEAR DIFFERENTIAL SYSTEM WITH THREE ZONES

MAN JIA, YOUFENG SU, HEBAI CHEN

Abstract. This article concerns the global dynamics of a continuous planar piecewise linear differential system with three zones. We give global phase portraits in the Poincaré disc and classify bifurcation diagrams under certain parametric conditions, when the dynamics of central linear zone is anti-saddle. Rich dynamical behaviors are demonstrated, from which we observe homoclinic loops appearing in three linear zones and limit cycles occurring in three linear zones which surround a node or node-focus.

1. Introduction

In several scientific fields, piecewise linear differential systems have attracted a lot of attention from a rather diverse group of scientists such as physicists and mathematicians [1, 11, 12, 17, 25, 26, 30, 33]. This is because, in addition to academic-theoretical significance [2, 4, 13, 14, 16, 18, 23, 31, 32, 36, 37], the study of piecewise linear differential systems has practical applications [5, 6, 15, 19, 20, 28, 34, 35]. Piecewise linear differential systems can model a large number of nonlinear problems arising in physics and engineering such as design of electric circuits [1, 3], some memristor oscillators [4, 5, 8, 9, 15, 23, 26, 27, 34] and FitzHugh-Nagumo system [30, 31, 35]. Although piecewise linear differential systems may be considered as some of the most tractable nonlinear ordinary differential equations, they display various rich and interesting dynamical behaviours, with all the dynamics of general smooth nonlinear systems (such as limit cycles, homoclinic loops, heteroclinic loops, strangle attractors and so on), and with special dynamical behaviors (such as jump bifurcation, grazing bifurcation, sliding bifurcation, singular continuous systems and so on) [15, 17].

In this article, we are interested in continuous planar piecewise linear (CPWL) differential systems. A CPWL differential system with three zones separated by two parallel lines is of the Liénard form:

$$\frac{dx}{dt} = F(x) - y, \quad \frac{dy}{dt} = g(x) - \alpha, \tag{1.1}$$

2020 *Mathematics Subject Classification.* 34C05, 34C23, 37G15, 37G20.
Key words and phrases. Piecewise linear system; global phase portrait; bifurcation; invariant manifold; limit cycle; homoclinic loop.

Submitted June 6, 2023. Published December 10, 2023.

where

$$F(x)=\begin{cases} t_r(x-1)+t_c, & \text{if } x>1,\\ t_c x, & \text{if } -1\le x\le 1,\\ t_l(x+1)-t_c, & \text{if } x<-1,\end{cases}$$

$$g(x)=\begin{cases} d_r(x-1)+d_c, & \text{if } x>1,\\ d_c x, & \text{if } -1\le x\le 1,\\ d_l(x+1)-d_c, & \text{if } x<-1,\end{cases}$$

with three open linear zones in the plane $\mathbb{R}^2$:

$$\mathcal{S}_l := \{(x,y)\in\mathbb{R}^2 : x<-1\},$$
$$\mathcal{S}_c := \{(x,y)\in\mathbb{R}^2 : -1<x<1\},$$
$$\mathcal{S}_r := \{(x,y)\in\mathbb{R}^2 : x>1\}$$

by two straight lines $\Gamma_l := \{(x,y)\in\mathbb{R}^2 : x=-1\}$ and $\Gamma_r := \{(x,y)\in\mathbb{R}^2 : x=1\}$. Considerable attention has been devoted to characterizing global dynamics of system (1.1) [6, 7, 9, 10, 17, 20, 24, 25, 26, 27, 29]. Jia-Su-Chen [21] once investigated global dynamics of system (1.1) in the region:

$$\mathcal{G} := \{(t_r,t_c,t_l,d_r,d_c,d_l,\alpha)\in\mathbb{R}^7 : t_r t_l>0,\ d_r d_l<0\},$$

where $\mathcal{G}$ is divided into four parametric regions:

$$\mathcal{G}_1 := \{(t_r,t_c,t_l,d_r,d_c,d_l,\alpha)\in\mathbb{R}^7 : t_r>0,\ t_l>0,\ d_r>0,\ d_l<0\},$$
$$\mathcal{G}_2 := \{(t_r,t_c,t_l,d_r,d_c,d_l,\alpha)\in\mathbb{R}^7 : t_r>0,\ t_l>0,\ d_r<0,\ d_l>0\},$$
$$\mathcal{G}_3 := \{(t_r,t_c,t_l,d_r,d_c,d_l,\alpha)\in\mathbb{R}^7 : t_r<0,\ t_l<0,\ d_r>0,\ d_l<0\},$$
$$\mathcal{G}_4 := \{(t_r,t_c,t_l,d_r,d_c,d_l,\alpha)\in\mathbb{R}^7 : t_r<0,\ t_l<0,\ d_r<0,\ d_l>0\}.$$

By a proper transformation, the regions $\mathcal{G}_2$, $\mathcal{G}_3$ and $\mathcal{G}_4$ can be changed into the region $\mathcal{G}_1$. So all discussions for system (1.1) were restricted in the region $\mathcal{G}_1$. When $d_c\le 0$, global phase portraits in the Poincaré disc and bifurcation diagrams of system (1.1) in the region $\mathcal{G}_1$ were presented [21]. Therefore, in this study we continue to explore global dynamics of system (1.1) in the region $\mathcal{G}_1$ when $d_c>0$.

The article is organized as follows. In Section 2, we state our main results of system (1.1) with $d_c>0$ in the region $\mathcal{G}_1$. To study the local dynamical behaviors of system (1.1), we introduce some preliminary results in Section 3. Local dynamics of system (1.1) are investigated in Section 4. Nonlocal dynamics of system (1.1) are explored in Section 5. The proofs of our main results are presented in Section 6, while numerical phase portraits are demonstrated in Section 7. A brief conclusion is given in Section 8.

2. Main results

In this section, we summarize our main results of system (1.1) with $d_c>0$ in the region $\mathcal{G}_1$, i.e., the bifurcation diagram in the (α,t_c)-plane and global phase portraits in the Poincaré disc. Notice that the condition $t_r^2-4d_r<0$ (resp. $=0$ or >0) implies that the dynamics of right linear zone of system (1.1) is a focus (resp. improper node or bidirectional node) (see Lemma 4.1 for more details). Moreover,

since system (1.1) has different qualitative properties of equilibrium points at infinity for the three conditions $t_r^2-4d_r<0$, $t_r^2-4d_r=0$ and $t_r^2-4d_r>0$ (see Lemma 4.2 for more details), our main results are achieved in the following three regions:

$$\begin{aligned}\mathcal{G}_{11} &:= \big\{(t_r,t_c,t_l,d_r,d_c,d_l,\alpha)\in\mathbb{R}^7 : t_r>0,\ t_l>0,\ d_r>0,\ d_c>0,\ d_l<0,\\ &\quad t_r^2-4d_r<0\big\}\subset\mathcal{G}_1,\\ \mathcal{G}_{12} &:= \big\{(t_r,t_c,t_l,d_r,d_c,d_l,\alpha)\in\mathbb{R}^7 : t_r>0,\ t_l>0,\ d_r>0,\ d_c>0,\ d_l<0,\\ &\quad t_r^2-4d_r=0\big\}\subset\mathcal{G}_1,\\ \mathcal{G}_{13} &:= \big\{(t_r,t_c,t_l,d_r,d_c,d_l,\alpha)\in\mathbb{R}^7 : t_r>0,\ t_l>0,\ d_r>0,\ d_c>0,\ d_l<0,\\ &\quad t_r^2-4d_r>0\big\}\subset\mathcal{G}_1.\end{aligned}$$

System (1.1) has two equilibrium points $E_l:((\alpha+d_c)/d_l-1, t_l(\alpha+d_c)/d_l-t_c)$ and $E_c:(\alpha/d_c, t_c\alpha/d_c)$ when $d_c>0$, $-d_c<\alpha<d_c$ and $t_c<0$ in $\mathcal{G}_1$, where E_l is a saddle, E_c is a stable node for ${t_c}^2-4d_c\geq 0$ or a stable focus for ${t_c}^2-4d_c<0$. Theorems 2.1-2.3 and Theorems 2.4-2.6 are presented according to the nonexistence of the homoclinic loop appearing in three linear zones which surrounds the stable node E_c. For simplicity, we set

$$t_c^* := -\frac{t_r(\alpha-d_c)+t_r\sqrt{(\alpha-d_c)^2+4\alpha d_r-\frac{d_r}{d_l}(\alpha+d_c)^2}}{2d_r}+\frac{t_l(\alpha+d_c)}{2d_l}$$
$$t_c^{***} := -\frac{t_r(\alpha-d_c+\sqrt{4\alpha d_r+(\alpha-d_c)^2})}{2d_r},$$

where t_c^* and t_c^{***} are continuous functions on α when t_r, d_r, d_c and d_l are fixed.

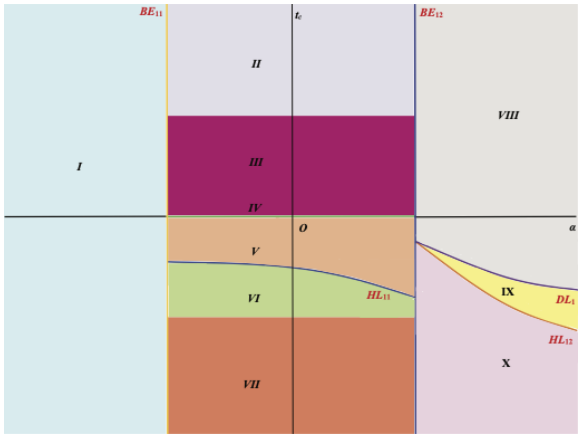

FIGURE 1. Bifurcation diagram in the (α,t_c)-plane of system (1.1) as $(t_r,t_c,t_l,d_r,d_c,d_l,\alpha)\in\mathcal{G}_{11}$.

Theorem 2.1. *When $(t_r,t_c,t_l,d_r,d_c,d_l,\alpha)\in\mathcal{G}_{11}$, the bifurcation diagram of system (1.1) in the (α,t_c)-plane consists of the following bifurcation curves:*

(a) *Boundary equilibrium bifurcation curves:*

$$BE_{11}=\{(\alpha,t_c)\in\mathbb{R}^2:\alpha=-d_c\},\quad BE_{12}=\{(\alpha,t_c)\in\mathbb{R}^2:\alpha=d_c\}.$$

(b) *Homoclinic bifurcation curves:*

$$HL_{11} = \{(\alpha, t_c) \in \mathbb{R}^2 : -d_c < \alpha \le d_c,\ t_c = \phi(\alpha)\},$$
$$HL_{12} = \{(\alpha, t_c) \in \mathbb{R}^2 : \alpha > d_c,\ t_c = \varphi(\alpha)\}.$$

(c) *Double limit cycle bifurcation curve:*

$$DL_1 = \{(\alpha, t_c) \in \mathbb{R}^2 : \alpha > d_c,\ t_c = h(\alpha)\},$$

where the function $t_c = \phi(\alpha)$ is continuous, monotonic and satisfies

$$\max\{t_c^*, -2\sqrt{d_c}\} < \phi(\alpha) < 0 \quad \text{for } -d_c < \alpha < d_c,$$
$$\max\{t_c^*, -2\sqrt{d_c}\} < \phi(\alpha) < -t_r\sqrt{d_c/d_r} \quad \text{for } \alpha = d_c,$$

and the function $t_c = h(\alpha)$ is continuous satisfying $\varphi(\alpha) < h(\alpha) < t_c^{***}$ for $\alpha > d_c$. Moreover, the bifurcation diagram and global phase portraits in the Poincaré disc of system (1.1) *in $\mathcal{G}_{11}$ are respectively shown in Figures 1 and 2, where $-d_c < \alpha^* < d_c$, and*

$$I = \{(\alpha, t_c) \in \mathbb{R}^2 : \alpha < -d_c\},$$
$$II = \{(\alpha, t_c) \in \mathbb{R}^2 : -d_c < \alpha < d_c,\ t_c \ge 2\sqrt{d_c}\},$$
$$III = \{(\alpha, t_c) \in \mathbb{R}^2 : -d_c < \alpha < d_c,\ 0 < t_c < 2\sqrt{d_c}\},$$
$$IV = \{(\alpha, t_c) \in \mathbb{R}^2 : -d_c < \alpha < d_c,\ t_c = 0\},$$
$$V = \{(\alpha, t_c) \in \mathbb{R}^2 : -d_c < \alpha < d_c,\ \phi(\alpha) < t_c < 0\},$$
$$VI = \{(\alpha, t_c) \in \mathbb{R}^2 : -d_c < \alpha < d_c,\ -2\sqrt{d_c} < t_c < \phi(\alpha)\},$$
$$VII = \{(\alpha, t_c) \in \mathbb{R}^2 : -d_c < \alpha < d_c,\ t_c \le -2\sqrt{d_c}\},$$
$$VIII = \{(\alpha, t_c) \in \mathbb{R}^2 : \alpha > d_c,\ t_c > h(\alpha)\},$$
$$IX = \{(\alpha, t_c) \in \mathbb{R}^2 : \alpha > d_c,\ \varphi(\alpha) < t_c < h(\alpha)\},$$
$$X = \{(\alpha, t_c) \in \mathbb{R}^2 : \alpha > d_c,\ t_c < \varphi(\alpha)\},$$
$$BE_{121} = \{(\alpha, t_c) \in \mathbb{R}^2 : \alpha = d_c,\ t_c \ge 2\sqrt{d_c}\},$$
$$BE_{122} = \{(\alpha, t_c) \in \mathbb{R}^2 : \alpha = d_c,\ -t_r\sqrt{d_c/d_r} < t_c < 2\sqrt{d_c}\},$$
$$BE_{123} = \{(\alpha, t_c) \in \mathbb{R}^2 : \alpha = d_c,\ t_c = -t_r\sqrt{d_c/d_r}\},$$
$$BE_{124} = \{(\alpha, t_c) \in \mathbb{R}^2 : \alpha = d_c,\ \phi(\alpha) < t_c < -t_r\sqrt{d_c/d_r}\},$$
$$BE_{125} = \{(\alpha, t_c) \in \mathbb{R}^2 : \alpha = d_c,\ -2\sqrt{d_c} < t_c < \phi(\alpha)\},$$
$$BE_{126} = \{(\alpha, t_c) \in \mathbb{R}^2 : \alpha = d_c,\ t_c \le -2\sqrt{d_c}\},$$
$$HL_{111} = \{(\alpha, t_c) \in \mathbb{R}^2 : -d_c < \alpha < \alpha^* < d_c,\ t_c = \phi(\alpha)\},$$
$$HL_{112} = \{(\alpha, t_c) \in \mathbb{R}^2 : -d_c < \alpha = \alpha^* < d_c,\ t_c = \phi(\alpha)\},$$
$$HL_{113} = \{(\alpha, t_c) \in \mathbb{R}^2 : -d_c < \alpha^* < \alpha < d_c,\ t_c = \phi(\alpha)\},$$
$$HL_{114} = \{(\alpha, t_c) \in \mathbb{R}^2 : \alpha = d_c,\ t_c = \phi(\alpha)\}.$$

In Figure 2, the stable limit cycle is marked by red color, the center is marked by baby blue color, the unstable limit cycle is marked by dark blue color, the semi-stable limit cycle is marked by yellow color and the unstable homoclinic loop is marked by green color. When there is a unique limit cycle (stable or unstable) in

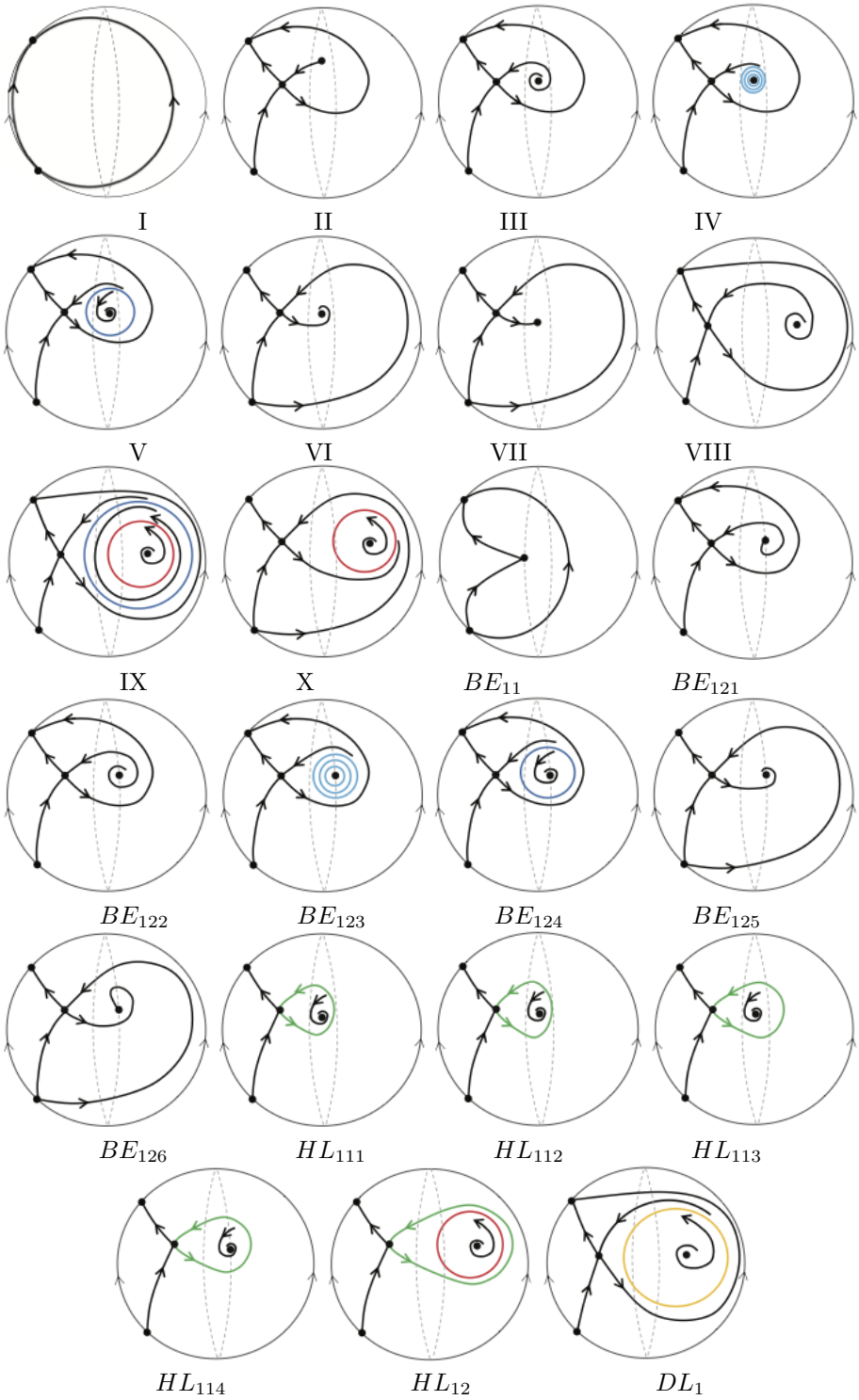

FIGURE 2. Global phase portraits in the Poincaré disc of system (1.1) as $(t_r, t_c, t_l, d_r, d_c, d_l, \alpha) \in \mathcal{G}_{11}$.

Theorem 2.1, it involves two or three linear zones, see global phase portraits in the Poincaré disc of V, X, BE_{124} and HL_{12}. When there are two limit cycles, the inner limit cycle involves two or three linear zones and the outer limit cycle involves three linear zones, see global phase portrait in the Poincaré disc of IX. The semi-stable limit cycle involves three linear zones, see global phase portrait in the Poincaré disc of DL_1. The homoclinic loop involves two (resp. three) linear zones, see global phase portraits in the Poincaré disc of HL_{111} and HL_{112} (resp. HL_{113}, HL_{114} and HL_{12}), and the homoclinic loop becomes tangent to Γ_r, see global phase portrait in the Poincaré disc of HL_{112}.

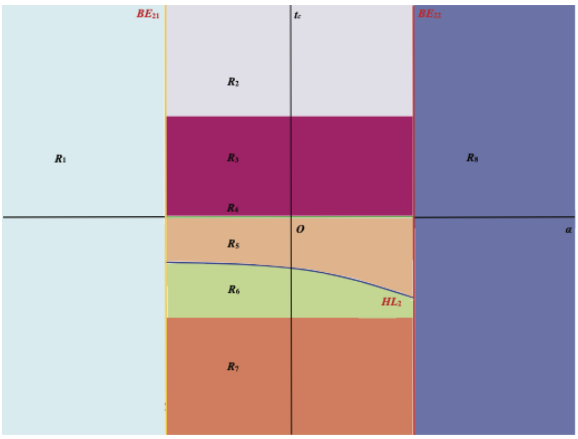

FIGURE 3. Bifurcation diagram in the (α, t_c)-plane of system (1.1) as $(t_r, t_c, t_l, d_r, d_c, d_l, \alpha) \in \mathcal{G}_{12}$.

Theorem 2.2. *When $(t_r, t_c, t_l, d_r, d_c, d_l, \alpha) \in \mathcal{G}_{12}$, the bifurcation diagram of system (1.1) in the (α, t_c)-plane consists of the following bifurcation curves:*

(a) *Boundary equilibrium bifurcation curves:*

$$BE_{21} = \{(\alpha, t_c) \in \mathbb{R}^2 : \alpha = -d_c\}, \quad BE_{22} = \{(\alpha, t_c) \in \mathbb{R}^2 : \alpha = d_c\}.$$

(b) *Homoclinic bifurcation curve:*

$$HL_2 = \{(\alpha, t_c) \in \mathbb{R}^2 : -d_c < \alpha < d_c,\ t_c = \phi(\alpha)\},$$

where the function $t_c = \phi(\alpha)$ is continuous, monotonic, satisfying $\max\{t_c^*, -2\sqrt{d_c}\} < \phi(\alpha) < 0$ for $-d_c < \alpha < d_c$. Moreover, the bifurcation diagram and global phase portraits in the Poincaré disc of system (1.1) in $\mathcal{G}_{12}$ are respectively shown in Figures 3 and 4, *where $-d_c < \alpha^* < d_c$, and*

$$R_1 = \{(\alpha, t_c) \in \mathbb{R}^2 : \alpha < -d_c\},$$
$$R_2 = \{(\alpha, t_c) \in \mathbb{R}^2 : -d_c < \alpha < d_c,\ t_c \geq 2\sqrt{d_c}\},$$
$$R_3 = \{(\alpha, t_c) \in \mathbb{R}^2 : -d_c < \alpha < d_c,\ 0 < t_c < 2\sqrt{d_c}\},$$
$$R_4 = \{(\alpha, t_c) \in \mathbb{R}^2 : -d_c < \alpha < d_c,\ t_c = 0\},$$
$$R_5 = \{(\alpha, t_c) \in \mathbb{R}^2 : -d_c < \alpha < d_c,\ \phi(\alpha) < t_c < 0\},$$
$$R_6 = \{(\alpha, t_c) \in \mathbb{R}^2 : -d_c < \alpha < d_c,\ -2\sqrt{d_c} < t_c < \phi(\alpha)\},$$

$$
\begin{aligned}
R_7 &= \{(\alpha, t_c) \in \mathbb{R}^2 : -d_c < \alpha < d_c,\ t_c \le -2\sqrt{d_c}\},\\
R_8 &= \{(\alpha, t_c) \in \mathbb{R}^2 : \alpha > d_c\},\\
BE_{221} &= \{(\alpha, t_c) \in \mathbb{R}^2 : \alpha = d_c,\ t_c \ge 2\sqrt{d_c}\},\\
BE_{222} &= \{(\alpha, t_c) \in \mathbb{R}^2 : \alpha = d_c,\ t_c < 2\sqrt{d_c}\},\\
HL_{21} &= \{(\alpha, t_c) \in \mathbb{R}^2 : -d_c < \alpha < \alpha^* < d_c,\ t_c = \phi(\alpha)\},\\
HL_{22} &= \{(\alpha, t_c) \in \mathbb{R}^2 : -d_c < \alpha = \alpha^* < d_c,\ t_c = \phi(\alpha)\},\\
HL_{23} &= \{(\alpha, t_c) \in \mathbb{R}^2 : -d_c < \alpha^* < \alpha < d_c,\ t_c = \phi(\alpha)\}.
\end{aligned}
$$

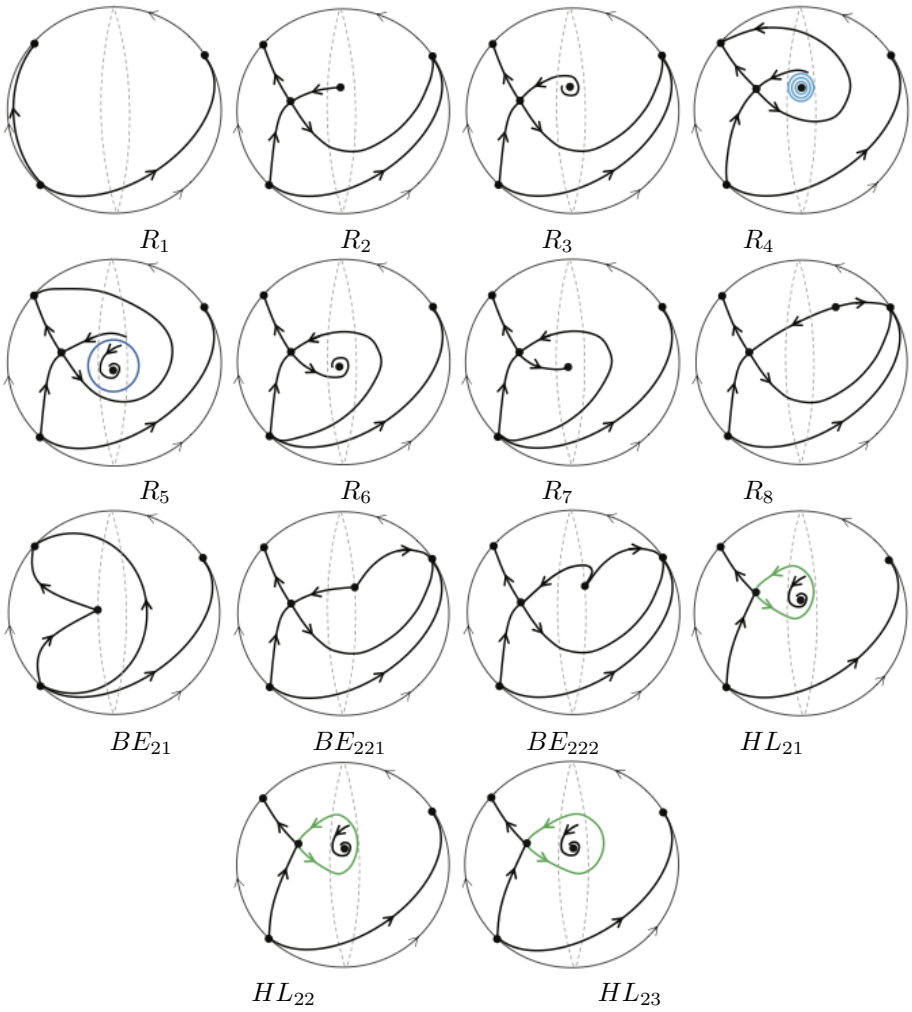

FIGURE 4. Global phase portraits in the Poincaré disc of system (1.1) as $(t_r, t_c, t_l, d_r, d_c, d_l, \alpha) \in \mathcal{G}_{12}$.

In Theorem 2.2, the unstable limit cycle involves two or three linear zones, see global phase portrait in the Poincaré disc of R_5. The homoclinic loop involves two (resp. three) linear zones, see global phase portraits in the Poincaré disc of HL_{21} and HL_{22} (resp. HL_{23}). The homoclinic loop becomes tangent to Γ_r, see global phase portrait in the Poincaré disc of HL_{22}.

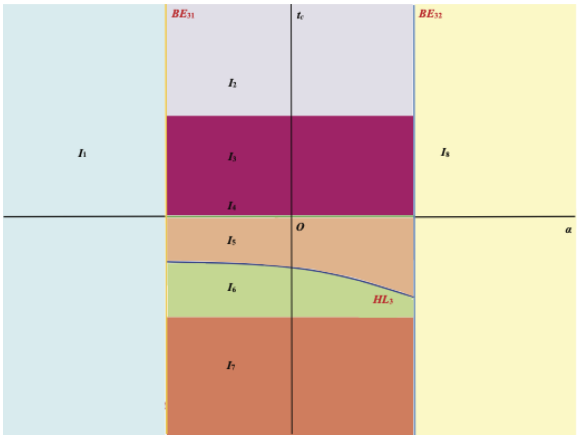

FIGURE 5. Bifurcation diagram in the (α, t_c)-plane of system (1.1) as $(t_r, t_c, t_l, d_r, d_c, d_l, \alpha) \in \mathcal{G}_{13}$.

Theorem 2.3. *When $(t_r, t_c, t_l, d_r, d_c, d_l, \alpha) \in \mathcal{G}_{13}$, the bifurcation diagram of system (1.1) in the (α, t_c)-plane consists of the following bifurcation curves:*

(a) *Boundary equilibrium bifurcation curves:*

$$BE_{31} = \{(\alpha, t_c) \in \mathbb{R}^2 : \alpha = -d_c\}, \quad BE_{32} = \{(\alpha, t_c) \in \mathbb{R}^2 : \alpha = d_c\}.$$

(b) *Homoclinic bifurcation curve:*

$$HL_3 = \{(\alpha, t_c) \in \mathbb{R}^2 : -d_c < \alpha < d_c,\ t_c = \phi(\alpha)\},$$

where the function $t_c = \phi(\alpha)$ is continuous and monotonic satisfying $\max\{t_c^*, -2\sqrt{d_c}\} < \phi(\alpha) < 0$ for $-d_c < \alpha < d_c$. Moreover, the bifurcation diagram and global phase portraits in the Poincaré disc of system (1.1) in $\mathcal{G}_{13}$ are respectively shown in Figures 5 and 6, *where $-d_c < \alpha^* < d_c$, and*

$$I_1 = \{(\alpha, t_c) \in \mathbb{R}^2 : \alpha < -d_c\},$$
$$I_2 = \{(\alpha, t_c) \in \mathbb{R}^2 : -d_c < \alpha < d_c,\ t_c \geq 2\sqrt{d_c}\},$$
$$I_3 = \{(\alpha, t_c) \in \mathbb{R}^2 : -d_c < \alpha < d_c,\ 0 < t_c < 2\sqrt{d_c}\},$$
$$I_4 = \{(\alpha, t_c) \in \mathbb{R}^2 : -d_c < \alpha < d_c,\ t_c = 0\},$$
$$I_5 = \{(\alpha, t_c) \in \mathbb{R}^2 : -d_c < \alpha < d_c,\ \phi(\alpha) < t_c < 0\},$$
$$I_6 = \{(\alpha, t_c) \in \mathbb{R}^2 : -d_c < \alpha < d_c,\ -2\sqrt{d_c} < t_c < \phi(\alpha)\},$$
$$I_7 = \{(\alpha, t_c) \in \mathbb{R}^2 : -d_c < \alpha < d_c,\ t_c \leq -2\sqrt{d_c}\},$$
$$I_8 = \{(\alpha, t_c) \in \mathbb{R}^2 : \alpha > d_c\},$$
$$BE_{321} = \{(\alpha, t_c) \in \mathbb{R}^2 : \alpha = d_c,\ t_c \geq 2\sqrt{d_c}\},$$

$$BE_{322} = \{(\alpha, t_c) \in \mathbb{R}^2 : \alpha = d_c,\ t_c < 2\sqrt{d_c}\},$$
$$HL_{31} = \{(\alpha, t_c) \in \mathbb{R}^2 : -d_c < \alpha < \alpha^* < d_c,\ t_c = \phi(\alpha)\},$$
$$HL_{32} = \{(\alpha, t_c) \in \mathbb{R}^2 : -d_c < \alpha = \alpha^* < d_c,\ t_c = \phi(\alpha)\},$$
$$HL_{33} = \{(\alpha, t_c) \in \mathbb{R}^2 : -d_c < \alpha^* < \alpha < d_c,\ t_c = \phi(\alpha)\}.$$

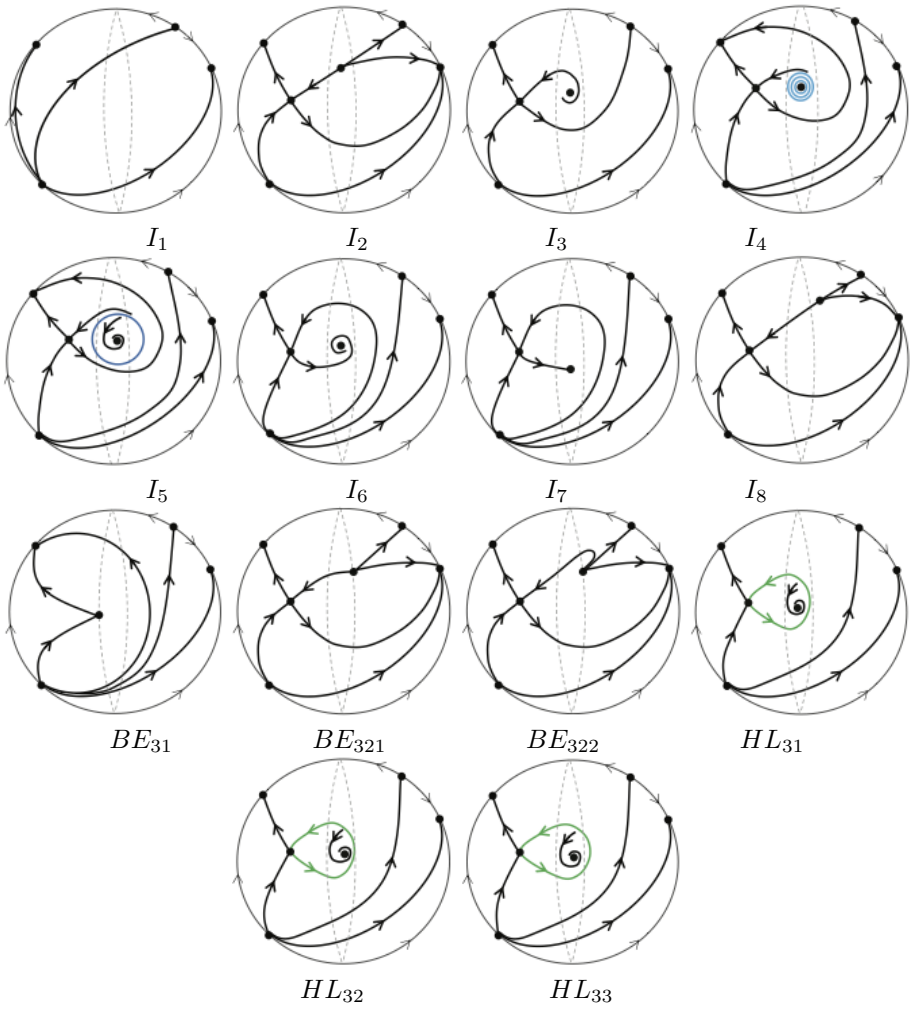

FIGURE 6. Global phase portraits in the Poincaré disc of system (1.1) as $(t_r, t_c, t_l, d_r, d_c, d_l, \alpha) \in \mathcal{G}_{13}$.

Theorem 2.4. *When $(t_r, t_c, t_l, d_r, d_c, d_l, \alpha) \in \mathcal{G}_{11}$, the bifurcation diagram of system (1.1) in the (α, t_c)-plane consists of the following bifurcation curves:*

(a) *Boundary equilibrium bifurcation curves:*

$$BE_{41} = \{(\alpha, t_c) \in \mathbb{R}^2 : \alpha = -d_c\}, \quad BE_{42} = \{(\alpha, t_c) \in \mathbb{R}^2 : \alpha = d_c\}.$$

(b) *Homoclinic bifurcation curves:*

$$HL_{41} = \{(\alpha, t_c) \in \mathbb{R}^2 : -d_c < \alpha \le d_c,\ t_c = \phi(\alpha)\},$$
$$HL_{42} = \{(\alpha, t_c) \in \mathbb{R}^2 : \alpha > d_c,\ t_c = \varphi(\alpha)\}.$$

(c) *Double limit cycle bifurcation curve:*

$$DL_4 = \{(\alpha, t_c) \in \mathbb{R}^2 : \alpha > d_c,\ t_c = h(\alpha)\},$$

where the function $t_c = \phi(\alpha)$ *is continuous and monotonic satisfying* $\max\{t_c^*, -2\sqrt{d_c}\} < \phi(\alpha) < 0$ *for* $-d_c < \alpha < \overline{\alpha}$, $\phi(\alpha) = -2\sqrt{d_c}$ *for* $\alpha = \overline{\alpha} = \phi^{-1}(-2\sqrt{d_c})$, $t_c^* < \phi(\alpha) < -2\sqrt{d_c}$ *for* $\overline{\alpha} < \alpha \le d_c$, *the function* $t_c = \varphi(\alpha)$ *is continuous and monotonic, and the function* $t_c = h(\alpha)$ *is continuous satisfying* $\varphi(\alpha) < h(\alpha) < t_c^{***}$ *for* $\alpha > d_c$. *Moreover, the bifurcation diagram and global phase portraits in the Poincaré disc of system* (1.1) *in* $\mathcal{G}_{11}$ *are shown in Figure 7, where* $-d_c < \alpha^* < \overline{\alpha} < d_c$, *and*

$$G_1 = \{(\alpha, t_c) \in \mathbb{R}^2 : \alpha < -d_c\},$$
$$G_2 = \{(\alpha, t_c) \in \mathbb{R}^2 : -d_c < \alpha < d_c,\ t_c \ge 2\sqrt{d_c}\},$$
$$G_3 = \{(\alpha, t_c) \in \mathbb{R}^2 : -d_c < \alpha < d_c,\ 0 < t_c < 2\sqrt{d_c}\},$$
$$G_4 = \{(\alpha, t_c) \in \mathbb{R}^2 : -d_c < \alpha < d_c,\ t_c = 0\},$$
$$G_5 = \{(\alpha, t_c) \in \mathbb{R}^2 : -d_c < \alpha < \overline{\alpha},\ \phi(\alpha) < t_c < 0\} \cup$$
$$\{(\alpha, t_c) \in \mathbb{R}^2 : \overline{\alpha} < \alpha < d_c,\ -2\sqrt{d_c} < t_c < 0\},$$
$$G_6 = \{(\alpha, t_c) \in \mathbb{R}^2 : -d_c < \alpha < \overline{\alpha},\ -2\sqrt{d_c} < t_c < \phi(\alpha)\},$$
$$G_7 = \{(\alpha, t_c) \in \mathbb{R}^2 : \overline{\alpha} < \alpha < d_c,\ \phi(\alpha) < t_c \le -2\sqrt{d_c}\},$$
$$G_8 = \{(\alpha, t_c) \in \mathbb{R}^2 : -d_c < \alpha < \overline{\alpha},\ t_c \le -2\sqrt{d_c}\} \cup$$
$$\{(\alpha, t_c) \in \mathbb{R}^2 : \overline{\alpha} < \alpha < d_c,\ t_c < \phi(\alpha)\},$$
$$G_9 = \{(\alpha, t_c) \in \mathbb{R}^2 : \alpha > d_c,\ t_c > h(\alpha)\},$$
$$G_{10} = \{(\alpha, t_c) \in \mathbb{R}^2 : \alpha > d_c,\ \varphi(\alpha) < t_c < h(\alpha)\},$$
$$G_{11} = \{(\alpha, t_c) \in \mathbb{R}^2 : \alpha > d_c,\ t_c < \varphi(\alpha)\},$$
$$BE_{421} = \{(\alpha, t_c) \in \mathbb{R}^2 : \alpha = d_c,\ t_c \ge 2\sqrt{d_c}\},$$
$$BE_{422} = \{(\alpha, t_c) \in \mathbb{R}^2 : \alpha = d_c,\ -t_r\sqrt{d_c/d_r} < t_c < 2\sqrt{d_c}\},$$
$$BE_{423} = \{(\alpha, t_c) \in \mathbb{R}^2 : \alpha = d_c,\ t_c = -t_r\sqrt{d_c/d_r}\},$$
$$BE_{424} = \{(\alpha, t_c) \in \mathbb{R}^2 : \alpha = d_c,\ -2\sqrt{d_c} < t_c < t_r\sqrt{d_c/d_r}\},$$
$$BE_{425} = \{(\alpha, t_c) \in \mathbb{R}^2 : \alpha = d_c,\ \phi(\alpha) < t_c \le -2\sqrt{d_c}\},$$
$$BE_{426} = \{(\alpha, t_c) \in \mathbb{R}^2 : \alpha = d_c,\ t_c < \phi(\alpha)\},$$
$$HL_{411} = \{(\alpha, t_c) \in \mathbb{R}^2 : -d_c < \alpha < \alpha^* < \overline{\alpha},\ t_c = \phi(\alpha)\},$$
$$HL_{412} = \{(\alpha, t_c) \in \mathbb{R}^2 : -d_c < \alpha = \alpha^* < \overline{\alpha},\ t_c = \phi(\alpha)\},$$
$$HL_{413} = \{(\alpha, t_c) \in \mathbb{R}^2 : -d_c < \alpha^* < \alpha < \overline{\alpha},\ t_c = \phi(\alpha)\},$$
$$HL_{414} = \{(\alpha, t_c) \in \mathbb{R}^2 : -d_c < \overline{\alpha} \le \alpha < d_c,\ t_c = \phi(\alpha)\},$$
$$HL_{415} = \{(\alpha, t_c) \in \mathbb{R}^2 : \alpha = d_c,\ t_c = \phi(\alpha)\}.$$

Bifurcation diagram in the (α, t_c)-plane of system (1.1) as $(t_r, t_c, t_l, d_r, d_c, d_l, \alpha) \in \mathcal{G}_{11}$

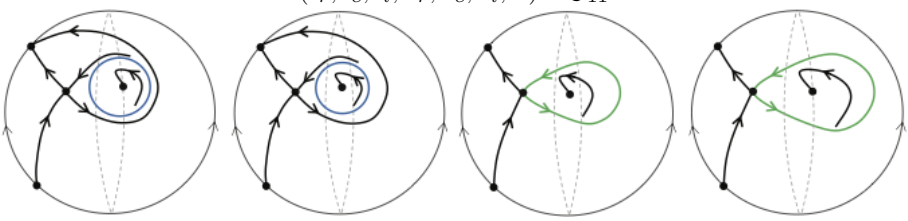

G_7 BE_{425} HL_{414} HL_{415}

FIGURE 7. Bifurcation diagram and global phase portraits in the Poincaré disc of system (1.1) as $(t_r, t_c, t_l, d_r, d_c, d_l, \alpha) \in \mathcal{G}_{11}$.

As we observe, the unstable limit cycle involves two or three linear zones in the global phase portrait in the Poincaré disc of G_7 or BE_{425}. The unstable homoclinic loop involves three linear zones in the global phase portrait in the Poincaré disc of HL_{414} or HL_{415}. The equilibrium point lying in $\mathcal{S}_c$ is a stable node in the global phase portrait in the Poincaré disc of G_7 or HL_{414}. However, in the global phase portrait in the Poincaré disc of BE_{425} or HL_{415}, the equilibrium point lying on the switching line Γ_r is a stable node (as seen from $\mathcal{S}_c$), and is an unstable focus (as seen from $\mathcal{S}_r$). Compared with Theorem 2.1, the homoclinic bifurcation curve of system (1.1) in Theorem 2.4 is different in the region $\{(\alpha, t_c) \in \mathbb{R}^2 | -d_c < \alpha \le d_c\}$ of the (α, t_c)-plane, while the other conditions are the same. Global phase portraits in the Poincaré disc of BE_{41}, BE_{421}, BE_{422}, BE_{423}, BE_{424}, BE_{426}, HL_{411}, HL_{412}, HL_{413}, HL_{42}, DL_4, G_1, G_2, G_3, G_4, G_5, G_6, G_8, G_9, G_{10} and G_{11} of Theorem 2.4 are the same as those in the Poincaré disc of BE_{11}, BE_{121}, BE_{122}, BE_{123}, BE_{124}, BE_{126}, HL_{111},HL_{112}, HL_{113}, HL_{12}, DL_1, I, II, III, IV, V, VI, VII, $VIII$, IX and X of Theorem 2.1, respectively. Therefore, we omit the details and only present global phase portraits in the Poincaré disc of G_7, BE_{425}, HL_{414} and HL_{415} in Theorem 2.4.

Theorem 2.5. *When $(t_r, t_c, t_l, d_r, d_c, d_l, \alpha) \in \mathcal{G}_{12}$, the bifurcation diagram of system (1.1) in the (α, t_c)-plane consists of the following bifurcation curves:*

(a) *Boundary equilibrium bifurcation curves:*

$$BE_{51} = \{(\alpha, t_c) \in \mathbb{R}^2 : \alpha = -d_c\}, \quad BE_{52} = \{(\alpha, t_c) \in \mathbb{R}^2 : \alpha = d_c\}.$$

(b) *Homoclinic bifurcation curve:*

$$HL_5 = \{(\alpha, t_c) \in \mathbb{R}^2 : -d_c < \alpha < d_c,\ t_c = \phi(\alpha)\},$$

where the function $t_c = \phi(\alpha)$ *is continuous and monotonic satisfying* $\max\{t_c^*, -2\sqrt{d_c}\} < \phi(\alpha) < 0$ *for* $-d_c < \alpha < \overline{\alpha}$, $\phi(\alpha) = -2\sqrt{d_c}$ *for* $\alpha = \overline{\alpha} = \phi^{-1}(-2\sqrt{d_c})$, *and* $t_c^* < \phi(\alpha) < -2\sqrt{d_c}$ *for* $\overline{\alpha} < \alpha < d_c$. *Moreover, the bifurcation diagram and global phase portraits in the Poincaré disc of system* (1.1) *in* $\mathcal{G}_{12}$ *are shown in Figure 8, where* $-d_c < \alpha^* < \overline{\alpha} < d_c$, *and*

$$\begin{gathered}
N_1 = \{(\alpha, t_c) \in \mathbb{R}^2 : \alpha < -d_c\},\\
N_2 = \{(\alpha, t_c) \in \mathbb{R}^2 : -d_c < \alpha < d_c,\ t_c \geq 2\sqrt{d_c}\},\\
N_3 = \{(\alpha, t_c) \in \mathbb{R}^2 : -d_c < \alpha < d_c,\ 0 < t_c < 2\sqrt{d_c}\},\\
N_4 = \{(\alpha, t_c) \in \mathbb{R}^2 : -d_c < \alpha < d_c,\ t_c = 0\},\\
N_5 = \{(\alpha, t_c) \in \mathbb{R}^2 : -d_c < \alpha < \overline{\alpha},\ \phi(\alpha) < t_c < 0\} \cup\\
\{(\alpha, t_c) \in \mathbb{R}^2 : \overline{\alpha} < \alpha < d_c,\ -2\sqrt{d_c} < t_c < 0\},\\
N_6 = \{(\alpha, t_c) \in \mathbb{R}^2 : -d_c < \alpha < \overline{\alpha},\ -2\sqrt{d_c} < t_c < \phi(\alpha)\},\\
N_7 = \{(\alpha, t_c) \in \mathbb{R}^2 : \overline{\alpha} < \alpha < d_c,\ \phi(\alpha) < t_c \leq -2\sqrt{d_c}\},\\
N_8 = \{(\alpha, t_c) \in \mathbb{R}^2 : -d_c < \alpha < \overline{\alpha},\ t_c \leq -2\sqrt{d_c}\}\\
\cup \{(\alpha, t_c) \in \mathbb{R}^2 : \overline{\alpha} < \alpha < d_c,\ t_c < \phi(\alpha)\},\\
N_9 = \{(\alpha, t_c) \in \mathbb{R}^2 : \alpha > d_c\},\\
BE_{521} = \{(\alpha, t_c) \in \mathbb{R}^2 : \alpha = d_c,\ t_c \geq 2\sqrt{d_c}\},\\
BE_{522} = \{(\alpha, t_c) \in \mathbb{R}^2 : \alpha = d_c,\ t_c < 2\sqrt{d_c}\},\\
HL_{51} = \{(\alpha, t_c) \in \mathbb{R}^2 : -d_c < \alpha < \alpha^* < \overline{\alpha},\ t_c = \phi(\alpha)\},\\
HL_{52} = \{(\alpha, t_c) \in \mathbb{R}^2 : -d_c < \alpha = \alpha^* < \overline{\alpha},\ t_c = \phi(\alpha)\},\\
HL_{53} = \{(\alpha, t_c) \in \mathbb{R}^2 : -d_c < \alpha^* < \alpha < \overline{\alpha},\ t_c = \phi(\alpha)\},\\
HL_{54} = \{(\alpha, t_c) \in \mathbb{R}^2 : -d_c < \overline{\alpha} \leq \alpha < d_c,\ t_c = \phi(\alpha)\}.
\end{gathered}$$

Although homoclinic bifurcation curves of system (1.1) in Theorem 2.5 are different from the ones described in Theorem 2.2 in the region $\{(\alpha, t_c) \in \mathbb{R}^2 | -d_c < \alpha < d_c\}$ of the (α, t_c)-plane, all other bifurcation curves of system (1.1) in Theorem 2.5 are the same as those shown in Theorem 2.2. It indicates that 14 global phase portraits in the Poincaré disc of Theorem 2.5 can be found in Theorem 2.2. In other words, global phase portraits in the Poincaré disc of BE_{51}, BE_{521}, BE_{522}, HL_{51}, HL_{52}, HL_{53}, N_1, N_2, N_3, N_4, N_5, N_6, N_8 and N_9 of Theorem 2.5 are the same as those in the Poincaré disc of BE_{21}, BE_{221}, BE_{222}, HL_{211}, HL_{212}, HL_{213}, R_1, R_2, R_3, R_4, R_5, R_6, R_7 and R_8 of Theorem 2.2, respectively. Hence, we only show global phase portraits in the Poincaré disc of N_7 and HL_{514} in Theorem 2.5.

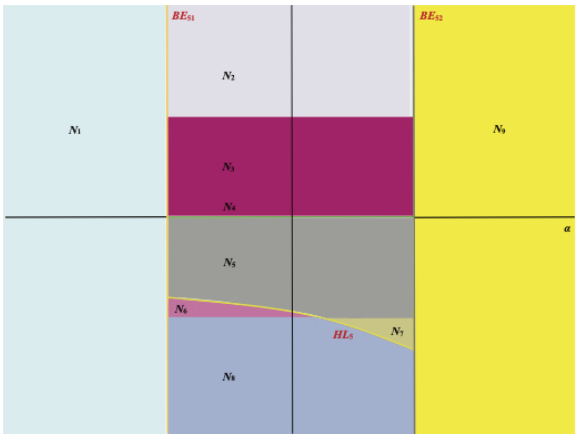

Bifurcation diagram in the (α, t_c)-plane of system (1.1) as $(t_r, t_c, t_l, d_r, d_c, d_l, \alpha) \in \mathcal{G}_{12}$

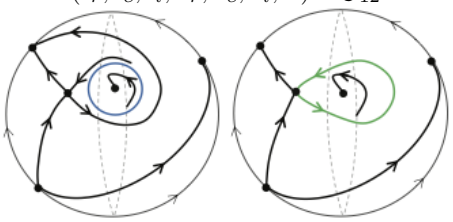

N_7 $\qquad$ HL_{54}

FIGURE 8. Bifurcation diagram and global phase portraits in the Poincaré disc of system (1.1) as $(t_r, t_c, t_l, d_r, d_c, d_l, \alpha) \in \mathcal{G}_{12}$.

Theorem 2.6. *When $(t_r, t_c, t_l, d_r, d_c, d_l, \alpha) \in \mathcal{G}_{13}$, the bifurcation diagram of system (1.1) in the (α, t_c)-plane consists of the following bifurcation curves:*

(a) *Boundary equilibrium bifurcation curves:*

$$BE_{61} = \{(\alpha, t_c) \in \mathbb{R}^2 : \alpha = -d_c\}, \quad BE_{62} = \{(\alpha, t_c) \in \mathbb{R}^2 : \alpha = d_c\};$$

(b) *Homoclinic bifurcation curve:*

$$HL_6 = \{(\alpha, t_c) \in \mathbb{R}^2 : -d_c < \alpha < d_c,\ t_c = \phi(\alpha)\},$$

where the function $t_c = \phi(\alpha)$ is continuous, monotonous and satisfies

$$\max\{t_c^*, -2\sqrt{d_c}\} < \phi(\alpha) < 0 \quad \text{for } -d_c < \alpha < \overline{\alpha},$$
$$\phi(\alpha) = -2\sqrt{d_c} \quad \text{for } \alpha = \overline{\alpha} = \phi^{-1}(-2\sqrt{d_c}),$$

and $t_c^* < \phi(\alpha) < -2\sqrt{d_c}$ for $\overline{\alpha} < \alpha < d_c$. Moreover, the bifurcation diagram and global phase portraits in the Poincaré disc of system (1.1) in $\mathcal{G}_{13}$ are shown in Figure 9, *where $-d_c < \alpha^* < \overline{\alpha} < d_c$, and*

$$U_1 = \{(\alpha, t_c) \in \mathbb{R}^2 : \alpha < -d_c\},$$
$$U_2 = \{(\alpha, t_c) \in \mathbb{R}^2 : -d_c < \alpha < d_c,\ t_c \geq 2\sqrt{d_c}\},$$
$$U_3 = \{(\alpha, t_c) \in \mathbb{R}^2 : -d_c < \alpha < d_c,\ 0 < t_c < 2\sqrt{d_c}\},$$
$$U_4 = \{(\alpha, t_c) \in \mathbb{R}^2 : -d_c < \alpha < d_c,\ t_c = 0\},$$

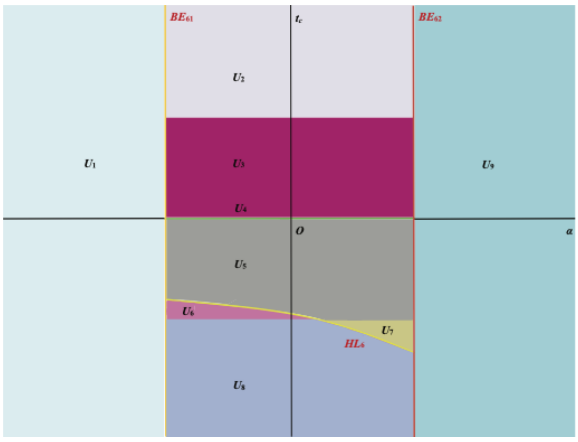

Bifurcation diagram in the (α, t_c)-plane of system (1.1) as $(t_r, t_c, t_l, d_r, d_c, d_l, \alpha) \in \mathcal{G}_{13}$

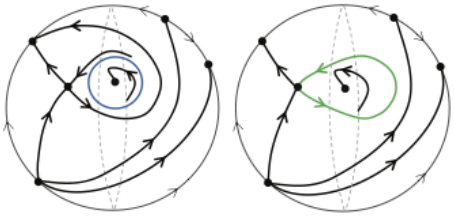

U_7 HL_{64}

FIGURE 9. Bifurcation diagram and global phase portraits in the Poincaré disc of system (1.1) as $(t_r, t_c, t_l, d_r, d_c, d_l, \alpha) \in \mathcal{G}_{13}$.

$$
\begin{aligned}
U_5 &= \{(\alpha, t_c) \in \mathbb{R}^2 : -d_c < \alpha < \overline{\alpha},\ \phi(\alpha) < t_c < 0\} \\
&\quad \cup \{(\alpha, t_c) \in \mathbb{R}^2 : \overline{\alpha} < \alpha < d_c,\ -2\sqrt{d_c} < t_c < 0\}, \\
U_6 &= \{(\alpha, t_c) \in \mathbb{R}^2 : -d_c < \alpha < \overline{\alpha},\ -2\sqrt{d_c} < t_c < \phi(\alpha)\}, \\
U_7 &= \{(\alpha, t_c) \in \mathbb{R}^2 : \overline{\alpha} < \alpha < d_c,\ \phi(\alpha) < t_c \le -2\sqrt{d_c}\}, \\
U_8 &= \{(\alpha, t_c) \in \mathbb{R}^2 : -d_c < \alpha < \overline{\alpha},\ t_c \le -2\sqrt{d_c}\} \\
&\quad \cup \{(\alpha, t_c) \in \mathbb{R}^2 : \overline{\alpha} < \alpha < d_c,\ t_c < \phi(\alpha)\}, \\
U_9 &= \{(\alpha, t_c) \in \mathbb{R}^2 : \alpha > d_c\}, \\
BE_{621} &= \{(\alpha, t_c) \in \mathbb{R}^2 : \alpha = d_c,\ t_c \ge 2\sqrt{d_c}\}, \\
BE_{622} &= \{(\alpha, t_c) \in \mathbb{R}^2 : \alpha = d_c,\ t_c < 2\sqrt{d_c}\}, \\
HL_{61} &= \{(\alpha, t_c) \in \mathbb{R}^2 : -d_c < \alpha < \alpha^* < \overline{\alpha},\ t_c = \phi(\alpha)\}, \\
HL_{62} &= \{(\alpha, t_c) \in \mathbb{R}^2 : -d_c < \alpha = \alpha^* < \overline{\alpha},\ t_c = \phi(\alpha)\}, \\
HL_{63} &= \{(\alpha, t_c) \in \mathbb{R}^2 : -d_c < \alpha^* < \alpha < \overline{\alpha},\ t_c = \phi(\alpha)\}, \\
HL_{64} &= \{(\alpha, t_c) \in \mathbb{R}^2 : -d_c < \overline{\alpha} \le \alpha < d_c,\ t_c = \phi(\alpha)\}.
\end{aligned}
$$

In Theorem 2.6, the homoclinic bifurcation curves of system (1.1) are different from the ones described in Theorem 2.3 in the region $\{(\alpha, t_c) \in \mathbb{R}^2 | -d_c < \alpha < d_c\}$ of the (α, t_c)-plane. However, the other bifurcation curves of system (1.1) in Theorem 2.6 are the same as those described in Theorem 2.3 under the same conditions. Therefore, 14 global phase portraits in the Poincaré disc of Theorem 2.6 can be found in Theorem 2.3. In other words, global phase portraits in the Poincaré disc of BE_{61}, BE_{621}, BE_{622}, HL_{61}, HL_{62}, HL_{63}, U_1, U_2, U_3, U_4, U_5, U_6, U_8 and U_9 of Theorem 2.6 are the same as the corresponding ones in the Poincaré disc of BE_{31}, BE_{321}, BE_{322}, HL_{311}, HL_{312}, HL_{313} and the regions I_1, I_2, I_3, I_4, I_5, I_6, I_7, I_8 of Theorem 2.3, respectively. Thus, we only illustrate global phase portraits in the Poincaré disc of U_7 and HL_{614} as given in Theorem 2.6.

In addition, note that system (1.1) is analytic in $\mathbb{R}^2 \backslash \{\Gamma_l \cup \Gamma_r\}$ and Lipschitz continuous in $\mathbb{R}^2$. Therefore, classical theorems on the existence, uniqueness and continuity of solutions hold for system (1.1) under the initial conditions [26].

3. Preliminaries

We consider a continuous planar piecewise linear differential system in the Liénard form

$$\dot{x} = F(x) - y, \quad \dot{y} = g(x), \tag{3.1}$$

where the functions $F(x)$ and $g(x)$ satisfy the following four conditions for $x \in (a, b)$ with $a < 0 < b$:

(C1) both $F(x)$ and $g(x)$ are Lipschitz continuous with respect to x;
(C2) $F(0) = g(0) = 0$ and $xg(x) > 0$ for $x \neq 0$;
(C3) there exists a unique switching line $x = 0$;
(C4) the unique equilibrium point $(0, 0)$, is a stable focus as seen from the left linear zone of the switching line $x = 0$, and is an unstable focus as seen from the right linear zone of the switching line $x = 0$.

Let $z(x) := \int_0^x g(s)ds$ with $z_1 := z(b)$ and $z_2 := z(a)$. Obviously, we have $z(x) > 0$ for $x \in (a, 0) \cup (0, b)$ and $z(x) = 0$ for $x = 0$. Denote two branches of the inverse of $z(x)$ as $x_1(z)$ and $x_2(z)$ when $x \geq 0$ and $x \leq 0$, respectively. Set

$$F_1(z) := F(x_1(z)), \quad F_2(z) := F(x_2(z)). \tag{3.2}$$

Re-write system (3.1) as

$$\frac{dz}{dy} = \frac{z'(x)dx}{dy} = \frac{g(x)dx}{dy} = F_1(z) - y, \quad z \in (0, z_1) \tag{3.3}$$

for $x > 0$, and

$$\frac{dz}{dy} = \frac{z'(x)dx}{dy} = \frac{g(x)dx}{dy} = F_2(z) - y, \quad z \in (0, z_2) \tag{3.4}$$

for $x < 0$. From (3.1)-(3.2), we have the following result.

Proposition 3.1. *If conditions* (C1)–(C4) *hold, then we have*

(i) *The unique equilibrium point $O(0, 0)$ of system* (3.1) *is an unstable focus if and only if $F_1(z) > F_2(z)$ for $0 < z \ll 1$.*
(ii) *The unique equilibrium point $O(0, 0)$ of system* (3.1) *is a stable focus if and only if $F_1(z) < F_2(z)$ for $0 < z \ll 1$.*
(iii) *The unique equilibrium point $O(0, 0)$ of system* (3.1) *is a center if and only if $F_1(z) = F_2(z)$ for $0 < z \ll 1$.*

Proof. Note that the existence, uniqueness and continuity of the solution of system (3.1) holds under the initial conditions, so the qualitative property of $O(0,0)$ depends on the qualitative property of the left-hand and right-hand linear zones of the switching line $x=0$. It follows from condition (C4) that $O(0,0)$ is a focus or center.

To prove that $O(0,0)$ of system (3.1) is an unstable focus if and only if $F_1(z) > F_2(z)$ for $0 < z \ll 1$, we suppose that $O(0,0)$ is a center, and take a closed orbit denoted by γ in a small neighborhood of $O(0,0)$. We denote by A and B the intersection points of γ with the positive and negative y-axis respectively, see Figure 10(a). Furthermore, we denote the corresponding integral curves of systems (3.3) and (3.4) by γ_1 and γ_2 respectively. Evidently, γ_1 and γ_2 are connected by A and B. We denote by P the intersection point of γ_1 with the curve $F_1(z)$, as shown in Figure 10(b). If $F_1(z) > F_2(z)$ holds in a small neighborhood of $O(0,0)$, by the comparison theorem [11, Corollary 6.3] to systems (3.3) and (3.4) we know that γ_2 passing through A intersects the curve $F_1(z)$ at C and γ_2 passing through B intersects the curve $F_1(z)$ at D, where C lies on the right side of P and D lies on the left side of P. This indicates that system (3.1) has no integral curves connecting A and B. This contradicts the existence of γ. In other words, $O(0,0)$ is a focus if $F_1(z) > F_2(z)$ holds in a small neighborhood of $O(0,0)$. It is easy to see that $O(0,0)$ is an unstable focus if and only if $F_1(z) > F_2(z)$ for $0 < z \ll 1$.

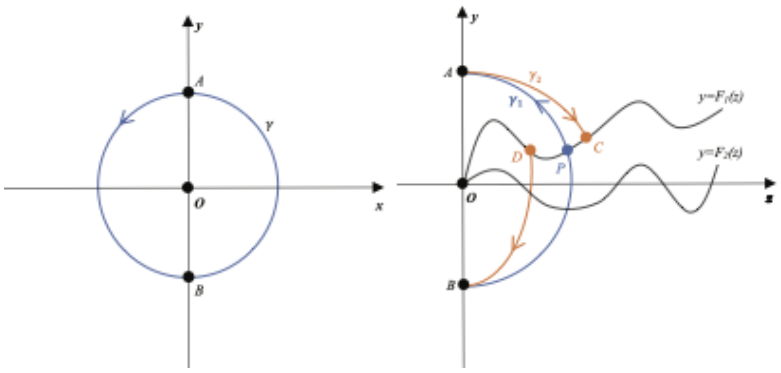

(a) (b)

FIGURE 10. (a) Closed orbit γ of system (3.1); (b) Closed orbits γ_1 and γ_2 of systems (3.3) and (3.4) when $F_1(z) > F_2(z)$.

Similarly, we can prove that $O(0,0)$ is a stable focus if and only if $F_1(z) < F_2(z)$ for $0 < z \ll 1$. If $F_1(z) = F_2(z)$ in a small neighborhood of $O(0,0)$, then γ_1 and γ_2 will coincide. This implies that $O(0,0)$ is a center if and only if $F_1(z) = F_2(z)$ for $0 < z \ll 1$. □

(C5) The unique equilibrium point $(0,0)$ is an unstable focus as seen from the left linear zone of the switching line $x=0$, and is a stable focus as seen from the right linear zone of the switching line $x=0$.

Proceeding in an analogous manner, we can derive the dual result of Proposition 3.1 as follows.

Proposition 3.2. *If conditions* (C1)–(C3), (C5) *hold, then we have*

(i) *The unique equilibrium point* $O(0,0)$ *of system* (3.1) *is a stable focus if and only if* $F_1(z) > F_2(z)$ *for* $0 < z \ll 1$.
(ii) *The unique equilibrium point* $O(0,0)$ *of system* (3.1) *is an unstable focus if and only if* $F_1(z) < F_2(z)$ *for* $0 < z \ll 1$.
(iii) *The unique equilibrium point* $O(0,0)$ *of system* (3.1) *is a center if and only if* $F_1(z) = F_2(z)$ *for* $0 < z \ll 1$.

4. Local dynamics of system (1.1)

Lemma 4.1. *When* $d_c > 0$ *in* $\mathcal{G}_1$, *system* (1.1) *has no equilibrium points if* $\alpha < -d_c$; *one equilibrium point* E_{cl} *if* $\alpha = -d_c$; *two equilibrium points* E_1 *and* E_c *if* $-d_c < \alpha < d_c$; *two equilibrium points* E_1 *and* E_{cr} *if* $\alpha = d_c$; *and two equilibrium points* E_l *and* E_r *if* $\alpha > d_c$. *The qualitative properties of these equilibrium points are shown in* Table 1, *where* $E_l : ((\alpha + d_c)/d_l - 1, t_l(\alpha + d_c)/d_l - t_c)$ *lies in* $\mathcal{S}_l$, $E_c : (\alpha/d_c, t_c\alpha/d_c)$ *lies in* $\mathcal{S}_c$, $E_r : ((\alpha - d_c)/d_r + 1, t_r(\alpha - d_c)/d_r + t_c)$ *lies in* $\mathcal{S}_r$, $E_{cl} : (-1, -t_c)$ *lies on the left switching line* Γ_l, *and* $E_{cr} : (1, t_c)$ *lies on the right switching line* Γ_r.

Table 1. Qualitative properties of finite equilibrium points of system (1.1) with $d_c > 0$ in $\mathcal{G}_1$

Possibilities $t_r, t_c, d_r, d_c, \alpha$				Number, Stability and Type
$\alpha < -d_c$				0
$\alpha = -d_c$	$t_c < 0$	${t_c}^2 - 4d_c < 0$		1, E_{cl} cusp (Fig. 11(a))
		${t_c}^2 - 4d_c \geq 0$		1, E_{cl} saddle-node (Fig. 11(b))
	$t_c = 0$			1, E_{cl} cusp (Fig. 11(c))
	$t_c > 0$	${t_c}^2 - 4d_c < 0$		1, E_{cl} cusp (Fig. 11(d))
		${t_c}^2 - 4d_c \geq 0$		1, E_{cl} saddle-node (Fig. 11(e))
$-d_c < \alpha < d_c$ $d_c > 0$	$t_c < 0$	${t_c}^2 - 4d_c < 0$		2, E_1 saddle, E_c stable focus
		${t_c}^2 - 4d_c \geq 0$		2, E_1 saddle, E_c stable node
	$t_c = 0$			2, E_1 saddle, E_c center
	$t_c > 0$	${t_c}^2 - 4d_c < 0$		2, E_1 saddle, E_c unstable focus
		${t_c}^2 - 4d_c \geq 0$		2, E_1 saddle, E_c unstable node
$\alpha = d_c$	$t_c < 0$	${t_c}^2 - 4d_c < 0$	${t_r}^2 - 4d_r < 0$	2, E_1 saddle, E_{cr} a focus or center
			${t_r}^2 - 4d_r \geq 0$	2, E_1 saddle, E_{cr} focus-node (Fig. 11(f))
		${t_c}^2 - 4d_c \geq 0$	${t_r}^2 - 4d_r < 0$	2, E_1 saddle, E_{cr} node-focus (Fig. 11(g))
			${t_r}^2 - 4d_r \geq 0$	2, E_1 saddle, E_{cr} node-node (Fig. 11(h))
	$t_c = 0$		${t_r}^2 - 4d_r < 0$	2, E_1 saddle, E_{cr} unstable focus (Fig. 11(i))
			${t_r}^2 - 4d_r \geq 0$	2, E_1 saddle, E_{cr} focus-node (Fig. 11(j))
	$t_c > 0$	${t_c}^2 - 4d_c < 0$	${t_r}^2 - 4d_r < 0$	2, E_1 saddle, E_{cr} unstable focus
			${t_r}^2 - 4d_r \geq 0$	2, E_1 saddle, E_{cr} focus-node (Fig. 11(k))
		${t_c}^2 - 4d_c \geq 0$	${t_r}^2 - 4d_r < 0$	2, E_1 saddle, E_{cr} node-focus (Fig. 11(l))
			${t_r}^2 - 4d_r \geq 0$	2, E_1 saddle, E_{cr} unstable node
$\alpha > d_c$			${t_r}^2 - 4d_r < 0$	2, E_1 saddle, E_r unstable focus
			${t_r}^2 - 4d_r \geq 0$	2, E_1 saddle, E_r unstable node

Proof. As we know, the number of equilibrium points of system (1.1) is determined by the number of roots of $g(x) = \alpha$. If $d_c > 0$ in $\mathcal{G}_1$, by a direct calculation, we see that system (1.1) exhibits two equilibrium points E_l and E_r for $\alpha > d_c$, two equilibrium points E_l and E_{cr} for $\alpha = d_c$, two equilibrium points E_l and E_c for $-d_c < \alpha < d_c$, one equilibrium point E_{cl} for $\alpha = -d_c$, and no equilibrium points

for $\alpha < -d_c$, as shown in Table 1. The Jacobian matrices at E_l, E_c and E_r have the forms respectively

$$J_{E_1} := \begin{bmatrix} t_1 & -1 \\ d_1 & 0 \end{bmatrix}, \quad J_{E_c} := \begin{bmatrix} t_c & -1 \\ d_c & 0 \end{bmatrix}, \quad J_{E_r} := \begin{bmatrix} t_r & -1 \\ d_r & 0 \end{bmatrix}.$$

From $\det J_{E_1} = d_1 < 0$, $\det J_{E_c} = d_c > 0$ and $\det J_{E_r} = d_r > 0$, it follows that E_l is a saddle and E_c and E_r are anti-saddles, as shown in Table 1.

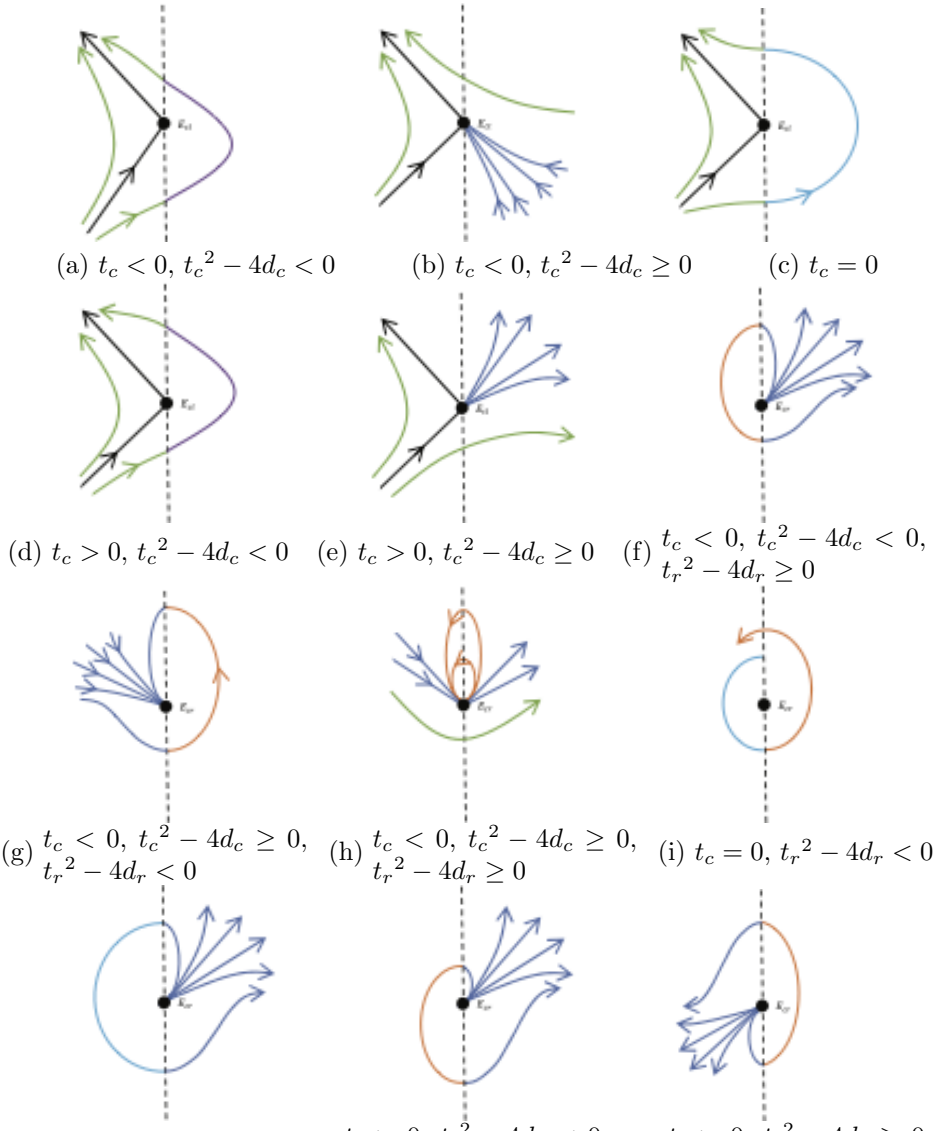

(a) $t_c < 0$, ${t_c}^2 - 4d_c < 0$ (b) $t_c < 0$, ${t_c}^2 - 4d_c \geq 0$ (c) $t_c = 0$

(d) $t_c > 0$, ${t_c}^2 - 4d_c < 0$ (e) $t_c > 0$, ${t_c}^2 - 4d_c \geq 0$ (f) $t_c < 0$, ${t_c}^2 - 4d_c < 0$, ${t_r}^2 - 4d_r \geq 0$

(g) $t_c < 0$, ${t_c}^2 - 4d_c \geq 0$, ${t_r}^2 - 4d_r < 0$ (h) $t_c < 0$, ${t_c}^2 - 4d_c \geq 0$, ${t_r}^2 - 4d_r \geq 0$ (i) $t_c = 0$, ${t_r}^2 - 4d_r < 0$

(j) $t_c = 0$, ${t_r}^2 - 4d_r \geq 0$ (k) $t_c > 0$, ${t_c}^2 - 4d_c < 0$, ${t_r}^2 - 4d_r \geq 0$ (l) $t_c > 0$, ${t_c}^2 - 4d_c \geq 0$, ${t_r}^2 - 4d_r < 0$

FIGURE 11. Qualitative properties of E_{cl} and E_{cr} of system (1.1) with $d_c > 0$ in $\mathcal{G}_1$

It follows that the qualitative property of E_{cl} (resp. E_{cr}) depends on the qualitative property of the left-hand and right-hand linear zones of the switching line Γ_l (resp. Γ_r). The equilibrium point E_{cr} is an unstable focus as seen from $\mathcal{S}_c$, and is an unstable focus as seen from $\mathcal{S}_r$ for $t_c > 0$, ${t_c}^2 - 4d_c < 0$ and ${t_r}^2 - 4d_r < 0$. Therefore, E_{cr} is an unstable focus in the above case. The equilibrium point E_{cr} is a stable focus as seen from $\mathcal{S}_c$, but is an unstable focus as seen from $\mathcal{S}_r$ for $t_c < 0$, ${t_c}^2 - 4d_c < 0$ and ${t_r}^2 - 4d_r < 0$. Then, E_{cr} can be a focus or center (see Lemma 5.9). The equilibrium point E_{cr} is a stable node as seen from $\mathcal{S}_c$, and is an unstable node as seen from $\mathcal{S}_r$. So E_{cr} is a node-node, as shown in Figure 11(h). More similar results are illustrated in Figure 11 as well. □

Lemma 4.2. [21] *Equilibrium points at infinity of system* (1.1) *in the Poincaré disc are shown in Figure 12 in the region* $\mathcal{G}_1$.

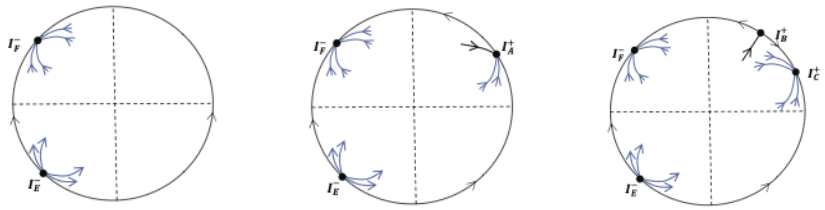

$t_r^2 - 4d_r < 0$ $t_r^2 - 4d_r = 0$ $t_r^2 - 4d_r > 0$

FIGURE 12. Equilibrium points at infinity of system (1.1) in the Poincaré disc in $\mathcal{G}_1$

5. Nonlocal dynamics of system (1.1)

In this section, we study limit cycles and homoclinic loops of system (1.1) with $d_c > 0$ in the region $\mathcal{G}_1$. By Lemma 4.1, E_{cl} lies on the left switching line Γ_l and is a half of a saddle in $\mathcal{S}_l$. Namely, system (1.1) has two invariant lines in $\mathcal{S}_l$. We know that system (1.1) has no limit cycles and homoclinic loops when $\alpha = -d_c < 0$. Therefore, we only need to investigate limit cycles and homoclinic loops of system (1.1) when $\alpha > -d_c$ and $d_c > 0$. When $d_c > 0$, we separate our discussions into three cases $-d_c < a < d_c$, $a = d_c$ and $\alpha > d_c$, respectively.

5.1. Limit cycles and homoclinic loops for $d_c > 0$ and $-d_c < \alpha < d_c$ in $\mathcal{G}_1$.

According to Lemma 4.1, system (1.1) has two equilibrium points E_l and E_c when $d_c > 0$ and $-d_c < \alpha < d_c$ in $\mathcal{G}_1$. Moreover, E_1 is a saddle and E_c is a node for $t_c^2 - 4d_c \geq 0$, $t_c \neq 0$ or a focus for $t_c^2 - 4d_c < 0$, $t_c \neq 0$ or a center for $t_c = 0$. Set $m := \alpha/d_c$. Then, the coordinates of E_c can be rewritten as $(m, t_c m)$. By making a linear transformation

$$x \to x + m, \quad y \to y + t_c m,$$

system (1.1) reduces to

$$\frac{dx}{dt} = \widetilde{F}(x) - y, \quad \frac{dy}{dt} = \widetilde{g}(x), \tag{5.1}$$

where

$$\widetilde{F}(x)=\begin{cases}t_r(x+m-1)+t_c(-m+1), & \text{if } x>-m+1,\\ t_cx, & \text{if } -m-1\le x\le -m+1,\\ t_l(x+m+1)+t_c(-m-1), & \text{if } x<-m-1,\end{cases}$$

$$\widetilde{g}(x)=\begin{cases}d_r(x+m-1)+d_c(-m+1), & \text{if } x>-m+1,\\ d_cx, & \text{if } -m-1\le x\le -m+1,\\ d_l(x+m+1)+d_c(-m-1), & \text{if } x<-m-1.\end{cases}$$

It is easy to see that E_c of system (1.1) is moved to $O(0,0)$ of system (5.1) and E_l of system (1.1) is moved to $N_l(d_c(m+1)/d_l-m-1, t_ld_c(m+1)/d_l-t_c(m+1))$ of system (5.1). Clearly, we have $-m+1>0$ and $-m-1<0$ because of $d_c>0$ and $-d_c<\alpha<d_c$. The plane $\mathbb{R}^2$ is divided into three open linear zones

$$\begin{aligned}\widetilde{\mathcal{S}}_l &:= \{(x,y)\in\mathbb{R}^2 : x<-m-1\},\\ \widetilde{\mathcal{S}}_c &:= \{(x,y)\in\mathbb{R}^2 : -m-1<x<-m+1\},\\ \widetilde{\mathcal{S}}_r &:= \{(x,y)\in\mathbb{R}^2 : x>-m+1\}\end{aligned}$$

by two straight lines $\widetilde{\Gamma}_l := \{(x,y)\in\mathbb{R}^2 : x=-m-1\}$ and $\widetilde{\Gamma}_r := \{(x,y)\in\mathbb{R}^2 : x=-m+1\}$. For simplicity, for system (5.1) we still use F and g to represent $\widetilde{F}$ and $\widetilde{g}$, respectively. Note that systems (1.1) and (5.1) are topologically equivalent. Therefore, we only need to study limit cycles and homoclinic loops of system (5.1) to obtain the corresponding results for system (1.1) by a translation.

In the following lemma, we show the nonexistence of limit cycles and homoclinic loops of system (1.1) with $d_c>0$ and $-d_c<\alpha<d_c$ in $\mathcal{G}_1$.

Lemma 5.1. *Assume that $d_c>0$ and $-d_c<\alpha<d_c$ in $\mathcal{G}_1$. System (1.1) exhibits neither limit cycles nor homoclinic loops when $t_c\ge 0$ or $t_c\le t_c^*$, where*

$$t_c^* := -\frac{t_r(\alpha-d_c)+t_r\sqrt{(\alpha-d_c)^2+4\alpha d_r-\frac{d_r}{d_l}(\alpha+d_c)^2}}{2d_r}+\frac{t_l(\alpha+d_c)}{2d_l}.$$

Proof. It follows from Lemma 4.1 that system (5.1) has two equilibrium points N_l and O when $d_c>0$ and $-d_c<\alpha<d_c$ in $\mathcal{G}_1$. Moreover, N_l is a saddle, and O is a node for $t_c^2-4d_c\ge 0$, $t_c\ne 0$ or a focus for $t_c^2-4d_c<0$, $t_c\ne 0$ or a center for $t_c=0$. To study the nonexistence of limit cycles and homoclinic loops of system (5.1), we set a generalized Filippov transformation

$$z(x) := \int_0^x g(s)ds,$$

where $x_1(z)$ and $x_2(z)$ are the branches of the inverse of $z(x)$ for $x\ge 0$ and $x<0$ respectively. Denote the abscissa of saddle point N_l by $x_{N_l} := d_c(m+1)/d_l-m-1$. We know that limit cycles of system (5.1) must only surround O by the index theory [38, Chapter 4] if they exist. Therefore, it suffices to consider $x\in(x_{N_l},+\infty)$. From

system (5.1) it follows that

$$z(x)=\begin{cases}\frac{d_r x^2}{2}+(d_r-d_c)(m-1)x+\frac{1}{2}(d_r-d_c)(m-1)^2\\ \quad \text{if } x>-m+1,\\ \frac{d_c x^2}{2} \quad \text{if } -m-1\le x\le -m+1,\\ \frac{d_l x^2}{2}+(d_l-d_c)(m+1)x+\frac{1}{2}(d_l-d_c)(m+1)^2\\ \quad \text{if } x_{N_l}<x<-m-1.\end{cases} \tag{5.2}$$

Moreover,

$$z(x)\in\begin{cases}(\frac{d_c(-m+1)^2}{2},+\infty), & \text{if } x>-m+1,\\ [0,\frac{d_c(-m+1)^2}{2}], & \text{if } 0\le x\le -m+1,\\ (0,\frac{d_c(m+1)^2}{2}], & \text{if } -m-1\le x<0,\\ (\frac{d_c(m+1)^2}{2},z_{N_l}), & \text{if } x_{N_l}<x<-m-1,\end{cases}$$

where $z_{N_l}:=d_c(d_l-d_c)(m+1)^2/(2d_l)$. It follows from (5.2) that

$$x_1(z)=\begin{cases}\sqrt{\frac{2z}{d_c}}, & \text{if } 0\le x\le -m+1,\\ h_1(z)-m+1, & \text{if } x>-m+1,\end{cases} \tag{5.3}$$

$$x_2(z)=\begin{cases}-\sqrt{\frac{2z}{d_c}}, & \text{if } -m-1\le x<0,\\ h_2(z)-m-1, & \text{if } x_{N_l}<x<-m-1,\end{cases} \tag{5.4}$$

with

$$h_1(z):=\frac{-d_c(-m+1)+\sqrt{(-d_r d_c+d_c^2)(-m+1)^2+2d_r z}}{d_r},$$
$$h_2(z):=\frac{-d_c(-m-1)-\sqrt{(-d_l d_c+d_c^2)(-m-1)^2+2d_l z}}{d_l}.$$

Let $F_1(z):=F(x_1(z))$ and $F_2(z):=F(x_2(z))$. Proving that $F_1(z)>F_2(z)$ or $F_1(z)<F_2(z)$ for $z\in(0,z_{N_l})$, is equivalent to that there are no limit cycles and homoclinic loops [27, Section 6]. Based on (5.3) and (5.4), we derive

$$F_1(z)=\begin{cases}t_c\sqrt{\frac{2z}{d_c}}, & \text{if } 0\le z\le \frac{d_c(-m+1)^2}{2},\\ t_r h_1(z)+t_c(-m+1), & \text{if } z>\frac{d_c(-m+1)^2}{2},\end{cases} \tag{5.5}$$

and

$$F_2(z)=\begin{cases}-t_c\sqrt{\frac{2z}{d_c}}, & \text{if } 0<z\le \frac{d_c(m+1)^2}{2},\\ t_l h_2(z)+t_c(-m-1), & \text{if } \frac{d_c(m+1)^2}{2}<z<z_{N_l}.\end{cases} \tag{5.6}$$

From (5.5) and (5.6) it follows that

$$\begin{aligned}&F_1(z)-F_2(z)\\ &=\begin{cases}2t_c\sqrt{\frac{2z}{d_c}}, & \text{if } 0<z\le \frac{d_c(-m+1)^2}{2},\\ t_r h_1(z)+t_c(-m+1)+t_c\sqrt{\frac{2z}{d_c}}, & \text{if } \frac{d_c(-m+1)^2}{2}<z\le \frac{d_c(m+1)^2}{2},\\ t_r h_1(z)-t_l h_2(z)+2t_c, & \text{if } \frac{d_c(m+1)^2}{2}<z<z_{N_l}\end{cases}\end{aligned} \tag{5.7}$$

for $0<\alpha<d_c$, and

$$F_1(z)-F_2(z)=\begin{cases}2t_c\sqrt{\frac{2z}{d_c}}, & \text{if } 0<z\le\frac{d_c}{2},\\ t_r\frac{-d_c+\sqrt{-d_rd_c+d_c^2+2d_rz}}{d_r}-t_l\frac{d_c-\sqrt{-d_ld_c+d_c^2+2d_lz}}{d_l}+2t_c, & \text{if } \frac{d_c}{2}<z<z_{N_l}\end{cases}\tag{5.8}$$

for $\alpha=0$, and

$$F_1(z)-F_2(z)=\begin{cases}2t_c\sqrt{\frac{2z}{d_c}}, & \text{if } 0<z\le\frac{d_c(m+1)^2}{2},\\ t_c\sqrt{\frac{2z}{d_c}}-t_lh_2(z)+t_c(m+1), & \text{if } \frac{d_c(m+1)^2}{2}<z\le\frac{d_c(-m+1)^2}{2},\\ t_rh_1(z)-t_lh_2(z)+2t_c, & \text{if } \frac{d_c(-m+1)^2}{2}<z<z_{N_l}\end{cases}\tag{5.9}$$

for $-d_c<\alpha<0$.

We consider the value of $F_1(z)-F_2(z)$ for $0<\alpha<d_c$ by three cases $t_c>0$, $t_c=0$ and $t_c<0$, see (5.7).

Case (a1) When $t_c>0$, we have $F_1(z)-F_2(z)>0$ for $z\in(0,d_c(-m+1)^2/2]$, and

$$F_1'(z)-F_2'(z)=\frac{t_r}{\sqrt{(-d_rd_c+d_c^2)(-m+1)^2+2d_rz}}+\frac{t_c}{\sqrt{2d_cz}}>0$$

for $z\in(d_c(-m+1)^2/2,d_c(m+1)^2/2]$, and

$$F_1'(z)-F_2'(z)=\frac{t_r}{\sqrt{(-d_rd_c+d_c^2)(-m+1)^2+2d_rz}}+\frac{t_l}{\sqrt{(-d_ld_c+d_c^2)(-m-1)^2+2d_lz}}>0$$

for $z\in(d_c(m+1)^2/2,z_{N_l})$. Therefore, we have $F_1(z)-F_2(z)>0$ for $z\in(0,z_{N_l})$. According to [27, Section 6], we know that system (5.1) has no limit cycles and homoclinic loops for $t_c>0$, $0<\alpha<d_c$ and $d_c>0$.

Case (a2) When $t_c=0$, we have $F_1(z)-F_2(z)=0$ for $z\in(0,d_c(-m+1)^2/2]$ and $F_1'(z)-F_2'(z)>0$ for $z\in(d_c(-m+1)^2/2,z_{N_l})$. Hence, we obtain $F_1(z)-F_2(z)\ge0$ for $z\in(0,z_{N_l})$, which implies that system (5.1) has no limit cycles and homoclinic loops according to [27, Section 6] when $t_c=0$, $0<\alpha<d_c$ and $d_c>0$.

Case (a3) When $t_c<0$, we have $F_1(z)-F_2(z)<0$ for $z\in(0,d_c(-m+1)^2/2]$. For $z\in(d_c(-m+1)^2/2,d_c(m+1)^2/2]$, a routine computation gives rise to

$$F_1'(z)-F_2'(z)=\frac{-t_c\sqrt{2d_rz}+t_c\sqrt{(-d_rd_c+d_c^2)(-m+1)^2+2d_rz}}{\sqrt{(-d_rd_c+d_c^2)(-m+1)^2+2d_rz}\cdot\sqrt{2d_cz}}$$

$$\begin{cases}<0, & \text{if } t_c<-t_r,\\ =0, & \text{if } t_c=-t_r,\\ >0, & \text{if } t_c>-t_r\end{cases}$$

for $t_r^2d_c-t_c^2d_r=0$; and

$$F_1'(z)-F_2'(z)\begin{cases}<0, & \text{if } z<z_0,\\ =0, & \text{if } z=z_0,\\ >0, & \text{if } z>z_0\end{cases}$$

for $t_r^2 d_c - t_c^2 d_r > 0$; and

$$F_1'(z) - F_2'(z) \begin{cases} > 0, & \text{if } z < z_0, \\ = 0, & \text{if } z = z_0, \\ < 0, & \text{if } z > z_0 \end{cases}$$

for $t_r^2 d_c - t_c^2 d_r < 0$, where

$$z_0 := \frac{t_c^2(-d_r d_c + d_c^2)(-m+1)^2}{2(t_r^2 d_c - t_c^2 d_r)}. \tag{5.10}$$

If $t_r^2 d_c - t_c^2 d_r < 0$ and $z_0 \in (d_c(-m+1)^2/2, d_c(m+1)^2/2]$, then

$$\begin{aligned}
&(F_1(z) - F_2(z))|_{z=z_0} \\
&= t_r \frac{-d_c(-m+1) + \sqrt{(-d_r d_c + d_c^2)(-m+1)^2 + 2d_r z_0}}{d_r} + t_c(-m+1) + t_c\sqrt{\frac{2z_0}{d_c}} \\
&= \Big(\frac{-t_r d_c + t_c d_r - \sqrt{(-d_r + d_c)(t_r^2 d_c - t_c^2 d_r)}}{d_r}\Big)(-m+1) < 0.
\end{aligned}$$

If $t_c < \overline{t_c}$, then

$$\begin{aligned}
&(F_1(z) - F_2(z))|_{z=\frac{d_c(m+1)^2}{2}} \\
&= t_r \frac{-d_c(-m+1) + \sqrt{d_c^2(-m+1)^2 + 4d_r d_c m}}{d_r} + t_c(-m+1) + t_c(m+1) \\
&= t_r \frac{-d_c(-m+1) + \sqrt{d_c^2(-m+1)^2 + 4d_r d_c m}}{d_r} + 2t_c < 0,
\end{aligned}$$

where

$$\overline{t_c} := -\frac{t_r(\alpha - d_c) + t_r\sqrt{(\alpha - d_c)^2 + 4\alpha d_r}}{2d_r}.$$

As $z \in (d_c(m+1)^2/2, z_{N_l})$, if $t_c < t_c^*$, then $F_1'(z) - F_2'(z) > 0$ and

$$\begin{aligned}
&(F_1(z) - F_2(z))|_{z=z_{N_l}} \\
&= t_r \frac{d_c(m-1) + \sqrt{d_c^2(-m+1)^2 + 4d_r d_c m - \frac{d_r d_c^2}{d_l}(m+1)^2}}{d_r} - \frac{t_l d_c(m+1)}{d_l} + 2t_c \\
&< 0.
\end{aligned}$$

It is easy to check that $t_c^* < \overline{t_c}$. So we have $F_1(z) - F_2(z) < 0$ for $z \in (0, z_{N_l})$ if $t_c < t_c^*$. According to [27, Section 6], system (5.1) exhibits no limit cycles and homoclinic loops when $t_c \le t_c^*$, $0 < \alpha < d_c$ and $d_c > 0$.

We now consider the value of $F_1(z) - F_2(z)$ for $\alpha = 0$ by three cases $t_c > 0$, $t_c = 0$ and $t_c < 0$, see (5.8).

Case (b1) When $t_c > 0$, we have $F_1(z) - F_2(z) > 0$ for $z \in (0, d_c/2]$, and

$$F_1'(z) - F_2'(z) = \frac{t_r}{\sqrt{-d_r d_c + d_c^2 + 2d_r z}} + \frac{t_l}{\sqrt{-d_l d_c + d_c^2 + 2d_l z}} > 0,$$

for $z \in (d_c/2, d_c(d_l - d_c)/(2d_l))$. Therefore, $F_1(z) - F_2(z) > 0$ for z in the interval $(0, d_c(d_l - d_c)/(2d_l))$. It follows from [27, Section 6] that system (5.1) exhibits no limit cycles and homoclinic loops when $t_c > 0$, $\alpha = 0$ and $d_c > 0$.

Case (b2) When $t_c = 0$, we have $F_1(z) - F_2(z) = 0$ for $z \in (0, d_c/2]$ and $F_1'(z) - F_2'(z) > 0$ for $z \in (d_c/2, z_{N_l})$. It implies that $F_1(z) - F_2(z) \ge 0$ for $z \in (0, z_{N_l})$.

Therefore, system (5.1) exhibits no limit cycles and homoclinic loops [27, Section 6], when $t_c = 0$, $\alpha = 0$ and $d_c > 0$.

Case (b3) When $t_c < 0$, it follows that $F_1(z) - F_2(z) < 0$ for $z \in (0, d_c/2]$ and $F_1'(z) - F_2'(z) > 0$ for $z \in (d_c/2, d_c(d_l - d_c)/(2d_l))$. Furthermore, we have

$$(F_1(z) - F_2(z))|_{z=\frac{d_c(d_l-d_c)}{2d_l}} = t_r \frac{-d_c + \sqrt{d_c^2 - \frac{d_r d_c^2}{d_l}}}{d_r} - \frac{t_l d_c}{d_l} + 2t_c < 0,$$

when

$$t_c < -\frac{-t_r d_c + t_r\sqrt{d_c^2 - \frac{d_r d_c^2}{d_l}}}{2d_r} + \frac{t_l d_c}{2d_l}.$$

Note that t_c^* with $\alpha = 0$ is

$$t_c^* - \left(-t_r d_c + t_r\sqrt{d_c^2 - d_r d_c^2/d_l}\right)/(2d_r) + t_l d_c/(2d_l).$$

Therefore, we obtain $F_1(z) - F_2(z) < 0$ for $z \in (0, d_c(d_l - d_c)/(2d_l))$ if $t_c < t_c^*$. Based on [27, Section 6], system (5.1) has no limit cycles and homoclinic loops when $t_c \le t_c^*$, $\alpha = 0$ and $d_c > 0$.

Next, we discuss the sign of $F_1(z) - F_2(z)$ for $-d_c < \alpha < 0$ by three cases $t_c > 0$, $t_c = 0$ and $t_c < 0$, see (5.9).

Case (c1) When $t_c > 0$, we have $F_1(z) - F_2(z) > 0$ for $z \in (0, d_c(m+1)^2/2]$, and

$$F_1'(z) - F_2'(z) = \frac{t_l}{\sqrt{(-d_l d_c + d_c^2)(-m-1)^2 + 2d_l z}} + \frac{t_c}{\sqrt{2d_c z}} > 0,$$

for $z \in (d_c(m+1)^2/2, d_c(-m+1)^2/2]$, and

$$F_1'(z) - F_2'(z) = \frac{t_r}{\sqrt{(-d_r d_c + d_c^2)(-m+1)^2 + 2d_r z}} + \frac{t_l}{\sqrt{(-d_l d_c + d_c^2)(-m-1)^2 + 2d_l z}} > 0$$

for $z \in (d_c(-m+1)^2/2, z_{N_l})$. Thus, we obtain $F_1(z) - F_2(z) > 0$ for $z \in (0, z_{N_l})$. From [27, Section 6], it follows that system (5.1) exhibits no limit cycles and homoclinic loops for $t_c > 0$, $-d_c < \alpha < 0$ and $d_c > 0$.

Case (c2). When $t_c = 0$, we find $F_1(z) - F_2(z) = 0$ for $z \in (0, d_c(m+1)^2/2]$ and $F_1'(z) - F_2'(z) > 0$ for $z \in (d_c(m+1)^2/2, z_{N_l})$, which means that $F_1(z) - F_2(z) \ge 0$ for $z \in (0, z_{N_l})$. Then, system (5.1) has no limit cycles and homoclinic loops according to [27, Section 6], when $t_c = 0$, $-d_c < \alpha < 0$ and $d_c > 0$.

Case (c3). When $t_c < 0$, we find $F_1(z) - F_2(z) < 0$ for $z \in (0, d_c(m+1)^2/2]$. For $z \in (d_c(m+1)^2/2, d_c(-m+1)^2/2]$, a routine computation gives rise to

$$F_1'(z) - F_2'(z) \begin{cases} < 0, & \text{if } z < z_0, \\ = 0, & \text{if } z = z_0, \\ > 0, & \text{if } z > z_0, \end{cases}$$

because $t_l^2 d_c - t_c^2 d_l > 0$, where z_0 is given in (5.10). When $t_c < \widehat{t_c}$, it follows that

$$(F_1(z) - F_2(z))|_{z=\frac{d_c(-m+1)^2}{2}}$$
$$= t_c(-m+1) - t_c(-m-1) - t_l \frac{-d_c(-m-1) - \sqrt{d_c^2(m+1)^2 - 4d_l d_c m}}{d_l}$$

$$= t_l \frac{d_c(-m-1) + \sqrt{d_c^2(m+1)^2 - 4d_l d_c m}}{d_l} + 2t_c < 0,$$

where

$$\widehat{t_c} := \frac{t_l(\alpha + d_c) - t_l\sqrt{(\alpha + d_c)^2 - 4\alpha d_l}}{2d_l}.$$

For $z \in (d_c(m+1)^2/2, z_{N_l})$, it holds that $F_1'(z) - F_2'(z) > 0$. If $t_c < t_c^*$, then

$$F_1(z) - F_2(z)|_{z=\frac{d_c(d_l-d_c)(m+1)^2}{2d_l}} < 0.$$

We see that $t_c^* < \widehat{t_c}$ implies $F_1(z) - F_2(z) < 0$ for $z \in (0, z_{N_l})$ if $t_c < t_c^*$. According to [27, Section 6], system (5.1) exhibits no limit cycles and homoclinic loops when $t_c \le t_c^*$, $-d_c < \alpha < 0$ and $d_c > 0$.

From Cases (a1), (a2), (b1), (b2), (c1), and (c2), we obtain that system (1.1) exhibits neither limit cycles nor homoclinic loops when $t_c \ge 0$, $-d_c < \alpha < d_c$ and $d_c > 0$ in $\mathcal{G}_1$. System (1.1) has neither limit cycles nor homoclinic loops by Cases (a3), (b3) and (c3), when $t_c \le t_c^*$, $-d_c < \alpha < d_c$, and $d_c > 0$ in $\mathcal{G}_1$. □

From Lemma 5.1, it suffices to study the existence of limit cycles of system (1.1) when $d_c > 0$, $-d_c < \alpha < d_c$ and $t_c^* < t_c < 0$ in $\mathcal{G}_1$. From Lemma 4.1, we know that system (1.1) has two equilibrium points E_l and E_c when $d_c > 0$, $-d_c < \alpha < d_c$ and $t_c^* < t_c < 0$ in $\mathcal{G}_1$. Moreover, E_1 is a saddle and E_c is a stable node for $t_c^2 - 4d_c \ge 0$ or a stable focus for $t_c^2 - 4d_c < 0$. Since E_c lies in $\mathcal{S}_c$ and limit cycles of system (1.1) must only surround E_c by the index theory [38, Chapter 4], we obtain the existence of small limit cycles of system (1.1) when $d_c > 0$, $-d_c < \alpha < d_c$ and $t_c^* < t_c < 0$ in $\mathcal{G}_1$ as follows.

Lemma 5.2. *Assume that $d_c > 0$ and $-d_c < \alpha < d_c$ in $\mathcal{G}_1$. If $t_c^* < t_c < 0$, then the following two assertions hold.*

(a) *System (1.1) exhibits no small limit cycles when ${t_c}^2 - 4d_c \ge 0$.*
(b) *System (1.1) exhibits at most one small limit cycle that is unstable when ${t_c}^2 - 4d_c < 0$. The small limit cycle lies in $\mathcal{S}_l \cup \Gamma_l \cup \mathcal{S}_c$ if $t_c > t_l d_c/d_l$ or in $\mathcal{S}_c \cup \Gamma_r \cup \mathcal{S}_r$ if $t_c > -t_r\sqrt{d_c/d_r}$.*

Proof. When $d_c > 0$, $-d_c < \alpha < d_c$ and $t_c < 0$ in $\mathcal{G}_1$, it follows from Lemma 4.1 that system (5.1) has two equilibrium points N_l and O, N_l is a saddle, and O is a stable node for ${t_c}^2 - 4d_c \ge 0$ or a stable focus for ${t_c}^2 - 4d_c < 0$. Applying the index theory [38, Chapter 4], we know that limit cycle of system (5.1) must surround O if it exists. Therefore, we study the existence of small limit cycles of system (5.1) by analyzing the dynamical behavior of O. Given ${t_c}^2 - 4d_c \ge 0$, since O is a stable node, system (5.1) has at least one invariant line in $\widetilde{\mathcal{S}}_c$, namely, there is no small limit cycle. Thus we arrive at the desire result (**a**). Given ${t_c}^2 - 4d_c < 0$, we note that small limit cycle of system (5.1) lies in $\widetilde{\mathcal{S}}_l \cup \widetilde{\Gamma}_l \cup \widetilde{\mathcal{S}}_c$ or in $\widetilde{\mathcal{S}}_c \cup \widetilde{\Gamma}_r \cup \widetilde{\mathcal{S}}_r$ if it exists. We discuss it by classification in what follows.

Firstly, we denote the small limit cycle of system (5.1) by Γ_1. The small limit cycle Γ_1 lies in $\widetilde{\mathcal{S}}_l \cup \widetilde{\Gamma}_l \cup \widetilde{\mathcal{S}}_c$, as shown in Figure 13(a). Moreover, A_1, B_1, C_1, D_1, E_1, F_1, G_1, and H_1 are points on Γ_1, the points A_1, G_1 lie on the line $x = 0$, the points B_1, F_1 lie on the left switching line $\widetilde{\Gamma}_l$, the points C_1, E_1 lie on the line $x = t_c(m+1)/t_l - m - 1$, and D_1, H_1 are the intersection points of Γ_1 and the curve $y = F(x)$. We claim that the intersection point of Γ_1 and the negative x-axis lies in the region $\{x \in \mathbb{R} | x_{N_l} < x < x^*\}$, where $x_{N_l} := d_c(m+1)/d_l - m - 1$ is

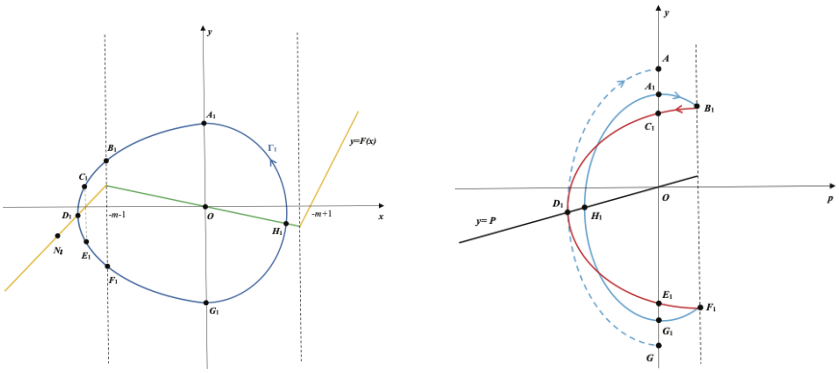

Small limit cycle of Γ_1 of (5.1) Γ_1 lies in the $(p-y)$-plane

FIGURE 13. Small limit cycles of system (5.1) in $\widetilde{\mathcal{S}}_l \cup \widetilde{\Gamma}_l \cup \widetilde{\mathcal{S}}_c$

the abscissa of saddle point N_l and $x^* := t_c(m+1)/t_l - m - 1$ satisfies $F(x^*) = 0$. Otherwise, we have

$$\oint_{\Gamma_1} dE = g(x)F(x) < 0,$$

when the intersection point of Γ_1 and the negative x-axis lies in the region $\{x \in \mathbb{R} | x^* \le x < 0\}$, where

$$E(x,y) := \int_0^x g(s)ds + \frac{y^2}{2}$$

is an energy function along the vector field of system (5.1). This contradicts the fact that $\oint_{\Gamma_1} dE = 0$.

To prove that

$$\oint_{\Gamma_1} F'(x)dt > 0, \tag{5.11}$$

which indicates that the small limit cycle Γ_1 is unstable and hyperbolic [7, Proposition 3.1], we let $p := F(x)$ and denote by $x_1(p)$ and $x_2(p)$ the branches of the inverse of $p(x)$ for $-m-1 < x < -m+1$ and $x_{N_l} < x < -m-1$, respectively. From system (5.1) it follows that

$$\begin{aligned} x_1(p) &= \frac{p}{t_c}, \quad \text{for } t_c(-m+1) < p < -t_c(m+1), \\ x_2(p) &= \frac{p}{t_l} + \frac{(t_c - t_l)(m+1)}{t_l}, \\ \text{for } & -t_c(m+1) + \frac{t_l d_c(m+1)}{d_l} < p < -t_c(m+1). \end{aligned} \tag{5.12}$$

We re-write (5.1) as

$$\begin{aligned} \frac{dy}{dp} &= \frac{\lambda_1(p)}{p-y}, \quad p \in (t_c(-m+1),\ -t_c(m+1)), \\ \frac{dy}{dp} &= \frac{\lambda_2(p)}{p-y}, \quad p \in (-t_c(m+1) + \frac{t_l d_c(m+1)}{d_l},\ -t_c(m+1)), \end{aligned} \tag{5.13}$$

where

$$\lambda_1(p) := \frac{g(x_1)}{F'(x_1)} = \frac{d_c p}{t_c^2}, \quad \lambda_2(p) := \frac{g(x_2)}{F'(x_2)} = \frac{d_l p}{t_l^2} + \frac{(t_c d_l - t_l d_c)(m+1)}{t_l^2}.$$

If $\lambda_1(p) = \lambda_2(p)$, then

$$p_0 := \frac{t_c^2(t_c d_l - t_l d_c)(m+1)}{t_l^2 d_c - t_c^2 d_l}. \tag{5.14}$$

From the sign of $\dot{y}$ of system (5.1), we know that $y_{A_1} > y_{B_1} > y_{C_1} > 0$ and $0 > y_{E_1} > y_{F_1} > y_{G_1}$, where y_{A_1}, y_{B_1}, y_{C_1}, y_{E_1}, y_{F_1} and y_{G_1} are the ordinates of A_1, B_1, C_1, E_1, F_1 and G_1, respectively. It means that $p_0 < 0$ if it exists. Then, $t_c > t_l d_c/d_l$. Denote $x_1^* := x_1(p_0)$ and $x_2^* := x_2(p_0)$. Evidently, we have

$$x_{N_l} < x_2^* < \frac{t_c(m+1)}{t_l} - m - 1 < 0 < x_1^* < -m + 1. \tag{5.15}$$

We claim that p_0 exists and $p_0 < 0$, i.e., Γ_1 intersects with the lines $x = x_1^*$ and $x = x_2^*$. Otherwise, it follows from the comparison theorem [11, Corollary 6.3] that it contradicts the existence of the small limit cycle Γ_1. We denote

$$\Gamma_1 := \cup_{i=1}^4 \Gamma_{1i},$$

where Γ_{11}, Γ_{12}, Γ_{13} and Γ_{14} are the parts of Γ_1 located in the regions $0 \le x < -m+1$, $-m-1 \le x < 0$, $x^* \le x < -m-1$, and $x_{N_l} < x < x^*$, respectively. The small limit cycle Γ_1 in the (p, y)-plane is indicated in Figure 13(b). We have

$$\begin{aligned}
&\int_{\Gamma_{12}} F'(x)dt + \int_{\Gamma_{13}} F'(x)dt \\
&= \int_0^{-t_c(m+1)} \frac{dp}{p - y_1} - \int_0^{-t_c(m+1)} \frac{dp}{p - z_1} - \int_0^{-t_c(m+1)} \frac{dp}{p - y_2} + \int_0^{-t_c(m+1)} \frac{dp}{p - z_2} \\
&= \int_0^{-t_c(m+1)} \frac{(y_1 - y_2)}{(p - y_1)(p - y_2)} + \int_0^{-t_c(m+1)} \frac{(z_2 - z_1)}{(p - z_1)(p - z_2)} > 0,
\end{aligned} \tag{5.16}$$

where y_1 and y_2 represent the orbit segments Γ_{12} and Γ_{13} respectively, which lie above $y = p$, and z_1 and z_2 represent the orbit segments Γ_{12} and Γ_{13} respectively, which lie below $y = p$. We now compare two integral curves Γ_{11} and Γ_{14}. By a change of coordinate transformation $p \to \mu p, y \to \mu y$ with $\mu = y_{D_1}/y_{H_1}$, $\overline{\Gamma}_{11}$ $(\widehat{AD_1G})$ is an orbit segment crossing through D_1, where $p \le 0$, and A and G are points on $\overline{\Gamma}_{11}$ and both lie on the y-axis. The functions $\overline{y}_1$ and $\overline{z}_1$ represent the orbit segments $\overline{\Gamma}_{11}$ respectively, which lie above and below the line $y = p$. Therefore,

$$\int_{\Gamma_{11}} F'(x)dt = \int_{\widehat{G_1H_1A_1}} F'(x)dt = \int_{\widehat{GD_1A}} F'(x)dt = \int_{\overline{\Gamma}_{11}} F'(x)dt. \tag{5.17}$$

Note that $\overline{y}_1(p_{D_1}) = y_2(p_{D_1}) = \overline{z}_1(p_{D_1}) = z_2(p_{D_1})$, $\overline{y}_1(0) > y_2(0)$ and $\overline{z}_1(0) < z_2(0)$. By the uniqueness of zero of the equation $\lambda_1(p) = \lambda_2(p)$, we have $\overline{y}_1(p) >$

$y_2(p)$ and $\overline{z}_1(p) < z_2(p)$ for $p \in (p_{D_1}, 0)$. Then

$$\begin{aligned}
&\int_{\overline{\Gamma}_{11}} F'(x)dt + \int_{\Gamma_{14}} F'(x)dt \\
&= -\int_0^{p_{D_1}} \frac{dp}{p-\overline{y}_1} + \int_0^{p_{D_1}} \frac{dp}{p-\overline{z}_1} + \int_0^{p_{D_1}} \frac{dp}{p-y_2} - \int_0^{p_{D_1}} \frac{dp}{p-z_2} \\
&= \int_0^{p_{D_1}} \frac{(y_2-\overline{y}_1)}{(p-\overline{y}_1)(p-y_2)} + \int_0^{p_{D_1}} \frac{(\overline{z}_1-z_2)}{(p-\overline{z}_1)(p-z_2)} > 0.
\end{aligned} \tag{5.18}$$

So, we see that (5.11) follows from (5.16)-(5.18) immediately when $t_c > t_l d_c/d_l$.

We claim that system (5.1) has at most one small limit cycle in $\widetilde{\mathcal{S}}_l \cup \widetilde{\Gamma}_l \cup \widetilde{\mathcal{S}}_c$. Otherwise, there are at least two small limit cycles denoted by Γ_{s1} and Γ_{s2} in $\widetilde{\mathcal{S}}_l \cup \widetilde{\Gamma}_l \cup \widetilde{\mathcal{S}}_c$, where Γ_{s1} and Γ_{s2} are adjacent to each other. From (5.11) it follows that

$$\oint_{\Gamma_{s1}} F'(x)dt > 0, \quad \oint_{\Gamma_{s2}} F'(x)dt > 0.$$

In other words, Γ_{s1} and Γ_{s2} are all unstable [7, Proposisition 3.1]. According to the Poincaré-Bendixson Theorem, there exists a stable limit cycle between Γ_{s1} and Γ_{s2}, which contradicts (5.11).

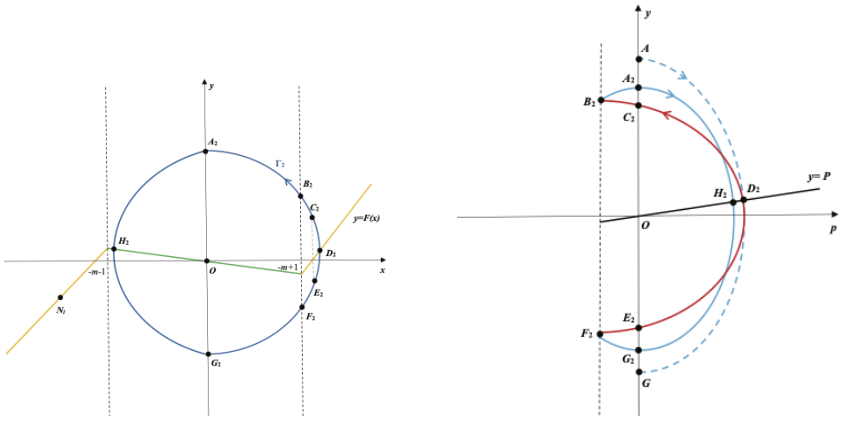

Small limit cycle Γ_2 of (5.1) Γ_2 lies in the (p, y)-plane

FIGURE 14. Small limit cycles of system (5.1) in $\widetilde{\mathcal{S}}_c \cup \widetilde{\Gamma}_r \cup \widetilde{\mathcal{S}}_r$

Secondly, we take the small limit cycle of system (5.1) that lies in $\widetilde{\mathcal{S}}_c \cup \widetilde{\Gamma}_r \cup \widetilde{\mathcal{S}}_r$, denoted by Γ_2, as shown in Figure 14(a). Note that $A_2, B_2, C_2, D_2, E_2, F_2, G_2, H_2$ are points on Γ_2, the points A_2, G_2 lie on the line $x = 0$, the points B_2, F_2 lie on the right switching line $\widetilde{\Gamma}_r$, the points C_2, E_2 lie on the line $x = t_c(m-1)/t_r - m + 1$, and D_2, H_2 are the intersection points of Γ_2 and the curve $y = F(x)$. Set $p := F(x)$. Then, the limit cycle Γ_2 in the (p, y)-plane is displayed in Figure 14(b). Similarly, we can prove that

$$\oint_{\Gamma_2} F'(x)dt > 0, \tag{5.19}$$

if $t_c > -t_r\sqrt{d_c/d_r}$, and system (5.1) has at most one small limit cycle in $\widetilde{\mathcal{S}}_c \cup \widetilde{\Gamma}_r \cup \widetilde{\mathcal{S}}_r$. In addition, it is impossible for a limit cycle to lie in $\widetilde{\mathcal{S}}_c \cup \widetilde{\Gamma}_r \cup \widetilde{\mathcal{S}}_r$, when a limit cycle lies in $\widetilde{\mathcal{S}}_l \cup \widetilde{\Gamma}_l \cup \widetilde{\mathcal{S}}_c$. The proof is complete. □

Lemma 5.3. *Assume that $d_c > 0$ and $-d_c < \alpha < d_c$ in $\mathcal{G}_1$. If $t_c^* < t_c < 0$, then the following two assertions hold:*

(a) *System (1.1) exhibits at most one limit cycle when ${t_c}^2 - 4d_c \geq 0$. Moreover, the limit cycle is large if it exists.*

(b) *System (1.1) exhibits at most two limit cycles when ${t_c}^2 - 4d_c < 0$. Moreover, it consists of a small limit cycle and a large limit cycle if they exist.*

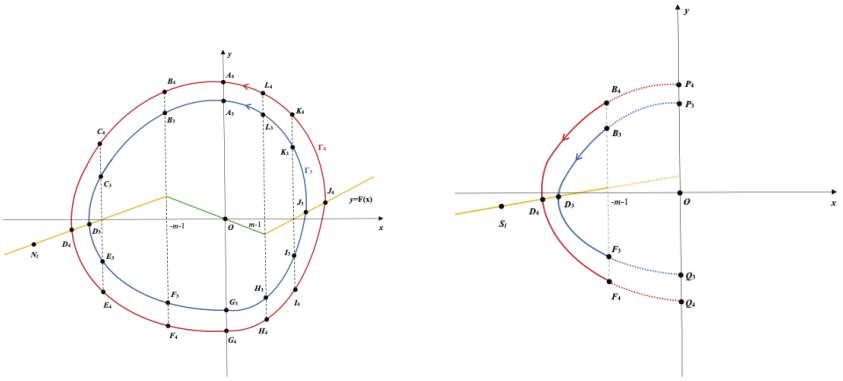

(a) (b)

FIGURE 15. (a) Two large limit cycles Γ_3 and Γ_4 of system (5.1); (b) Orbit segments $\widehat{B_3D_3F_3}$ and $\widehat{B_4D_4F_4}$.

Proof. It follows from Lemma 4.1 that system (5.1) has two equilibrium points N_l and O as $d_c > 0$, $-d_c < \alpha < d_c$ and $t_c < 0$ in $\mathcal{G}_1$. A straightforward calculation shows that N_l is a saddle, and O is a stable node for ${t_c}^2 - 4d_c \geq 0$ or a stable focus for ${t_c}^2 - 4d_c < 0$. By the index theory [38, Chapter 4], we know that the limit cycle of system (5.1) only surrounds O if it exists. Based on Lemma 5.2, we continue to investigate the existence of large limit cycles of system (5.1). We take any two large limit cycles of system (5.1) denoted by Γ_3 and Γ_4 that are adjacent to each other, as indicated in Figure 15(a). The large limit cycle Γ_3 is the innermost one, $A_i, B_i, C_i, D_i, E_i, F_i, G_i, H_i, I_i, J_i, K_i, L_i$ are points on Γ_i, the abscissa of B_i, F_i is $-m-1$, the abscissa of C_i, E_i is $t_c(m+1)/t_l - m - 1$, the abscissa of H_i, L_i is $m-1$, and the abscissa of I_i, K_i is $t_c(m-1)/t_r - m + 1$ for $i = 3, 4$. Following [9], we now prove that

$$\oint_{\Gamma_3} F'(x)dt < \oint_{\Gamma_4} F'(x)dt. \tag{5.20}$$

Let $y_3(x)$ and $y_4(x)$ represent the orbit segments $\widehat{L_3A_3B_3}$ and $\widehat{L_4A_4B_4}$, respectively. It follows that

$$\begin{aligned}
&\int_{\widehat{L_3A_3B_3}} F'(x)dt - \int_{\widehat{L_4A_4B_4}} F'(x)dt \\
&= \int_{m-1}^{-m-1} \frac{F'(x)}{F(x) - y_3(x)}dx - \int_{m-1}^{-m-1} \frac{F'(x)}{F(x) - y_4(x)}dx \\
&= \int_{m-1}^{-m-1} \frac{F'(x)(y_3(x) - y_4(x))}{(F(x) - y_3(x))(F(x) - y_4(x))}dx < 0,
\end{aligned} \tag{5.21}$$

because of $F'(x) = t_c < 0$, $y_3(x) - y_4(x) < 0$ and $(F(x) - y_3(x))(F(x) - y_4(x)) > 0$ for $x \in (-m-1, m-1)$. Similarly, we can obtain

$$\int_{\widehat{F_3G_3H_3}} F'(x)dt - \int_{\widehat{F_4G_4H_4}} F'(x)dt < 0. \tag{5.22}$$

Consider a system without the switching lines

$$\begin{aligned} \frac{dx}{dt} &= t_l(x+m+1) + t_c(-m-1) - y := \overline{F}(x) - y, \\ \frac{dy}{dt} &= d_l(x+m+1) + d_c(-m-1) := \overline{g}(x), \end{aligned} \tag{5.23}$$

in the region $\{(x,y) \in \mathbb{R}^2 : x \le 0\}$. Since systems (5.1) and (5.23) are the same in the region $\{(x,y) \in \mathbb{R}^2 : x \le -m-1\}$, we turn to study two orbit segments $\widehat{B_3D_3F_3}$ and $\widehat{B_4D_4F_4}$ in system (5.23) for simplicity, as displayed in Figure 15(b). We denote by P_i and Q_i the first intersection point of the orbit segment $\widehat{B_iD_iF_i}$ and y-axis for $i = 3, 4$ respectively, as t decreases and increases. To show that

$$\int_{\widehat{P_3D_3Q_3}} \overline{F}'(x)dt = \int_{\widehat{P_4D_4Q_4}} \overline{F}'(x)dt, \tag{5.24}$$

using $p = \overline{F}(x)$ we re-write system (5.23) as

$$\frac{dy}{dp} = \frac{d_l p + t_c d_l(m+1) - t_l d_c(m+1)}{t_l^2(p-y)}. \tag{5.25}$$

By making a change of coordinate transformation $p \to \mu p$, $y \to \mu y$ with $\mu = y_{D_4}/y_{D_3}$, $\widehat{P_3D_3Q_3}$ becomes an orbit segment crossing through D_4 of system (5.25). Therefore, we obtain (5.24). A routine computation gives rise to

$$\begin{aligned} &\int_{\widehat{P_3B_3}} \overline{F}'(x)dt - \int_{\widehat{P_4B_4}} \overline{F}'(x)dt \\ &= \int_0^{-m-1} \frac{\overline{F}'(x)}{\overline{F}(x) - \overline{y_3}(x)}dx - \int_0^{-m-1} \frac{\overline{F}'(x)}{\overline{F}(x) - \overline{y_4}(x)}dx \\ &= \int_0^{-m-1} \frac{\overline{F}'(x)\left(\overline{y_3}(x) - \overline{y_4}(x)\right)}{\left(\overline{F}(x) - \overline{y_3}(x)\right)\left(\overline{F}(x) - \overline{y_4}(x)\right)}dx > 0, \end{aligned} \tag{5.26}$$

where $\overline{y_3}(x)$ and $\overline{y_4}(x)$ represent the orbit segments $\widehat{P_3B_3}$ and $\widehat{P_4B_4}$ respectively. Combining (5.24) and (5.26) yields

$$\int_{\widehat{B_3D_3F_3}} F'(x)dt - \int_{\widehat{B_4D_4F_4}} F'(x)dt < 0. \tag{5.27}$$

Similarly, we have

$$\int_{\widehat{H_3J_3L_3}} F'(x)dt - \int_{\widehat{H_4J_4L_4}} F'(x)dt < 0. \tag{5.28}$$

Hence, inequality (5.20) follows from (5.21)-(5.22) and (5.27)-(5.28) immediately.

(a) When ${t_c}^2 - 4d_c \ge 0$, we suppose that system (5.1) has at least two large limit cycles denoted by Γ_{l1} and Γ_{l2}, where Γ_{l1} and Γ_{l2} are adjacent to each other and Γ_{l1} lies in the interior of Γ_{l2}. By Lemma 5.2, system (5.1) has no small limit cycles

when ${t_c}^2 - 4d_c \geq 0$. It means that Γ_{l1} is internally unstable. From (5.20) it follows that

$$\oint_{\Gamma_{l1}} F'(x)dt = 0, \quad \oint_{\Gamma_{l2}} F'(x)dt > 0.$$

In other words, Γ_{l1} is semi-stable (internally unstable and externally stable) and Γ_{l2} is unstable [7, Proposisition 3.1]. When $a_1 < a_2$, we obtain

$$\begin{vmatrix} F(x)|_{t_c=a_1} - y & g(x) \\ F(x)|_{t_c=a_2} - y & g(x) \end{vmatrix} (-m+1)g(x)(a_1 - a_2) \leq 0, \quad x > -m+1,$$
$$xg(x)(a_1 - a_2) < 0, \quad -m-1 \leq x \leq -m+1,$$
$$-(m+1)g(x)(a_1 - a_2) < 0, \quad \frac{d_c(m+1)}{d_l} - m - 1 < x < -m-1,$$

where the equality sign obviously cannot hold for the entire closed orbit of system (5.1). Hence, the vector field $(F(x) - y, g(x))$ of system (5.1) is rotated about t_c by [22, Definition 1.6] or [38, Definition 3.3]. It follows from [38, Theorem 3.4] that the semi-stable limit cycle Γ_{l1} will bifurcate into at least one unstable limit cycle and one stable limit cycle when t_c varies in the suitable direction. This contradicts (5.20). Thus, we infer that system (5.1) has at most one limit cycle when ${t_c}^2 - 4d_c \geq 0$. Moreover, the limit cycle is large if it exists.

(b) When ${t_c}^2 - 4d_c < 0$, we know that system (5.1) has at most one small limit cycle by Lemma 5.2 and the small limit cycle is unstable if it exists. If system (5.1) has no small limit cycles for ${t_c}^2 - 4d_c < 0$, the proof of which there is at most one large limit cycle is the same as the proof of Part (a), Therefore, we omit it.

We denote the small limit cycle of system (5.1) by γ_s. We only need to study the existence of large limit cycles when γ_s exists. Assume that system (5.1) exhibits at least three large limit cycles when γ_s exists, denoted by γ_{l1}, γ_{l2} and γ_{l3}, where γ_{l1} lies in the interior of γ_{l2} and γ_{l2} lies in the interior of γ_{l3}. Since the small limit cycle γ_s is unstable, by (5.20) we have

$$\oint_{\gamma_{l1}} F'(x)dt < 0, \quad \oint_{\gamma_{l2}} F'(x)dt = 0, \quad \oint_{\gamma_{l3}} F'(x)dt > 0.$$

In other words, γ_{l1} is stable, γ_{l2} is semi-stable (internally unstable and externally stable) and γ_{l3} is unstable [7, Proposisition 3.1]. When t_c varies in the suitable direction, it follows from [38, Theorem 3.4] that the semi-stable limit cycle γ_{l2} will bifurcate into at least one unstable limit cycle and one stable limit cycle. This contradicts (5.20).

We then suppose that system (5.1) has two large limit cycles when γ_s exists, denoted by γ_1 and γ_2, where γ_1 lies in the interior of γ_2. Since the small limit cycle γ_s is unstable, we find that γ_1 is internally stable. If γ_1 or γ_2 is semi-stable, then there are three large limit cycles by [38, Theorem 3.4] when t_c varies in the suitable direction. This is a contradiction. Therefore, we infer that γ_1 is stable and γ_2 is unstable, i.e.,

$$\oint_{\gamma_1} F'(x)dt < 0, \quad \oint_{\gamma_2} F'(x)dt > 0.$$

According to [38, Theorem 3.3], it follows that the attracting limit cycle of system (5.1) contracts and the repelling limit cycle of system (5.1) expands when t_c decreases. Therefore, γ_s and γ_1 will coincide and become a semi-stable limit cycle

γ (internally unstable and externally stable) when t_c decreases to a certain value. If t_c continues to decrease, then the semi-stable limit cycle γ will disappear by [38, Theorem 3.3] again. It implies that system (5.1) has one limit cycle γ_2 when $t_c \to -\infty$. This contradicts the nonexistence of limit cycles of system (1.1) when $t_c \to -\infty$ (see Lemma 5.1). Therefore, we have arrived at the desired result. □

From Lemma 5.1, we only need to study homoclinic loops of system (1.1) when $d_c > 0$, $-d_c < \alpha < d_c$ and $t_c^* < t_c < 0$ in $\mathcal{G}_1$. It follows from Lemma 4.1 that E_l of system (1.1) is a saddle and E_c of system (1.1) is a stable focus for ${t_c}^2 - 4d_c < 0$ or a stable node for ${t_c}^2 - 4d_c \geq 0$ when $d_c > 0$, $-d_c < \alpha < d_c$ and $t_c^* < t_c < 0$ in $\mathcal{G}_1$. It is notable that t_c^* may be greater than or less than or equal to $-2\sqrt{d_c}$. Therefore, we study homoclinic loops of system (1.1) for two cases $\max\{t_c^*, -2\sqrt{d_c}\} < t_c < 0$ and $t_c^* < t_c \leq -2\sqrt{d_c}$. In the case of $\max\{t_c^*, -2\sqrt{d_c}\} < t_c < 0$, homoclinic loops of system (1.1) may involve two or three linear zones because E_c is a stable focus. In the case of $t_c^* < t_c \leq -2\sqrt{d_c}$, homoclinic loops of system (1.1) only involve three linear zones because E_c is a stable node, so there is invariant line in $\mathcal{S}_c$.

Lemma 5.4. *When $d_c > 0$, $-d_c < \alpha < d_c$ and $\max\{t_c^*, -2\sqrt{d_c}\} < t_c < 0$ in $\mathcal{G}_1$, there is a continuous function $t_c = \phi(\alpha) \in (\max\{t_c^*, -2\sqrt{d_c}\}, 0)$ and a value $\alpha^* \in (-d_c, d_c)$ such that the following three assertions are true.*

(a) *System (1.1) exhibits a unique homoclinic loop involving two linear zones when $t_c = \phi(\alpha)$ for $\alpha < \alpha^*$, and the homoclinic loop is unstable.*
(b) *System (1.1) exhibits a unique homoclinic loop that is tangent to Γ_r when $t_c = \phi(\alpha)$ for $\alpha = \alpha^*$, and the homoclinic loop is unstable.*
(c) *System (1.1) exhibits a unique homoclinic loop involving three linear zones when $t_c = \phi(\alpha)$ for $\alpha > \alpha^*$, and the homoclinic loop unstable.*

Proof. For simplicity, we consider a continuous planar piecewise linear differential system with two zones:

$$\frac{dx}{dt} = F(x) - y, \quad \frac{dy}{dt} = g(x), \tag{5.29}$$

where

$$F(x) = \begin{cases} t_c x, & \text{if } x \geq -m-1, \\ t_l(x+m+1) + t_c(-m-1), & \text{if } x < -m-1, \end{cases}$$
$$g(x) = \begin{cases} d_c x, & \text{if } x \geq -m-1, \\ d_l(x+m+1) + d_c(-m-1), & \text{if } x < -m-1. \end{cases}$$

Note that systems (5.1) and (5.29) are the same in the region $\{(x,y) \in \mathbb{R}^2 : x \leq -m+1\}$. Therefore, we consider the existence, uniqueness and stability of homoclinic loops of system (5.29) in the region $\{(x,y) \in \mathbb{R}^2 : x \leq -m+1\}$. System (5.29) has two equilibrium points N_l and O when $d_c > 0$ and $-d_c < \alpha < d_c$ in $\mathcal{G}_1$, where N_l is a saddle and O is a stable focus if $-2\sqrt{d_c} < t_c < 0$.

To prove the existence of homoclinic loops of system (5.29), we denote the eigenvalues of the corresponding Jacobian matrix at the saddle point N_1 by λ_1 and λ_2, where

$$\lambda_1 := \frac{t_l - \sqrt{t_l^2 - 4d_l}}{2}, \quad \lambda_2 := \frac{t_l + \sqrt{t_l^2 - 4d_l}}{2}, \quad \lambda_1 + \lambda_2 = t_l, \quad \lambda_1\lambda_2 = d_l. \tag{5.30}$$

We then obtain that the λ_1-eigenvector and λ_2-eigenvector of

$$J_{N_1} := \begin{bmatrix} t_1 & -1 \\ d_1 & 0 \end{bmatrix} = \begin{bmatrix} \lambda_1+\lambda_2 & -1 \\ \lambda_1\lambda_2 & 0 \end{bmatrix}$$

are $(1,\lambda_2)^T$ and $(1,\lambda_1)^T$ respectively. Denote the intersection point of the linear λ_1 (resp. λ_2) invariant manifold that emanates from the saddle point N_l along the eigenvector $(1,\lambda_2)^T$ (resp. $(1,\lambda_1)^T$) with the line $x=-m-1$ by $E:(-m-1,y_1)$ (resp. $A:(-m-1,z_1)$). That is,

$$\begin{bmatrix} \frac{\alpha+d_c}{\lambda_1\lambda_2} - m - 1 \\ \frac{(\lambda_1+\lambda_2)(\alpha+d_c)}{\lambda_1\lambda_2} - t_c(m+1) \end{bmatrix} + \rho \begin{bmatrix} 1 \\ \lambda_2 \end{bmatrix} = \begin{bmatrix} -m-1 \\ y_1 \end{bmatrix} \tag{5.31}$$

and

$$\begin{bmatrix} \frac{\alpha+d_c}{\lambda_1\lambda_2} - m - 1 \\ \frac{(\lambda_1+\lambda_2)(\alpha+d_c)}{\lambda_1\lambda_2} - t_c(m+1) \end{bmatrix} + \rho \begin{bmatrix} 1 \\ \lambda_2 \end{bmatrix} = \begin{bmatrix} -m-1 \\ z_1 \end{bmatrix}, \tag{5.32}$$

where $\rho = -\frac{\alpha+d_c}{\lambda_1\lambda_2}$. It follows from (5.31) and (5.32) that

$$z_1 = \frac{\alpha+d_c}{\lambda_1} - t_c(m+1), \quad y_1 = \frac{\alpha+d_c}{\lambda_2} - t_c(m+1).$$

We denote the eigenvalues of the stable focus point O of system (5.29) by $\sigma \pm \omega i$, where

$$\sigma = \frac{t_c}{2}, \quad \omega = \frac{\sqrt{4d_c - t_c^2}}{2}, \quad \sigma^2+\omega^2 = d_c.$$

Set $\eta := \frac{\sigma}{\omega} = \frac{t_c}{\sqrt{4d_c-t_c^2}}$. Let (x_b,y_b) be the initial point of an orbit of system (5.29) with $x \geq -m-1$ and (x_f,y_f) be the terminal point after a time t. By the phase angle $\theta = -\omega t$, we have

$$\begin{pmatrix} x_f \\ y_f \end{pmatrix} = e^{-\eta\theta} \begin{pmatrix} -\frac{1}{d_c}\cos\theta + \frac{\eta}{d_c}\sin\theta & \frac{1}{d_c}\sin\theta + \frac{\eta}{d_c}\cos\theta \\ \frac{\sin\theta}{\omega} & \frac{\cos\theta}{\omega} \end{pmatrix} \begin{pmatrix} x_b \\ y_b \end{pmatrix}. \tag{5.33}$$

When $E:(-m-1,y_1)$ is the beginning point for an orbit, we want to know the point $D:(0,y_2)$ along the orbit as t decreases. From (5.33) it follows that

$$\begin{pmatrix} 0 \\ y_2 \end{pmatrix} = e^{-\eta\theta} \begin{pmatrix} -\frac{1}{d_c}\cos\theta + \frac{\eta}{d_c}\sin\theta & \frac{1}{d_c}\sin\theta + \frac{\eta}{d_c}\cos\theta \\ \frac{\sin\theta}{\omega} & \frac{\cos\theta}{\omega} \end{pmatrix} \begin{pmatrix} -m-1 \\ y_1 \end{pmatrix} \tag{5.34}$$

From the first coordinate of (5.34) we obtain

$$\tan\theta = \frac{\eta y_1 + m + 1}{-y_1 + \eta m + \eta},$$

$$\sin\theta = \sqrt{\frac{(\eta y_1 + m + 1)^2}{(\eta^2+1)[y_1^2 + (m+1)^2]}},$$

$$\cos\theta = \sqrt{\frac{(-y_1 + \eta m + \eta)^2}{(\eta^2+1)[y_1^2 + (m+1)^2]}}.$$

From the second coordinate of (5.34) we derive

$$y_2 = e^{-\eta\theta}\Big(-\frac{m+1}{\omega}\sqrt{\frac{(\eta y_1 + m + 1)^2}{(\eta^2+1)[y_1^2 + (m+1)^2]}} + \frac{y_1}{\omega}\sqrt{\frac{(-y_1 + \eta m + \eta)^2}{(\eta^2+1)[y_1^2 + (m+1)^2]}}\Big).$$

When $A:(-m-1,z_1)$ is the beginning point for an orbit, we want to know the point $B\,(0,z_2)$ along the orbit as t increases. From (5.33) it follows that

$$\begin{pmatrix}0\\ z_2\end{pmatrix}=e^{-\eta\theta}\begin{pmatrix}-\frac{1}{d_c}\cos\theta+\frac{\eta}{d_c}\sin\theta & \frac{1}{d_c}\sin\theta+\frac{\eta}{d_c}\cos\theta\\ \frac{\sin\theta}{\omega} & \frac{\cos\theta}{\omega}\end{pmatrix}\begin{pmatrix}-m-1\\ z_1\end{pmatrix}.$$

Similarly, we have

$$z_2=e^{-\eta\theta}\Big(\frac{m+1}{\omega}\sqrt{\frac{(\eta z_1+m+1)^2}{(\eta^2+1)[z_1^2+(m+1)^2]}}+\frac{z_1}{\omega}\sqrt{\frac{(-z_1+\eta m+\eta)^2}{(\eta^2+1)[z_1^2+(m+1)^2]}}\Big).$$

We define the Poincaé map $P:(0,z_2)\to(0,z^*)$ for system (5.29) with $x\geq 0$, where z_2 and z^* lie on the same orbit. We have

$$P(z^*)=-e^{-\eta\pi}z_2$$

with

$$\begin{aligned}z^*=-e^{-\eta\pi}e^{-\eta\theta}\Big(&\frac{m+1}{\omega}\sqrt{\frac{(\eta z_1+m+1)^2}{(\eta^2+1)[z_1^2+(m+1)^2]}}\\&+\frac{z_1}{\omega}\sqrt{\frac{(-z_1+\eta m+\eta)^2}{(\eta^2+1)[z_1^2+(m+1)^2]}}\Big).\end{aligned}$$

If $z^*=y_2$, then

$$\begin{aligned}&e^{-\eta\pi}\Big(\frac{m+1}{\omega}\sqrt{\frac{(\eta z_1+m+1)^2}{(\eta^2+1)[z_1^2+(m+1)^2]}}+\frac{z_1}{\omega}\sqrt{\frac{(-z_1+\eta m+\eta)^2}{(\eta^2+1)[z_1^2+(m+1)^2]}}\Big)\\&=-\frac{m+1}{\omega}\sqrt{\frac{(\eta y_1+m+1)^2}{(\eta^2+1)[y_1^2+(m+1)^2]}}+\frac{y_1}{\omega}\sqrt{\frac{(-y_1+\eta m+\eta)^2}{(\eta^2+1)[y_1^2+(m+1)^2]}}.\end{aligned}\tag{5.35}$$

Thus, system (5.29) has a homoclinic loop.

Note that system (5.29) is piecewise linear, Lipschitz continuous in $\mathbb{R}^2$ and analytic in $\mathbb{R}^2\backslash\{(x,y)\in\mathbb{R}^2:x=-m-1\}$. By [12, Theorem 3.3] and $\lambda_++\lambda_-=t_l>0$, the homoclinic loop of system (5.29) is unstable.

As $a_1<a_2$, it follows that

$$\begin{aligned}&\begin{vmatrix}F(x)|_{t_c=a_1}-y & g(x)\\ F(x)|_{t_c=a_2}-y & g(x)\end{vmatrix}\\&=\begin{cases}xg(x)(a_1-a_2)\leq 0 & \text{for } x\geq -m-1,\\ -(m+1)g(x)(a_1-a_2)<0, & \text{for } \frac{d_c(m+1)}{d_l}-m-1<x<-m-1,\end{cases}\end{aligned}$$

where the equality sign cannot hold for the entire closed orbit of system (5.29). Hence, the vector field $(F(x)-y,g(x))$ of system (5.29) is rotated about t_c [22, Definition 1.6] or [38, Definition 3.3]. From [21, Lemma 5.3], it follows that the manifolds W_N^+ and W_N^- of the saddle point N_l of system (5.29) rotate clockwise when t_c increases and t_l,d_c,d_l,α are fixed, where W_N^+ is the stable manifold of the right-hand side of N_l and W_N^- is the unstable manifold of the right-hand side of N_l. This indicates that system (5.29) exhibits at most one homoclinic loop.

To prove that the amplitude of the homoclinic loop of system (5.29) increases as α increases, we use the transformation

$$x\to x-m-1,\quad y\to y-t_c(m+1),$$

to change (5.29) to

$$\frac{dx}{dt} = \widehat{F}(x) - y, \quad \frac{dy}{dt} = \widehat{g}(x), \tag{5.36}$$

where

$$\widehat{F}(x) = \begin{cases} t_c x, & \text{if } x \geq 0, \\ t_l x, & \text{if } x < 0, \end{cases}$$

$$\widehat{g}(x) = \begin{cases} d_c(x - m - 1), & \text{if } x \geq 0, \\ d_l x + d_c(-m - 1), & \text{if } x < 0. \end{cases}$$

By the scaling transformation

$$x \to d_c(m+1)x, \quad y \to d_c(m+1)y, \tag{5.37}$$

system (5.36) reduces to

$$\frac{dx}{dt} = F(x) - y, \quad \frac{dy}{dt} = g(x), \tag{5.38}$$

where

$$F(x) = \begin{cases} t_c x, & \text{if } x \geq 0, \\ t_l x, & \text{if } x < 0, \end{cases}$$

$$g(x) = \begin{cases} d_c x - 1, & \text{if } x \geq 0, \\ d_l x - 1, & \text{if } x < 0. \end{cases}$$

Evidently, system (5.38) is independent on α, so the homoclinic loop of system (5.38) is independent on α as well. Since systems (5.29) and (5.38) are topologically equivalent, it follows from the scaling transformation (5.37) that the amplitude of the homoclinic loop of system (5.29) is increasing as α increases.

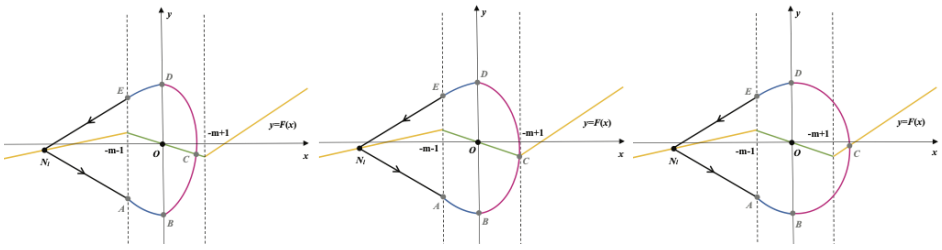

$t_c = \phi(\alpha)$ for $\alpha < \alpha^*$ $t_c = \phi(\alpha)$ for $\alpha = \alpha^*$ $t_c = \phi(\alpha)$ for $\alpha > \alpha^*$

FIGURE 16. Homoclinic loops of system (5.1)

We denote by $C{:}(x_c, t_c x_c)$ the right intersection point of the homoclinic loop of system (5.29) with the curve $y = F(x)$ If the point C is on the line $x = -m + 1$, then

$$\frac{t_c^2}{2} - d_c = \frac{d_c t_c(-m+1)\omega}{e^{-\eta\pi} z_2}. \tag{5.39}$$

By solving equations (5.35) and (5.39) and using the implicit function theorem, there exists a continuous function $t_c = \phi(\alpha)$ and a value α^* such that system (5.29) has one homoclinic loop that is tangent to the line $x = -m+1$ when $t_c = \phi(\alpha)$ for $\alpha = \alpha^*$, where $\phi(\alpha) \in (\max\{t_c^*, -2\sqrt{d_c}\}, 0)$ and $\alpha^* \in (-d_c, d_c)$. Since systems (5.1)

and (5.29) are the same in the region $\{(x,y)\in\mathbb{R}^2 : x\le -m+1\}$, we can plot the homoclinic loop for system (5.1) which is unstable, see Figure 16(b). In view of the monotonicity of the amplitude of the homoclinic loop of system (5.1) in the region $\{(x,y)\in\mathbb{R}^2 : x\le -m+1\}$, we are led to the conclusion that the homoclinic loop of system (5.1) involves two linear zones when $t_c=\phi(\alpha)$ for $\alpha<\alpha^*$, as shown in Figure 16(a). In addition, given the existence, uniqueness and continuity of system (5.1) under the initial conditions, we can obtain that the homoclinic loop of system (5.1) involves three linear zones when $t_c=\phi(\alpha)$ for $\alpha>\alpha^*$, as shown in Figure 16(c). The proof of Lemma 5.4 is completed. □

The following lemma is concerning the existence, uniqueness and stability of homoclinic loops of system (1.1) when $d_c>0$, $-d_c<\alpha<d_c$ and $t_c^*<t_c\le -2\sqrt{d_c}$ in $\mathcal{G}_1$. The proof is closely similar to the one of Lemma 5.4, so we omit it.

Lemma 5.5. *If $d_c>0$, $-d_c<\alpha<d_c$ and $t_c^*<t_c\le -2\sqrt{d_c}$ in $\mathcal{G}_1$, then system (1.1) exhibits a unique homoclinic loop involving three linear zones that is unstable when $t_c=\phi(\alpha)$ for $\alpha>\alpha^*$, where $t_c=\phi(\alpha)\in(t_c^*,-2\sqrt{d_c}]$ is a continuous function and $\alpha^*\in(-d_c,d_c)$ is a constant.*

For the uniqueness of limit cycle of system (1.1) with $d_c>0$ and $-d_c<\alpha<d_c$, we have the following lemma.

Lemma 5.6. *If $d_c>0$, $-d_c<\alpha<d_c$ and $\max\{t_c^*,-2\sqrt{d_c}\}<t_c<0$ in $\mathcal{G}_1$, then there is a continuous function $t_c=\phi(\alpha)\in(\max\{t_c^*,-2\sqrt{d_c}\},0)$ such that (a) system (1.1) exhibits no limit cycles when $t_c\in(\max\{t_c^*,-2\sqrt{d_c}\},\phi(\alpha)]$; and (b) system (1.1) exhibits a unique limit cycle that is unstable when $t_c\in(\phi(\alpha),0)$.*

Proof. When $d_c>0$, $-d_c<\alpha<d_c$ and $\max\{t_c^*,-2\sqrt{d_c}\}<t_c<0$ in $\mathcal{G}_1$, system (1.1) has two equilibrium points E_l and E_c by Lemma 4.1, where E_l is a saddle and E_c is a stable focus. Denote by $W_{E_1}^+$ and $W_{E_l}^-$ the stable and unstable manifolds of the right-hand side of E_l of system (1.1), respectively. According to Lemma 5.4, system (1.1) exhibits a unique homoclinic loop that is unstable when $t_c=\phi(\alpha)\in(\max\{t_c^*,-2\sqrt{d_c}\},0)$, see Figure 17(b). However, the unstable homoclinic loop breaks when $t_c=\phi(\alpha)\pm\varepsilon$, even $\varepsilon>0$ is sufficiently small. According to [21, Lemma 5.3], the manifolds $W_{E_l}^+$ and $W_{E_l}^-$ rotate clockwise when t_c increases and $t_r,t_l,d_r,d_c,d_l,\alpha$ are fixed. When $t_c=\phi(\alpha)-\varepsilon$ and $t_c=\phi(\alpha)+\varepsilon$, the relative locations of the manifolds $W_{E_l}^+$ and $W_{E_l}^-$ are depicted in Figure 17(a) and (c), respectively. By Lemma 5.4 again, we know that the unstable homoclinic loop involves two or three linear zones depending on α and α^*, where $\alpha^*\in(-d_c,d_c)$. It implies that we need to consider the nonexistence of limit cycles of system (1.1) in the interior of the unstable homoclinic loop by two cases $\alpha\le\alpha^*$ and $\alpha>\alpha^*$.

FIGURE 17. Homoclinic loop bifurcation of system (1.1)

For $\alpha \le \alpha^*$, from Lemma 5.4 we know that the unstable homoclinic loop of system (1.1) involves two linear zones when $t_c = \phi(\alpha)$ for $\alpha \le \alpha^*$, and the unstable homoclinic loop is tangent to Γ_r when $t_c = \phi(\alpha)$ for $\alpha = \alpha^*$. Now we claim that there is no limit cycle in the interior of the unstable homoclinic loop. Suppose that there exists a small limit cycle because system (1.1) has at most one small limit cycle from Lemma 5.2. Since E_c is a stable focus and the homoclinic loop is unstable, the small limit cycle is semi-stable by the Poincaré-Bendixson theorem. This contradicts the fact that the small limit cycle of system (1.1) is unstable by Lemma 5.2 if it exists. Therefore, system (1.1) exhibits no limit cycles when $t_c = \phi(\alpha)$ for $\alpha \le \alpha^*$.

For $\alpha > \alpha^*$, it follows from Lemma 5.4 that the unstable homoclinic loop involves three linear zones when $t_c = \phi(\alpha)$ for $\alpha > \alpha^*$. We claim that there is no limit cycle in the interior of the unstable homoclinic loop. Otherwise, there exist two limit cycles because system (1.1) has at most two limit cycles from Lemma 5.3. Since E_c is a stable focus and the homoclinic loop is unstable, we infer that the two limit cycles consist of an unstable limit cycle and a stable limit cycle, where the unstable limit cycle lies in the interior of the stable limit cycle. When $t_c = \phi(\alpha) + \varepsilon$, the relative locations of the manifolds $W^+_{E_l}$ and $W^-_{E_l}$ are shown in Figure 17(c). However, by the Poincaré-Bendixson theorem, there exist three limit cycles when $t_c \in (\phi(\alpha), \phi(\alpha) + \varepsilon)$, which contradicts the fact that system (1.1) has at most two limit cycles according to Lemma 5.3. Therefore, system (1.1) exhibits no limit cycles when $t_c = \phi(\alpha)$ for $\alpha > \alpha^*$. □

By an analogous argument, we can obtain the following result.

Lemma 5.7. *If $d_c > 0$, $-d_c < \alpha < d_c$ and $t_c^* < t_c \le -2\sqrt{d_c}$ in $\mathcal{G}_1$, then there is a continuous function $t_c = \phi(\alpha) \in (t_c^*, -2\sqrt{d_c}]$ such that (a) system (1.1) exhibits no limit cycles when $\phi(\alpha) \in (t_c^*, \phi(\alpha)]$; and (b) system (1.1) exhibits a unique limit cycle that is unstable when $t_c \in (\phi(\alpha), -2\sqrt{d_c}]$.*

5.2. **Limit cycles and homoclinic loops for $\alpha = d_c > 0$ in $\mathcal{G}_1$.** It follows from Lemma 4.1 that system (1.1) exhibits two equilibrium points E_l and E_{cr} when $\alpha = d_c > 0$ in $\mathcal{G}_1$, where E_l lies in $\mathcal{S}_l$ and E_{cr} lies on Γ_r. Since E_l is a saddle, it follows that limit cycles of system (1.1) must only surround E_{cr} by the index theory of [38, Chapter 4] and homoclinic loops of system (1.1) must involve three linear zones by the location of E_{cr}. Note that the condition $t_r^2 - 4d_r < 0$ (resp. $= 0$ or > 0) means that the dynamic of right linear zone of system (1.1) is a focus (resp. improper node or bidirectional node) by Lemma 4.1. Hence, there is at least one invariant line in $\mathcal{S}_r$ when $t_r^2 - 4d_r \ge 0$. This implies that system (1.1) has no limit cycles and homoclinic loops when $\alpha = d_c > 0$ and $t_r^2 - 4d_r \ge 0$. In other words, we only need to investigate limit cycles and homoclinic loops of system (1.1) when $\alpha = d_c > 0$ and $t_r^2 - 4d_r < 0$.

With the translation transformation $x \to x + 1, \quad y \to y + t_c$, system (1.1) becomes

$$\frac{dx}{dt} = \widehat{F}(x) - y, \quad \frac{dy}{dt} = \widehat{g}(x), \tag{5.40}$$

where

$$\widehat{F}(x) = \begin{cases} t_r x, & \text{if } x > 0, \\ t_c x, & \text{if } -2 \le x \le 0, \\ t_l(x+2) - 2t_c, & \text{if } x < -2, \end{cases}$$

$$\widehat{g}(x)=\begin{cases} d_r x, & \text{if } x>0,\\ d_c x, & \text{if } -2\le x\le 0,\\ d_l(x+2)-2d_c, & \text{if } x<-2. \end{cases}$$

That is, E_{cr} of system (1.1) is moved to $O_1(0,0)$ of system (5.40) and E_l of system (1.1) is moved to $M_l(2d_c/d_l-2,-2t_c+2t_l d_c/d_l)$ of system (5.40). The plane $\mathbb{R}^2$ is divided into three open linear zones

$$\widehat{\mathcal{S}}_l=\{(x,y)\in\mathbb{R}^2: x<-2\},$$
$$\widehat{\mathcal{S}}_c=\{(x,y)\in\mathbb{R}^2: -2<x<0\},$$
$$\widehat{\mathcal{S}}_r=\{(x,y)\in\mathbb{R}^2: x>0\}$$

by two straight lines $\widehat{\Gamma}_l=\{(x,y)\in\mathbb{R}^2: x=-2\}$ and $\widehat{\Gamma}_r=\{(x,y)\in\mathbb{R}^2: x=0\}$. For the sake of convenience, for system (5.40) we still use F and g to represent $\widehat{F}$ and $\widehat{g}$, respectively. Clearly, system (5.40) is topologically equivalent to system (1.1), so for the existence of limit cycles and homoclinic loops of system (1.1) we may start by analyzing system (5.40).

Lemma 5.8. *If $\alpha=d_c>0$ and $t_r^2-4d_r<0$ in $\mathcal{G}_1$, then system (1.1) exhibits neither limit cycles nor homoclinic loops when $t_c\ge -t_r\sqrt{d_c/d_r}$ or $t_c\le t_c^{**}$, where*

$$t_c^{**}:=-t_r\sqrt{\frac{d_c d_l-d_c^2}{d_r d_l}}+\frac{t_l d_c}{d_l}.$$

Proof. When $\alpha=d_c>0$ and $t_r^2-4d_r<0$ in $\mathcal{G}_1$, it follows from Lemma 4.1 that system (5.40) exhibits two equilibrium points O_1 and M_l, where M_l is a saddle. We define a generalized Filippov transformation

$$z(x):=\int_0^x g(s)ds.$$

Let $x_1(z)$ and $x_2(z)$ be the branches of the inverse of $z(x)$ for $x\ge 0$ and $x<0$, respectively. Let $F_1(z):=F(x_1(z))$ and $F_2(z):=F(x_2(z))$. Denote the abscissa of M_l by $x_{M_l}:=2d_c/d_l-2$. Then we obtain

$$z(x)=\begin{cases} \frac{d_r x^2}{2}\in[0,+\infty), & \text{if } x\ge 0,\\ \frac{d_c x^2}{2}\in(0,2d_c], & \text{if } -2\le x<0,\\ \frac{d_l x^2}{2}+2(d_l-d_c)x+2(d_l-d_c)\in(2d_c,z_{M_l}), & \text{if } x_{M_l}<x<-2, \end{cases}\tag{5.41}$$

where $z_{M_l}:=2d_c-2d_c^2/d_l$. It follows from (5.41) that

$$x_1(z)=\sqrt{\frac{2z}{d_r}},\quad \text{if } z\ge 0,\tag{5.42}$$

$$x_2(z)=\begin{cases} -\sqrt{\frac{2z}{d_c}}, & \text{if } 0<z\le 2d_c,\\ \frac{-2(d_l-d_c)-\sqrt{-4d_c(d_l-d_c)+2d_l z}}{d_l}, & \text{if } 2d_c<z<z_{M_l}. \end{cases}\tag{5.43}$$

From (5.42) and (5.43) we deduce

$$F_1(z)=t_r\sqrt{\frac{2z}{d_r}},\quad \text{if } z\ge 0,$$

$$F_2(z)=\begin{cases}-t_c\sqrt{\frac{2z}{d_c}}, & \text{if } 0<z\le 2d_c,\\ t_l\frac{2d_c-\sqrt{-4d_c(d_l-d_c)+2d_lz}}{d_l}-2t_c, & \text{if } 2d_c<z<z_{M_l}.\end{cases}$$

Then we have

$$F_1(z)-F_2(z)=\sqrt{2z}(\frac{t_r}{\sqrt{d_r}}+\frac{t_c}{\sqrt{d_c}})\begin{cases}>0, & \text{if } t_c>-t_r\sqrt{\frac{d_c}{d_r}},\\ =0, & \text{if } t_c=-t_r\sqrt{\frac{d_c}{d_r}},\\ <0, & \text{if } t_c<-t_r\sqrt{\frac{d_c}{d_r}}\end{cases} \tag{5.44}$$

for $z\in(0,2d_c]$, and

$$F_1'(z)-F_2'(z)=\frac{t_r}{\sqrt{2d_rz}}+\frac{t_l}{\sqrt{-4d_c(d_l-d_c)+2d_lz}}>0 \tag{5.45}$$

for $z\in(2d_c,z_{M_l})$. From (5.44) and (5.45) we find $F_1(z)-F_2(z)\ge 0$ for $z\in(0,z_{M_l})$ if $t_c\ge -t_r\sqrt{d_c/d_r}$. However, when $t_c<-t_r\sqrt{d_c/d_r}$, $F_1(z)-F_2(z)<0$ holds for $z\in(0,z_{M_l})$ if and only if

$$(F_1(z)-F_2(z))|_{z=z_{M_l}}=2t_r\sqrt{\frac{d_cd_l-d_c^2}{d_rd_l}}-\frac{2t_ld_c}{d_l}+2t_c<0. \tag{5.46}$$

Solving (5.46) gives $t_c<t_c^{**}$. It is easy to check $t_c^{**}<-t_r\sqrt{d_c/d_r}$, so $F_1(z)-F_2(z)<0$ holds for $z\in(0,z_{M_l})$ if $t_c<t_c^{**}$. From [27, Section 6], it follows that system (5.40) with $\alpha=d_c>0$ and $t_r^2-4d_r<0$ has neither limit cycles nor homoclinic loops when $t_c\ge -t_r\sqrt{d_c/d_r}$ or $t_c\le t_c^{**}$. □

Note that in Lemma 4.1 it is unclear whether E_{cr} of system (1.1) is a focus or a center when $\alpha=d_c>0$, $t_c<0$, ${t_c}^2-4d_c<0$ and ${t_r}^2-4d_r<0$ in $\mathcal{G}_1$. Now we are ready to answer this question.

Lemma 5.9. *If $\alpha=d_c>0$, $t_c<0$, ${t_c}^2-4d_c<0$ and ${t_r}^2-4d_r<0$ in $\mathcal{G}_1$, then the equilibrium point E_{cr} of system (1.1) is an unstable focus for $t_c>-t_r\sqrt{d_c/d_r}$ or a center for $t_c=-t_r\sqrt{d_c/d_r}$ or a stable focus for $t_c<-t_r\sqrt{d_c/d_r}$.*

Proof. From Lemma 4.1 we know that E_{cr} of system (1.1) lies on Γ_r. When $\alpha=d_c>0$, $t_c<0$, ${t_c}^2-4d_c<0$ and ${t_r}^2-4d_r<0$ in $\mathcal{G}_1$, E_{cr} is a stable focus as seen from $\mathcal{S}_c$, but is an unstable focus as seen from $\mathcal{S}_r$, so is O_1 of system (5.40). This implies condition **(C4)** of Proposition 3.1. In order to study the local dynamics of O_1 of system (5.40), it suffice to consider system (5.40) in the region $\{(x,y)\in\mathbb{R}^2:-2<x<2\}$. This implicitly implies that conditions (C1)–(C3) of Proposition 3.1 hold. According to Proposition 3.1, we know that O_1 of system (5.40) is an unstable focus for $t_c>-t_r\sqrt{d_c/d_r}$ or a stable focus for $t_c<-t_r\sqrt{d_c/d_r}$ or a center for $t_c=-t_r\sqrt{d_c/d_r}$ by (5.44), so is E_{cr} of system (1.1). □

By Lemma 5.8, it suffices to study limit cycles of system (1.1) when $\alpha=d_c>0$, ${t_r}^2-4d_r<0$ and $t_c^{**}<t_c<-t_r\sqrt{d_c/d_r}$ in $\mathcal{G}_1$. It follows from Lemmas 4.1 and 5.9 that E_l of system (1.1) is a saddle and E_{cr} of system (1.1) is a stable focus for ${t_c}^2-4d_c<0$ or node-focus (see Figure 11(g)) for ${t_c}^2-4d_c\ge 0$ when $\alpha=d_c>0$, ${t_r}^2-4d_r<0$ and $t_c^{**}<t_c<-t_r\sqrt{d_c/d_r}$ in $\mathcal{G}_1$. Obviously, we have $-2\sqrt{d_c}<-t_r\sqrt{d_c/d_r}$ because of ${t_r}^2-4d_r<0$. However, t_c^{**} may be greater than or less than or equal to $-2\sqrt{d_c}$. Therefore, we study limit cycles of system

(1.1) by two cases $\max\{t_c^{**}, -2\sqrt{d_c}\} < t_c < -t_r\sqrt{d_c/d_r}$ and $t_c^{**} < t_c \le -2\sqrt{d_c}$, while $\alpha = d_c > 0$ and ${t_r}^2 - 4d_r < 0$ in $\mathcal{G}_1$. In what follows, we discuss the existence of limit cycles of system (1.1) with $\alpha = d_c > 0$ and ${t_r}^2 - 4d_r < 0$ when $\max\{t_c^{**}, -2\sqrt{d_c}\} < t_c < -t_r\sqrt{d_c/d_r}$ (see Lemma 5.10) or $t_c^{**} < t_c \le -2\sqrt{d_c}$ (see Lemma 5.11) in $\mathcal{G}_1$.

Lemma 5.10. *If $\alpha = d_c > 0$ and ${t_r}^2 - 4d_r < 0$ in $\mathcal{G}_1$, and $\max\{t_c^{**}, -2\sqrt{d_c}\} < t_c < -t_r\sqrt{d_c/d_r}$, then system* (1.1) *exhibits at most one limit cycle, which is large if it exists.*

Proof. When $\alpha = d_c > 0$, ${t_r}^2 - 4d_r < 0$ and $\max\{t_c^{**}, -2\sqrt{d_c}\} < t_c < -t_r\sqrt{d_c/d_r}$ in $\mathcal{G}_1$, it follows from Lemmas 4.1 and 5.9 that E_l of system (1.1) is a saddle and E_{cr} of system (1.1) is a stable focus. By the index theory of [38, Chapter 4], we know that limit cycles of system (1.1) must only surround E_{cr}. Since E_{cr} lies on Γ_r and E_l lies in $\mathcal{S}_l$, it follows that limit cycle of system (1.1) may be a small limit cycle or a large limit cycle if it exists. If it is the small limit cycle, it only lies in $\mathcal{S}_c \cup \Gamma_r \cup \mathcal{S}_r$.

We claim that system (1.1) has no small limit cycles when $\alpha = d_c > 0$, ${t_r}^2 - 4d_r < 0$ and $\max\{t_c^{**}, -2\sqrt{d_c}\} < t_c < -t_r\sqrt{d_c/d_r}$ in $\mathcal{G}_1$. Otherwise, there is at least one small limit cycle in $\mathcal{S}_c \cup \Gamma_r \cup \mathcal{S}_r$. Recall that system (1.1) exhibits at most one small limit cycle that lies in $\mathcal{S}_c \cup \Gamma_r \cup \mathcal{S}_r$ only if $t_c > -t_r\sqrt{d_c/d_r}$ by Lemma 5.2 when $d_c > 0$, $-d_c < \alpha < d_c$ and $\max\{t_c^*, -2\sqrt{d_c}\} < t_c < 0$ in $\mathcal{G}_1$. When $d_c > 0$ and $\alpha \to d_c$, we know that t_c^* changes to t_c^{**} and the equilibrium point E_c of system (1.1) changes to E_{cr} by Lemma 4.1. In view of the existence, uniqueness and continuity of solutions of (1.1), there is at most one small limit cycle in $\mathcal{S}_c \cup \Gamma_r \cup \mathcal{S}_r$ only if $t_c > -t_r\sqrt{d_c/d_r}$ when $\alpha = d_c > 0$, $\max\{t_c^{**}, -2\sqrt{d_c}\} < t_c < 0$ in $\mathcal{G}_1$. This contradicts the condition $t_c < -t_r\sqrt{d_c/d_r}$.

To prove that (1.1) has at most one large limit cycle when $\alpha = d_c > 0$, ${t_r}^2 - 4d_r < 0$ and $\max\{t_c^{**}, -2\sqrt{d_c}\} < t_c < -t_r\sqrt{d_c/d_r}$ in $\mathcal{G}_1$, by way of contradiction we assume that there are two large limit cycles of system (1.1) denoted by Γ_1 and Γ_2, where Γ_1 and Γ_2 are adjacent to each other and Γ_1 is the innermost one. As discussing in the proof of Lemma 5.3, we can prove that

$$\oint_{\Gamma_1} F'(x)dt < \oint_{\Gamma_2} F'(x)dt.$$

Consequently, we obtain that system (1.1) has at most one large limit cycle if it exists. □

When $\alpha = d_c > 0$, ${t_r}^2 - 4d_r < 0$ and $t_c^{**} < t_c \le -2\sqrt{d_c}$ in $\mathcal{G}_1$, from Lemma 4.1 we know that E_l of system (1.1) is a saddle and E_{cr} of system (1.1) is node-focus as shown in Figure 11(g). Proceeding in analogous manner, we obtain the following lemma.

Lemma 5.11. *When $\alpha = d_c > 0$ and ${t_r}^2 - 4d_r < 0$ in $\mathcal{G}_1$, if $t_c^{**} < t_c \le -2\sqrt{d_c}$, then system* (1.1) *exhibits at most one limit cycle, which is large if it exists.*

From Lemma 5.8, for homoclinic loops of system (1.1) we need to consider the case of $\alpha = d_c > 0$, ${t_r}^2 - 4d_r < 0$ and $t_c^{**} < t_c < -t_r\sqrt{d_c/d_r}$ in $\mathcal{G}_1$. Since E_1 of system (1.1) lies in $\mathcal{S}_l$ and E_{cr} of system (1.1) lies on Γ_r, it follows that homoclinic loops of system (1.1) must involve three linear zones. Thus, we obtain the following result.

Lemma 5.12. *If $\alpha = d_c > 0$, ${t_r}^2 - 4d_r < 0$ and $\max\{t_c^{**}, -2\sqrt{d_c}\} < t_c < -t_r\sqrt{d_c/d_r}$ in $\mathcal{G}_1$, then system (1.1) exhibits a unique homoclinic loop involving three linear zones that is unstable when $t_c = \phi(\alpha)$, where $t_c = \phi(\alpha)$ is a continuous function satisfying $\phi(\alpha) \in (\max\{t_c^{**}, -2\sqrt{d_c}\}, -t_r\sqrt{d_c/d_r})$.*

Proof. When $\alpha = d_c > 0$, ${t_r}^2 - 4d_r < 0$ and $\max\{t_c^{**}, -2\sqrt{d_c}\} < t_c < -t_r\sqrt{d_c/d_r}$ in $\mathcal{G}_1$, system (5.40) exhibits two equilibrium points M_l and O_1 by Lemmas 4.1 and 5.9, where M_l is a saddle and O_1 is a stable focus.

To prove the existence of homoclinic loops of system (5.40), we denote by $W^+_{M_l}$ and $W^-_{M_l}$ the stable and unstable manifolds of the right-hand side of M_l of system (5.40) respectively. If ${t_r}^2 - 4d_r < 0$, there is no equilibrium point at infinity in the right half plane of system (5.40) by Lemma 4.2 (see Figure 12(a)). So the manifolds $W^+_{M_l}$ and $W^-_{M_l}$ must intersect the curve $y = F(x)$. Denote the first intersection point of $W^+_{M_l}$ (resp. $W^-_{M_l}$) with the curve $y = F(x)$ by $P(x_P, F(x_P))$ (resp. $Q(x_Q, F(x_Q))$). Evidently, system (5.40) has a homoclinic loop if and only if $x_P - x_Q = 0$. To show the existence of homoclinic loops of system (5.40), we need to prove $x_P - x_Q > 0$ for $t_c = t_c^{**}$ and $x_P - x_Q < 0$ for $t_c = -t_r\sqrt{d_c/d_r}$.

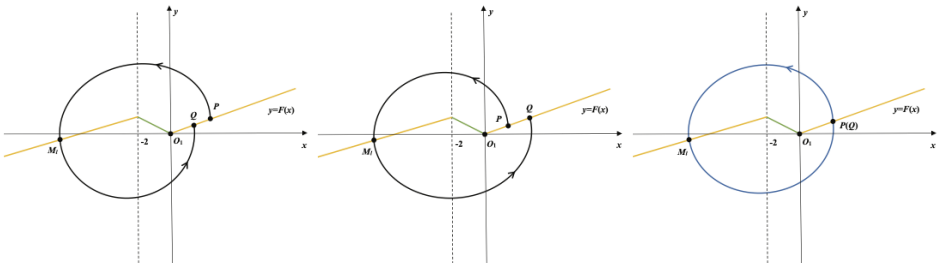

FIGURE 18. Homoclinic loops of system (5.40)

When $t_c = t_c^{**}$, it follows from Lemma 5.8 that system (5.40) exhibits neither limit cycles nor homoclinic loops. So $x_P - x_Q \neq 0$ and it must be $x_P - x_Q > 0$, as shown in Figure 18(a). Otherwise, there exists at least one limit cycle by the Poincaré-Bendixson theorem. This yields a contradiction.

When $t_c = -t_r\sqrt{d_c/d_r}$, from Lemma 5.8 system (5.40) exhibits neither limit cycles nor homoclinic loops, i.e., $x_P - x_Q \neq 0$. Form (5.44) and (5.45), we see $F_1(z) - F_2(z) = 0$ for $z \in (0, 2d_c]$ and $F_1(z) - F_2(z) > 0$ for $z \in (2d_c, 2d_c - 2d_c^2/d_l]$. We can directly get $x_P - x_Q < 0$ as we discussed for Proposition 3.1, see Figure 18(b).

There are some values $t_c \in (\max\{t_c^{**}, -2\sqrt{d_c}\}, -t_r\sqrt{d_c/d_r})$ so that $x_P - x_Q = 0$ for system (5.40) by the mean value theorem. Therefore, we obtain the existence of homoclinic loops of system (5.40).

For the uniqueness of homoclinic loops of system (5.40), by following [21, Lemma 5.3], we know that the manifolds $W^+_{M_l}$ and $W^-_{M_l}$ of M_l of system (5.40) rotate clockwise when t_c increases and $t_r, t_l, d_r, d_c, d_l, \alpha$ are fixed. So there is a unique value $t_c \in (\max\{t_c^{**}, -2\sqrt{d_c}\}, -t_r\sqrt{d_c/d_r})$ satisfying $x_P - x_Q = 0$ for system (5.40). Namely, there is a continuous and monotonous function $\phi(\alpha)$ on t_c such

that (5.40) exhibits a unique homoclinic loop, as shown in Figure 18(c), where $\phi(\alpha) \in (\max\{t_c^{**}, -2\sqrt{d_c}\}, -t_r\sqrt{d_c/d_r})$.

For the stability of homoclinic loop of system (5.40), at the saddle point M_l of system (5.40), two eigenvalues of the associated Jacobian matrix are λ_- and λ_+ satisfying $\lambda_- + \lambda_+ = t_l$. Due to $t_l > 0$, by virtue of [12, Theorem 3.3], we know that the homoclinic loop of system (5.40) is unstable. □

Similarly, we have the following lemma.

Lemma 5.13. *If $\alpha = d_c > 0$, ${t_r}^2 - 4d_r < 0$ and $t_c^{**} < t_c \le -2\sqrt{d_c}$ in $\mathcal{G}_1$, then system (1.1) exhibits a unique homoclinic loop involving three linear zones that is unstable when $t_c = \phi(\alpha)$, where $t_c = \phi(\alpha)$ is a continuous function satisfying $\phi(\alpha) \in (t_c^{**}, -2\sqrt{d_c}]$.*

It is notable that system (1.1) also exhibits a unique homoclinic loop involving three linear zones that is unstable if $\alpha = d_c > 0$, ${t_r}^2 - 4d_r < 0$ and $t_c = \phi(\alpha)$, where $t_c = \phi(\alpha)$ is a continuous function satisfying $\phi(\alpha) \in (t_c^{**}, -t_r\sqrt{d_c/d_r})$. The arguments are almost the same as we did for Lemma 5.12, so we skip them.

Lemma 5.14. *When $\alpha = d_c > 0$, ${t_r}^2 - 4d_r < 0$ and $t_c^{**} < t_c < -t_r\sqrt{d_c/d_r}$ in $\mathcal{G}_1$, there is a continuous function $t_c = \phi(\alpha) \in (t_c^{**}, -t_r\sqrt{d_c/d_r})$ such that the following two assertions hold.*

(a) *System (1.1) exhibits no limit cycles when $t_c \in (t_c^{**}, \phi(\alpha)]$.*
(b) *When $t_c \in (\phi(\alpha), -t_r\sqrt{d_c/d_r})$, system (1.1) exhibits a unique limit cycle which is large and unstable.*

Proof. When $\alpha = d_c > 0$, ${t_r}^2 - 4d_r < 0$ and $t_c^{**} < t_c < -t_r\sqrt{d_c/d_r}$ in $\mathcal{G}_1$, from Lemmas 4.1 and 5.9 it follows that E_l of system (1.1) is a saddle and E_{cr} of system (1.1) is a stable focus for ${t_c}^2 - 4d_c < 0$ or node-focus for ${t_c}^2 - 4d_c \ge 0$, see Figure 11(g). We also know that system (1.1) has a unique homoclinic loop involving three linear zones that is unstable when $\alpha = d_c > 0$, ${t_r}^2 - 4d_r < 0$ and $t_c = \phi(\alpha)$ in $\mathcal{G}_1$. We claim that there is no limit cycle in the interior of the unstable homoclinic loop. Otherwise, there is a semi-stable limit cycle (internally unstable and externally stable) in the interior of the unstable homoclinic loop by the Poincaré-Bendixson theorem. Moreover, there are two limit cycles if the unstable homoclinic loop breaks. This contradicts Lemmas 5.10 and 5.11 Therefore, system (1.1) has no limit cycles when $\alpha = d_c > 0$, ${t_r}^2 - 4d_r < 0$ and $t_c = \phi(\alpha)$ in $\mathcal{G}_1$.

Denote by $W_{E_l}^+$ and $W_{E_l}^-$ the stable and unstable manifolds of the right-hand side of E_l of system (1.1) respectively. From the proof of Lemma 5.18, we know that the relative locations of the manifolds $W_{E_l}^+$ and $W_{E_l}^-$ is shown in Figures 17(a) and 17(c) respectively when $t_c \in (t_c^{**}, \phi(\alpha))$ and $t_c \in (\phi(\alpha), -t_r\sqrt{d_c/d_r})$. In view of the fact that the interior of the unstable homoclinic loop of system (1.1) exhibits no limit cycles, we arrive at the desired result. □

5.3. **Limit cycles and homoclinic loops for $\alpha > d_c > 0$ in $\mathcal{G}_1$.** By Lemma 4.1, we know that system (1.1) exhibits two equilibrium points E_l and E_r when $\alpha > d_c > 0$ in $\mathcal{G}_1$, and E_l in $\mathcal{S}_l$ is a saddle and E_r in $\mathcal{S}_r$ is an unstable focus for $t_r^2 - 4d_r < 0$ or an unstable node for $t_r^2 - 4d_r \ge 0$. Therefore, limit cycle of system (1.1) must only surround E_r by the index theory of [38, Chapter 4] which can be a small limit cycle or a large limit cycle. However, homoclinic loops of system (1.1) only involve three linear zones. Note that system (1.1) has no limit

cycles and homoclinic loops because of the invariant line in $\mathcal{S}_r$ when $\alpha > d_c > 0$ and $t_r^2 - 4d_r \geq 0$ in $\mathcal{G}_1$. Therefore, we only need to investigate limit cycles and homoclinic loops of system (1.1) when $\alpha > d_c > 0$ and $t_r^2 - 4d_r < 0$ in $\mathcal{G}_1$.

By setting $e := (\alpha - d_c)/d_r > 0$, the coordinates of E_r of system (1.1) can be represented by $(e+1, t_r e + t_c)$. By the transformation

$$x \to x + e + 1, \quad y \to y + t_r e + t_c,$$

we change system (1.1) to

$$\frac{dx}{dt} = \overline{F}(x) - y, \quad \frac{dy}{dt} = \overline{g}(x), \tag{5.47}$$

where

$$\overline{F}(x) = \begin{cases} t_r x, & \text{if } x > -e, \\ t_c x + (t_c - t_r)e, & \text{if } -e-2 \leq x \leq -e, \\ t_l(x+e+2) - t_r e - 2t_c, & \text{if } x < -e-2, \end{cases}$$

$$\overline{g}(x) = \begin{cases} d_r x, & \text{if } x > -e, \\ d_c x + (d_c - d_r)e, & \text{if } -e-2 \leq x \leq -e, \\ d_l(x+e+2) - d_r e - 2d_c, & \text{if } x < -e-2. \end{cases}$$

As we see, E_r of system (1.1) changes to $O_2(0,0)$ of system (5.47) and E_l of system (1.1) changes to $P_l((d_r/d_l - 1)e + 2d_c/d_l - 2, (t_l d_r/d_l - t_r)e - 2t_c + 2t_l d_c/d_l)$ of system (5.47). The plane $\mathbb{R}^2$ can be divided into three open linear zones

$$\overline{\mathcal{S}}_l = \{(x,y) \in \mathbb{R}^2 : x < -e-2\},$$
$$\overline{\mathcal{S}}_c = \{(x,y) \in \mathbb{R}^2 : -e-2 < x < -e\},$$
$$\overline{\mathcal{S}}_r = \{(x,y) \in \mathbb{R}^2 : x > -e\}$$

by two straight lines $\overline{\Gamma}_l = \{(x,y) \in \mathbb{R}^2 : x = -e-2\}$ and $\overline{\Gamma}_r = \{(x,y) \in \mathbb{R}^2 : x = -e\}$. For convenience, for system (5.47) we still use F and g to represent $\overline{F}$ and $\overline{g}$ respectively. Since system (5.47) is topologically equivalent to system (1.1), we can study limit cycles and homoclinic loops of system (1.1) through analyzing system (5.47).

Lemma 5.15. *If $\alpha > d_c > 0$ and $t_r^2 - 4d_r < 0$ in $\mathcal{G}_1$, then system (1.1) exhibits neither limit cycles nor homoclinic loops when $t_c \geq t_c^{***}$, where*

$$t_c^{***} := -\frac{t_r(\alpha - d_c + \sqrt{4\alpha d_r + (\alpha - d_c)^2})}{2d_r}.$$

Proof. When $\alpha > d_c > 0$ and $t_r^2 - 4d_r < 0$ in $\mathcal{G}_1$, system (5.47) has two equilibrium points P_l and O_2, where P_l is a saddle and O_2 is an unstable focus by Lemma 4.1. To prove the nonexistence of limit cycles and homoclinic loops of system (5.47), we define the Filippov transformation

$$z(x) := \int_0^x g(s)ds.$$

It follows from system (5.47) that

$$z(x)=\begin{cases}\frac{d_r x^2}{2}, & \text{if } x>-e,\\ \frac{d_c}{2}(x+e)^2-d_r e x-\frac{d_r}{2}e^2, & \text{if } -e-2\le x\le -e,\\ \frac{d_l}{2}(x+e+2)^2-(d_r e+2d_c)x-\frac{d_r}{2}e^2-2d_c-2d_c e, & \text{if } x_{P_l}<x<-e-2,\end{cases} \tag{5.48}$$

and

$$z(x)\in\begin{cases}[0,+\infty), & \text{if } x\ge 0,\\ (0,\frac{d_r e^2}{2}), & \text{if } -e<x<0,\\ [\frac{d_r e^2}{2},2d_c+2d_r e+\frac{d_r e^2}{2}], & \text{if } -e-2\le x\le -e,\\ (2d_c+2d_r e+\frac{d_r e^2}{2},z_{P_l}), & \text{if } x_{P_l}<x<-e-2,\end{cases} \tag{5.49}$$

where $x_{P_l}:=(d_r/d_l-1)e+2d_c/d_l-2$, $z_{P_l}:=2d_c+2d_r e+d_r e^2/2-(d_r e+2d_c)^2/(2d_l)$.

Let $x_1(z)$ and $x_2(z)$ be the branches of the inverse of $z(x)$ for $x\ge 0$ and $x_{P_l}<x<0$ respectively. From (5.48) we derive

$$x_1(z)=\sqrt{\frac{2z}{d_r}},\quad \text{if } x\ge 0, \tag{5.50}$$

$$x_2(z)=\begin{cases}-\sqrt{\frac{2z}{d_r}}, & \text{if } -e<x<0,\\ \frac{(d_r-d_c)e-\sqrt{d_r^2e^2-d_r d_c e^2+2d_c z}}{d_c}, & \text{if } -e-2\le x\le -e.\end{cases} \tag{5.51}$$

We define $F_1(z):=F(x_1(z))$ and $F_2(z):=F(x_2(z))$. It follows from (5.50) and (5.51) that

$$F_1(z)=t_r\sqrt{\frac{2z}{d_r}},\quad \text{if } z>0,$$

$$F_2(z)=\begin{cases}-t_r\sqrt{\frac{2z}{d_r}}, & \text{if } 0<z<\frac{d_r e^2}{2},\\ t_c\frac{d_r e-\sqrt{d_r^2e^2-d_r d_c e^2+2d_c z}}{d_c}-t_r e, & \text{if } \frac{d_r e^2}{2}\le z\le 2d_c+2d_r e+\frac{d_r e^2}{2}.\end{cases}$$

By the two equalities above, we find that

$$F_1(z)-F_2(z)=\begin{cases}2t_r\sqrt{\frac{2z}{d_r}}, & \text{if } 0<z<\frac{d_r e^2}{2},\\ t_r\sqrt{\frac{2z}{d_r}}-t_c\frac{d_r e-\sqrt{d_r^2e^2-d_r d_c e^2+2d_c z}}{d_c}+t_r e, & \text{if } \frac{d_r e^2}{2}\le z\le 2d_c+2d_r e+\frac{d_r e^2}{2}\end{cases}$$

for $z\in(0,2d_c+2d_r e+d_r e^2/2]$. Clearly, from the above equality we have $F_1(z)-F_2(z)>0$ when $z\in(0,d_r e^2/2)$. When $z\in[d_r e^2/2,2d_c+2d_r e+d_r e^2/2]$, a direct calculation gives rise to

$$F_1'(z)-F_2'(z)=\frac{t_r\sqrt{d_r^2e^2-d_r d_c e^2+2d_c z}+t_c\sqrt{2d_r z}}{\sqrt{d_r^2e^2-d_r d_c e^2+2d_c z}\cdot\sqrt{2d_r z}}>0 \tag{5.52}$$

for $t_c\ge 0$. For $t_c<0$ we have

$$F_1'(z)-F_2'(z)=\frac{t_r\sqrt{d_r^2e^2-d_r d_c e^2+2d_c z}+t_c\sqrt{2d_r z}}{\sqrt{d_r^2e^2-d_r d_c e^2+2d_c z}\cdot\sqrt{2d_r z}}\begin{cases}<0, & \text{if } z<z_0,\\ =0, & \text{if } z=z_0,\\ >0, & \text{if } z>z_0,\end{cases} \tag{5.53}$$

as $t_r^2 d_c - t_c^2 d_r > 0$, or

$$F_1'(z) - F_2'(z) = \begin{cases} < 0, & \text{if } d_r < d_c, \\ = 0, & \text{if } d_r = d_c, \\ > 0, & \text{if } d_r > d_c, \end{cases} \tag{5.54}$$

as $t_r^2 d_c - t_c^2 d_r = 0$, or

$$F_1'(z) - F_2'(z) \begin{cases} > 0, & \text{if } z < z_0, \\ = 0, & \text{if } z = z_0, \\ < 0, & \text{if } z > z_0, \end{cases} \tag{5.55}$$

as $t_r^2 d_c - t_c^2 d_r < 0$, where

$$z_0 := \frac{t_r^2(d_r d_c e^2 - d_r^2 e^2)}{2(t_r^2 d_c - t_c^2 d_r)}. \tag{5.56}$$

When $z \in (2d_c + 2d_r e + d_r e^2/2, z_{P_l})$, from the monotonicity of $F_1(z)$ and $F_2(z)$, we have

$$F_1(z) > F_1(2d_c + 2d_r e + d_r e^2/2), \quad F_2(z) < F_2(2d_c + 2d_r e + d_r e^2/2).$$

That is, $F_1(z) - F_2(z) > 0$.

When $t_c \geq 0$, from (5.52) it follows that $F_1(z) - F_2(z) > 0$ for $z \in (0, z_{P_l})$. When $-t_r\sqrt{d_c/d_r} < t_c < 0$, we have

$$(F_1(z) - F_2(z))|_{z=z_0} = t_r\sqrt{\frac{2z_0}{d_r}} - t_c\frac{d_r e - \sqrt{d_r^2 e^2 - d_r d_c e^2 + 2d_c z_0}}{d_c} + t_r e > 0.$$

That is, $F_1(z) - F_2(z) > 0$ for $z \in (0, z_{P_l})$. When $t_c \leq -t_r\sqrt{d_c/d_r}$, from (5.54) and (5.55), we have $F_1(z) - F_2(z) > 0$ for $z \in (0, z_{P_l})$ if and only if

$$(F_1(z) - F_2(z))|_{z=2d_c+2d_r e+\frac{d_r e^2}{2}} = t_r\sqrt{\frac{4d_c + 4d_r e + d_r e^2}{d_r}} + 2t_c + t_r e > 0. \tag{5.57}$$

Solving (5.57) leads to $t_c^{***} < t_c \leq -t_r\sqrt{d_c/d_r}$. According to [27, Section 6], we know that system (5.47) exhibits neither limit cycles nor homoclinic loops when $\alpha > d_c > 0$, $t_r^2 - 4d_r < 0$ and $t_c \geq t_c^{***}$ in $\mathcal{G}_1$. □

Similarly, we can obtain the following result.

Lemma 5.16. *If $\alpha > d_c > 0$, ${t_r}^2 - 4d_r < 0$ and $t_c < t_c^{***}$ in $\mathcal{G}_1$, then system (1.1) exhibits at most two limit cycles.*

Following [21, Lemma 5.3], we have the following lemma.

Lemma 5.17. *if $\alpha > d_c > 0$, $t_r^2 - 4d_r < 0$ and $t_c < t_c^{***}$ in $\mathcal{G}_1$, then system (1.1) exhibits a unique homoclinic loop that is unstable when $t_c = \varphi(\alpha) \in (-\infty, t_c^{***})$, where the function $t_c = \varphi(\alpha)$ is continuous and monotonous. Moreover, there exists a unique limit cycle that is stable in the interior of the homoclinic loop .*

Following [21, Lemma 5.4], we can further have the following lemma.

Lemma 5.18. *If $\alpha > d_c > 0$, $t_r^2 - 4d_r < 0$ and $t_c < t_c^{***}$ in $\mathcal{G}_1$ then there is a continuous function $t_c = h(\alpha)$ and a continuous and monotonous function $t_c = \varphi(\alpha)$ such that the following assertions are true, where $-\infty < \varphi(\alpha) < h(\alpha) < t_c^{***}$.*

(a) *System (1.1) has a unique limit cycle that is stable when $t_c \in (-\infty, \varphi(\alpha))$.*

(b) *System* (1.1) *has exactly two limit cycles when* $t_c \in (\varphi(\alpha), h(\alpha))$. *The inner limit cycle is stable and the outer limit cycle is unstable.*
(c) *System* (1.1) *has a unique limit cycle that is semi-stable when* $t_c = h(\alpha)$.
(d) *System* (1.1) *has no limit cycles when* $t_c \in (h(\alpha), t_c^{***})$.

6. Proofs of main results

Proof of Theorem 2.1. When the parameters lie in the region $\mathcal{G}_{11}$, it follows from Lemma 4.1 that system (1.1) has one equilibrium point E_{cl} for $\alpha = -d_c$ and two equilibrium points E_l and E_{cr} for $\alpha = d_c$. If $\alpha = -d_c \pm \varepsilon$ or $\alpha = d_c \pm \varepsilon$ with small $\varepsilon > 0$, then E_{cl} or E_{cr} will vanish. Thus, BE_{11} and BE_{12} are the boundary equilibrium bifurcation curves.

When the function $t_c = \phi(\alpha)$ is continuous and monotonous satisfying $\phi(\alpha) \in (\max\{t_c^*, -2\sqrt{d_c}\}, 0)$ (resp. $(\max\{t_c^*, -2\sqrt{d_c}\}, -t_r\sqrt{d_c/d_r})$ for $-d_c < \alpha < d_c$ (resp. $\alpha = d_c$), from Lemma 5.4 it follows that system (1.1) exhibits a unique homoclinic loop that is unstable (resp. Lemma 5.12) when $t_c = \phi(\alpha)$. When the function the function $t_c = \varphi(\alpha)$ is continuous and monotonous satisfying $\varphi(\alpha) \in (-\infty, t_c^{***})$ for $\alpha > d_c$, from Lemma 5.17 it follows that system (1.1) has a unique homoclinic loop that is unstable when $t_c = \varphi(\alpha)$. Therefore, HL_{11} and HL_{12} are the homoclinic bifurcation curves.

From Lemma 5.18, it follows that system (1.1) exhibits a unique limit cycle that is semi-stable when $t_c = h(\alpha)$, where the function $t_c = h(\alpha)$ is continuous satisfying $h(\alpha) \in (\varphi(\alpha), t_c^{***})$ for $\alpha > d_c$. If $t_c = h(\alpha) \pm \varepsilon$ with small $\varepsilon > 0$, then the semi-stable limit cycle will vanish. Moreover, there are two limit cycles accompanied by the vanishing of the semi-stable limit cycle if $\varepsilon < 0$. Hence, we call DL the double limit cycle bifurcation curve.

It follows from Lemma 5.6 that there is a unique limit cycle that is unstable when parameters lie in the region V. By Lemma 5.14, system (1.1) exhibits a unique limit cycle that is large and unstable when parameters lie in the region BE_{124}. By Lemma 5.18, there are two limit cycles when parameters lie in the region IX. Moreover, the inner limit cycle is stable and the outer limit cycle is unstable. From Lemma 5.18 again, there is a unique limit cycle that is stable when parameters lie in the region X. By virtue of Lemmas 4.1 and 4.2, we depict global phase portraits of system (1.1) in the Poincaré disc. □

Because the primary procedures in the proofs of Theorems 2.2–2.6 are closely similar to the proof of Theorem 2.1, we omit them to avoid unnecessary repetition and redundancy.

7. Numerical results

In this section we perform numerical phase portraits for system (1.1) to demonstrate our theoretical results.

In Theorem 2.1, system (1.1) has 23 global phase portraits in the Poincaré disc. Since there is no finite equilibrium point when parameters lie in the region I, we show the remaining numerical phase portraits of system (1.1) in Figure 19. Table 2 is offered to help facilitate understanding comparisons between global phase portraits in the Poincaré disc in Theorem 2.1 and numerical phase portraits in Figure 19. Similarly, we demonstrate numerical phase portraits of system (1.1) in Figures 20 and 21 with the associated Tables, as stated in Theorems 2.2 and 2.4.

TABLE 2. Numerical values chosen for plotting phase portraits of Theorem 2.1

Figure	Case	α	t_c	t_r	t_l	d_r	d_c	d_l
19 (a)	II	-0.5	2	1	1	1	1	-1
19 (b)	III	-0.5	1	1	1	1	1	-1
19 (c)	IV	-0.5	0	1	1	1	1	-1
19 (d)	V	-0.5	-0.1	1	1	1	1	-1
19 (e)	VI	-0.5	-0.2	1	1	1	1	-1
19 (f)	VII	-0.5	-2	1	1	1	1	-1
19 (g)	VIII	1.2	-1	1	1	1	1	-1
19 (h)	IV	1.2	-1.7	1	1	1	1	-1
19 (i)	X	1.2	-4	1	1	1	1	-1
19 (j)	BE_{11}	-1	0	1	1	1	1	-1
19 (k)	BE_{121}	1	2	1	1	1	1	-1
19 (l)	BE_{122}	1	0	1	1	1	1	-1
19 (m)	BE_{123}	1	-1	1	1	1	1	-1
19 (n)	BE_{124}	1	-1.009	1	1	1	1	-1
19 (o)	BE_{125}	1	-1.8	1	1	1	1	-1
19 (p)	BE_{216}	1	-2	1	1	1	1	-1
19 (q)	HL_{111}	-0.5	-0.171	1	1	1	1	-1
19 (r)	HL_{112}	-0.21	-0.1712	1	1	1	1	-1
19 (s)	HL_{113}	0	-0.338	1	1	1	1	-1
19 (t)	HL_{114}	1	-1.61	1	1	1	1	-1
19 (u)	HL_{12}	1.2	-1.929	1	1	1	1	-1
19 (v)	DL_1	1.2	-1.3766	1	1	1	1	-1

TABLE 3. Numerical values chosen for plotting phase portraits of Theorem 2.2

Figure	Case	α	t_c	t_r	t_l	d_r	d_c	d_l
20 (a)	R_2	-0.5	2	2	1	1	1	-1
20 (b)	R_3	-0.5	1	2	1	1	1	-1
20 (c)	R_4	-0.5	0	2	1	1	1	-1
20 (d)	R_5	-0.5	-0.1	2	1	1	1	-1
20 (e)	R_6	-0.5	-0.2	2	1	1	1	-1
20 (f)	R_7	-0.5	-2	2	1	1	1	-1
20 (g)	R_8	1.2	-1	2	1	1	1	-1
20 (h)	BE_{21}	-1	0	2	1	1	1	-1
20 (i)	BE_{221}	1	2	2	1	1	1	-1
20 (j)	BE_{222}	1	-2	2	1	1	1	-1
20 (k)	HL_{21}	-0.5	-0.171	2	1	1	1	-1
20 (l)	HL_{22}	-0.21	-0.1712	2	1	1	1	-1
20 (m)	HL_{23}	0.1	-0.57	2	1	1	1	-1

8. CONCLUSION

In this article, we studied global dynamics of a continuous planar piecewise linear differential system with three zones. Combining with results obtained in [21], we have achieved our goal to fully present complicated and rich dynamical behaviors through demonstrating global phase portraits in the Poincaré disc and bifurcation diagrams of system (1.1) for the case $t_r t_l > 0$ and $d_r d_l < 0$.

TABLE 4. Numerical values chosen for plotting phase portraits of Theorem 2.4

Figure	Case	α	t_c	t_r	t_l	d_r	d_c	d_l
21 (a)	G_5	0.5	-1	1	4	1	1	-1
21 (b)	G_6	0.2	-1.9	1	4	1	1	-1
21 (c)	G_7	0.8	-3	1	4	1	1	-1
21 (d)	G_8	0.8	-4	1	4	1	1	-1
21 (e)	BE_{421}	1	2	1	4	1	1	-1
21 (f)	BE_{422}	1	0	1	4	1	1	-1
21 (g)	BE_{423}	1	-1	1	4	1	1	-1
21 (h)	BE_{424}	1	-1.5	1	4	1	1	-1
21 (i)	BE_{425}	1	-3	1	4	1	1	-1
21 (j)	BE_{425}	1	-4	1	4	1	1	-1
21 (k)	HL_{411}	-0.6	-0.565	1	4	1	1	-1
21 (l)	HL_{412}	-0.446	-0.566	1	4	1	1	-1
21 (m)	HL_{413}	0	-1.38	1	4	1	1	-1
21 (n)	HL_{414}	0.8	-3.2	1	4	1	1	-1
21 (o)	HL_{42}	1	-3.7	1	4	1	1	-1

Specifically, we discussed limit cycles and homoclinic loops of system (1.1) with $d_c > 0$ and $-d_c < \alpha < d_c$ in $\mathcal{G}_1$ in Section 5.1. The obtained results are totally distinguished from [21]. If $\phi(\alpha) \in (\max\{t_c^*, -2\sqrt{d_c}\}, 0)$ (resp. $\phi(\alpha) \in (t_c^*, -2\sqrt{d_c}]$), system (1.1) exhibits a unique limit cycle that is unstable surrounding E_c when $t_c \in (\phi(\alpha), 0)$ (resp. $t_c \in (\phi(\alpha), -2\sqrt{d_c}]$), see Lemma 5.6 (resp. Lemma 5.7). E_c lies in $\mathcal{S}_c$ and is a stable focus (resp. a stable node). However, homoclinic loops of system (1.1) may involve two or three linear zones. For example, system (1.1) exhibits a unique homoclinic loop involving two (resp. three) linear zones when $t_c = \phi(\alpha)$ for $\alpha < \alpha^*$ (resp. $\alpha > \alpha^*$) and exhibits a unique homoclinic loop that is tangent to Γ_r when $t_c = \phi(\alpha)$ for $\alpha = \alpha^*$, when $\phi(\alpha) \in (\max\{t_c^*, -2\sqrt{d_c}\}, 0)$, see Lemmas 5.4-5.5. Limit cycles and homoclinic loops of system (1.1) with $\alpha = d_c > 0$ in $\mathcal{G}_1$ and with $\alpha > d_c > 0$ in $\mathcal{G}_1$ were explored in Sections 5.2 and 5.3 respectively.

In the future, we will develop the methods described herein to the Liénard system with perturbations and present dynamical behaviors on limit cycles and homoclinic loops in a subsequent paper somewhere else.

Acknowledgments. This work was supported by the National Natural Science Foundation of China (Nos. 12322109, 62173092, and 12171485), by the Science and Technology Innovation Program of Hunan Province (No. 2023RC3040), and by the China Postdoctoral Science Foundation (No. 2023M743969).

REFERENCES

[1] J. H. Bonsel, R. H. B. Fey, H. Nijmeijer; Application of a dynamic vibration absorber to a piecewise linear beam system, *Nonlinear Dyn.*, **37** (2004), 227–243.

[2] J. Borghetti, G. S. Snider, P. J. Kuekes, J. J. Jang, D. R. Stewart, R. S. Williams; 'Memristive' switches enable 'stateful' logic operations via material implication, *Nature*, **468** (2010), 873–876.

[3] Q. Cao, M. Wiercigroch, E. E. Pavlovskaia, J. M. T. Thompson, C. Grebogi; Piecewise linear approach to an archetypal oscillator for smooth and discontinuous dynamics, *Phil. Trans. R. Soc. A*, **366** (2008), 635–652.

[4] V. Carmona, E. Freire, E. Ponce, F. Torres; On simplifying and classifying piecewise linear systems, *IEEE Trans. Circuits. Syst. I*, **49** (2002), 609–620.

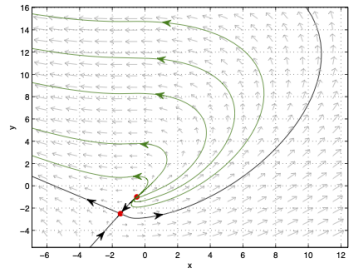

$(\alpha, t_c) = (-0.5, 2)$

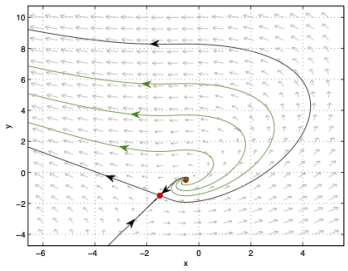

$(\alpha, t_c) = (-0.5, 1)$

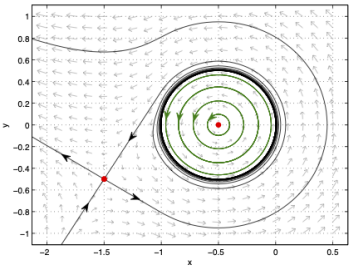

$(\alpha, t_c) = (-0.5, 0)$

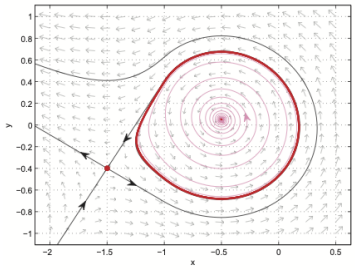

$(\alpha, t_c) = (-0.5, -0.1)$

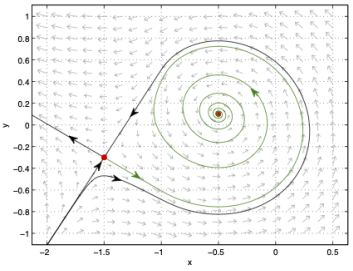

$(\alpha, t_c) = (-0.5, -0.2)$

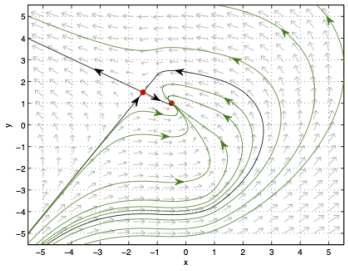

$(\alpha, t_c) = (-0.5, -2)$

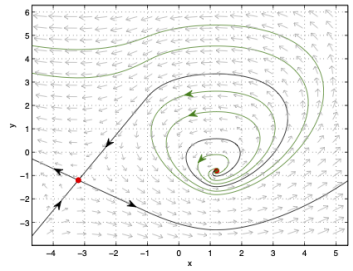

$(\alpha, t_c) = (1.2, -1)$

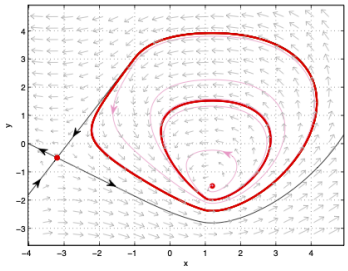

$(\alpha, t_c) = (1.2, -1.7)$

FIGURE 19. Numerical phase portraits of Theorem 2.1 with $(t_r, t_l, d_r, d_c, d_l) = (1, 1, 1, 1, -1) \in \mathcal{G}_{11}$

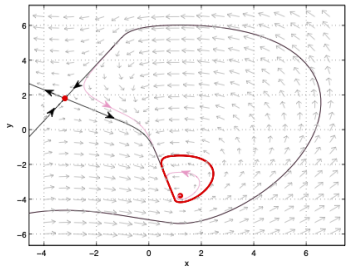

$(\alpha, t_c) = (1.2, -4)$

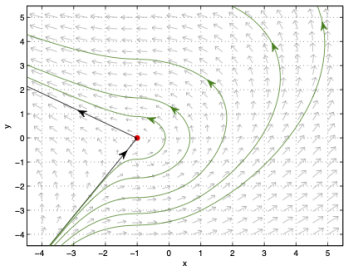

$(\alpha, t_c) = (-1, 0)$

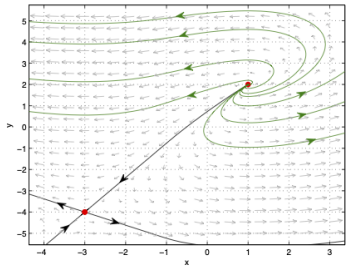

$(\alpha, t_c) = (1, 2)$

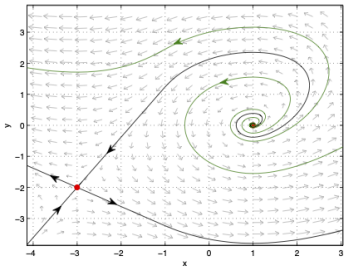

$(\alpha, t_c) = (1, 0)$

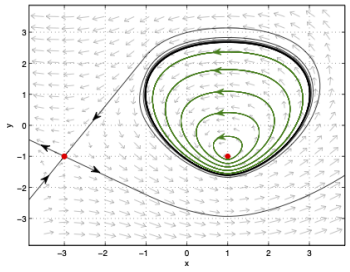

$(\alpha, t_c) = (1, -1)$

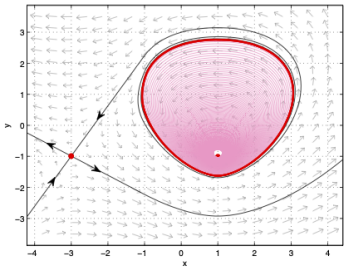

$(\alpha, t_c) = (1, -1.009)$

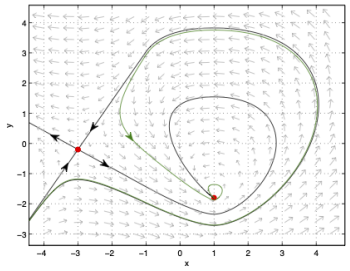

$(\alpha, t_c) = (1, -1.8)$

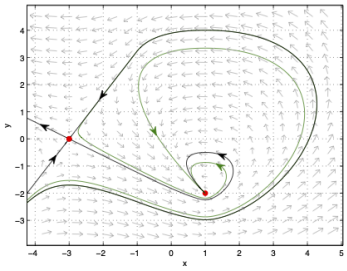

$(\alpha, t_c) = (1, -2)$

FIGURE 19. Numerical phase portraits of Theorem 2.1 with $(t_r, t_l, d_r, d_c, d_l) = (1, 1, 1, 1, -1) \in \mathcal{G}_{11}$

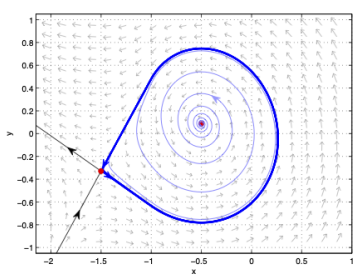

$(\alpha, t_c) = (-0.5, -0.171)$

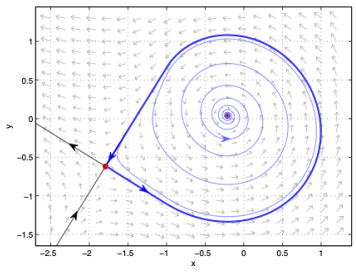

$(\alpha, t_c) = (-0.21, -0.1712)$

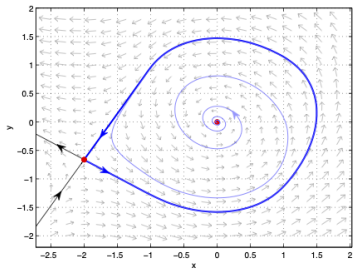

$(\alpha, t_c) = (0, -0.338)$

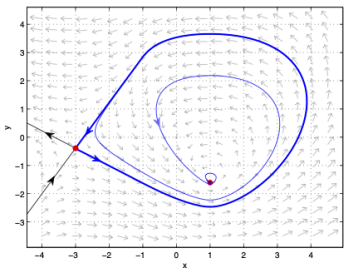

$(\alpha, t_c) = (1, -1.61)$

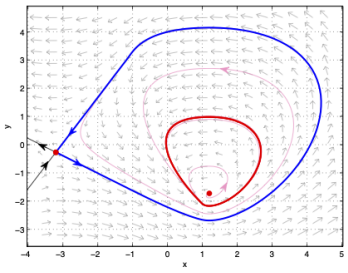

$(\alpha, t_c) = (1.2, -1.929)$

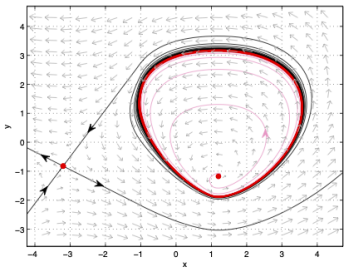

$(\alpha, t_c) = (1.2, -1.3766)$

FIGURE 19. Numerical phase portraits of Theorem 2.1 with $(t_r, t_l, d_r, d_c, d_l) = (1, 1, 1, 1, -1) \in \mathcal{G}_{11}$

[5] H. Chen; Global dynamics of memristor oscillators, *Int. J. Bifurcation and Chaos*, **26** (2016), 1650198, 1–29.

[6] H. Chen, M. Jia, Y. Tang; A degenerate planar piecewise linear differential system with three zones, *J. Differential Equations*, **297** (2021) 433–468.

[7] H. Chen, D. Li, J. Xie, Y. Yue; Limit cycles in planar continuous piecewise linear systems, *Commun. Nonlinear Sci. Numer. Simulat.*, **47** (2017), 438–454.

[8] H. Chen, X. Li; Global phase portraits of memristor oscillators, *Int. J. Bifurcation and Chaos*, **24** (2014), 1450152, 1–31.

[9] H. Chen, Y. Tang; At most two limit cycles in a piecewise linear differential system with three zones and asymmetry, *Physica D*, **386-387** (2019), 23–30.

[10] H. Chen, Y. Tang; A proof of Euzébio-Pazim-Ponce's conjectures for a degenerate planar piecewise linear differential system with three zones, *Physica D*, **401** (2020), 132150, 1–22.

[11] H. Chen, F. Wei, Y. Xia, D. Xiao; Global dynamics of an asymmetry piecewise linear differential system: theory and applications, *Bull. Sci. Math.*, **160** (2020), 102858, 1–43.

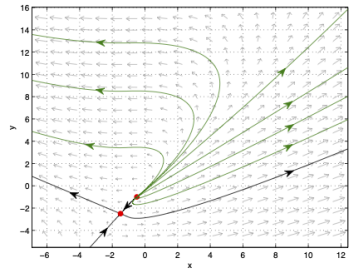

$(\alpha, t_c) = (-0.5, 2)$

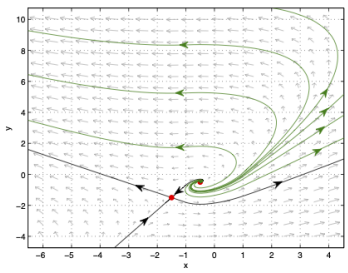

$(\alpha, t_c) = (-0.5, 1)$

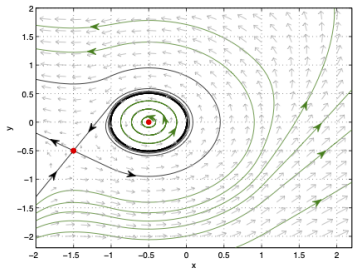

$(\alpha, t_c) = (-0.5, 0)$

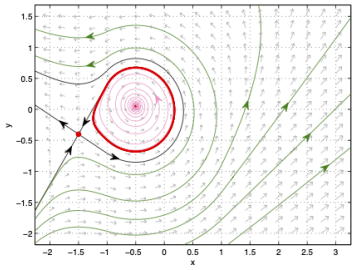

$(\alpha, t_c) = (-0.5, -0.1)$

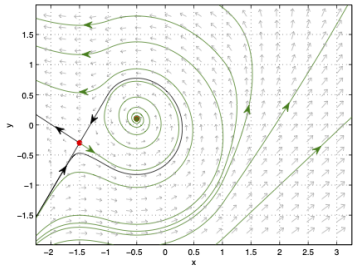

$(\alpha, t_c) = (-0.5, -0.2)$

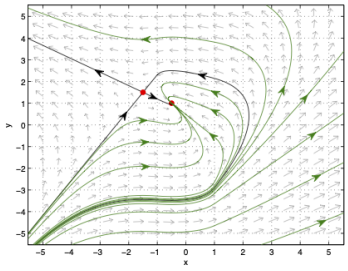

$(\alpha, t_c) = (-0.5, -2)$

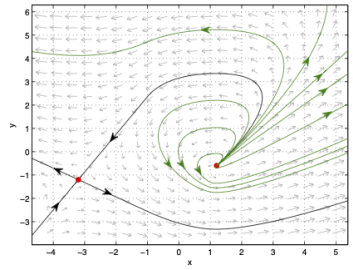

$(\alpha, t_c) = (1.2, -1)$

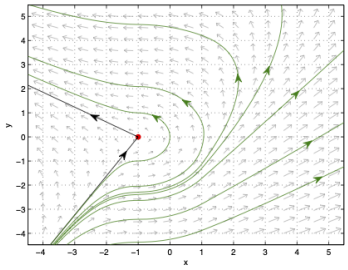

$(\alpha, t_c) = (-1, 0)$

FIGURE 20. Numerical phase portraits of Theorem 2.2 with $(t_r, t_l, d_r, d_c, d_l) = (2, 1, 1, 1, -1) \in \mathcal{G}_{12}$

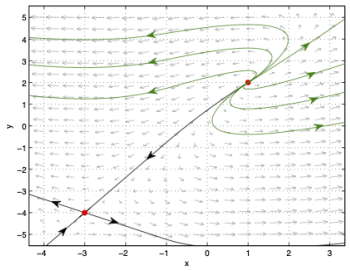

$(\alpha, t_c) = (1, 2)$

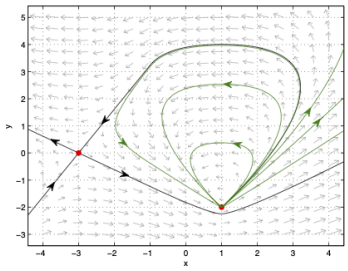

$(\alpha, t_c) = (1, -2)$

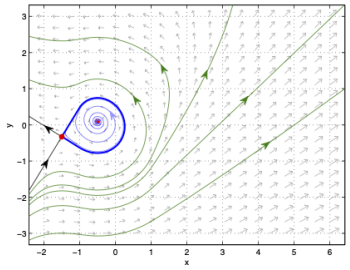

$(\alpha, t_c) = (-0.5, -0.171)$

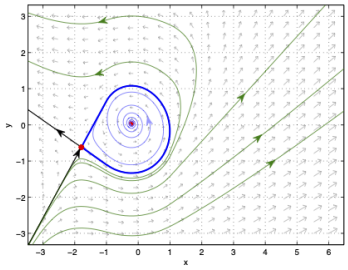

$(\alpha, t_c) = (-0.21, -0.1712)$

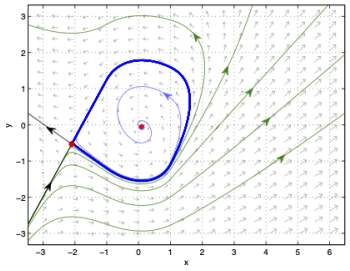

$(\alpha, t_c) = (0.1, -0.57)$

FIGURE 20. Numerical phase portraits of Theorem 2.2 with $(t_r, t_l, d_r, d_c, d_l) = (2, 1, 1, 1, -1) \in \mathcal{G}_{12}$

[12] S.-N. Chow, C. Li, D. Wang; *Normal Forms and Bifurcation of Planar Vector Fields*, Cambridge. Press, 1994.

[13] L. O. Chua; Memristor: The missing circuit element, *IEEE Trans. Circuit Theory*, **CT-18** (1971), 507–519.

[14] F. Corinto, A. Ascoli, M. Gilli, Nonlinear dynamics of memristor oscillators, *IEEE Trans. Ciruits Syst. I: Regul. Pap.*, **58** (2011), 1323–1336.

[15] M. di Bernardo, C. J. Budd, A. R. Champneys, P. Kowalczyk; *Piecewise-smooth Dynamical Systems: Theory and Applications*, Springer-Verlag, London, 2008.

[16] E. Diz-Pita, J. Llibre, M. V. Otero-Espinar; Phase portraits of a family of Kolmogorov systems depending on six parameters, *Electron. J. Differential Equations*, **2021** (2021), no. 35, 1-38.

[17] R. Euzébio, R. Pazim, E. Ponce; Jump bifurcations in some degenerate planar piecewise linear differential systems with three zones, *Physica D* **325** (2016), 74–85.

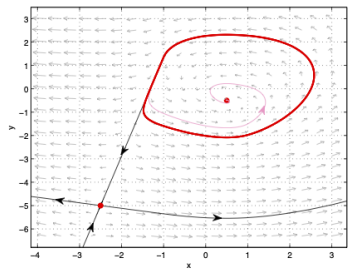

$(\alpha, t_c) = (0.5, -1)$

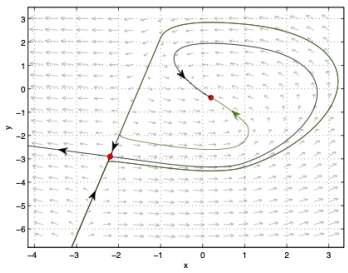

$(\alpha, t_c) = (0.2, -1.9)$

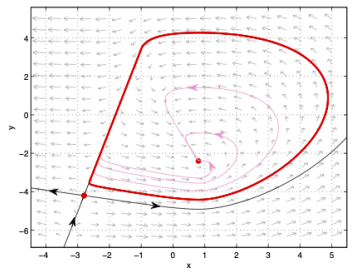

$(\alpha, t_c) = (0.8, -3)$

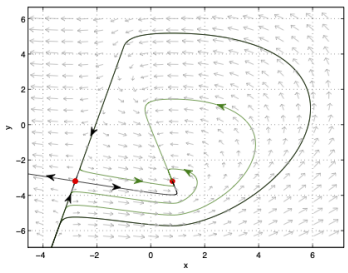

$(\alpha, t_c) = (0.8, -4)$

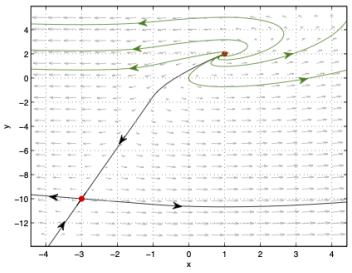

$(\alpha, t_c) = (1, 2)$

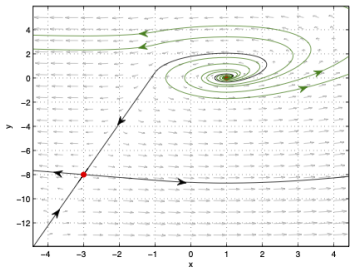

$(\alpha, t_c) = (1, 0)$

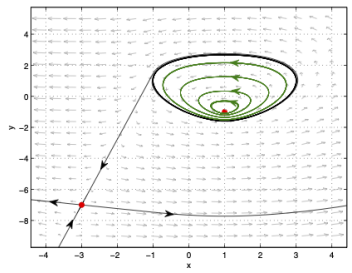

$(\alpha, t_c) = (1, -1)$

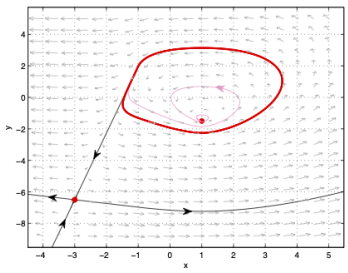

$(\alpha, t_c) = (1, -1.5)$

FIGURE 21. Numerical phase portraits of Theorem 2.4 with $(t_r, t_l, d_r, d_c, d_l) = (1, 4, 1, 1, -1) \in \mathcal{G}_{11}$

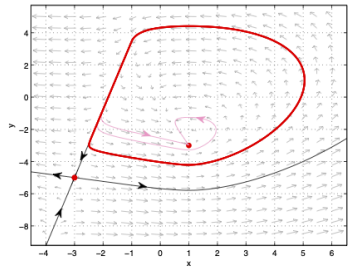

$(\alpha, t_c) = (1, -3)$

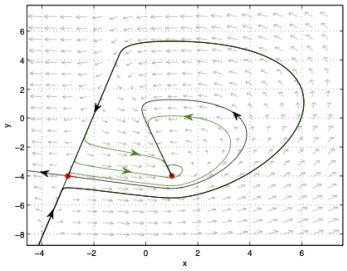

$(\alpha, t_c) = (1, -4)$

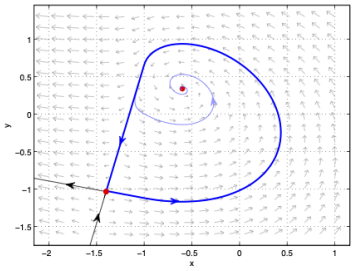

$(\alpha, t_c) = (-0.6, -0.565)$

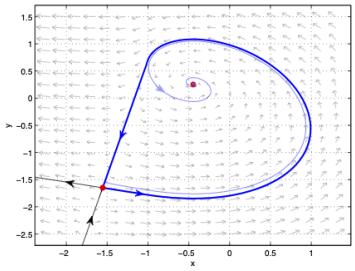

$(\alpha, t_c) = (-0.446, -0.566)$

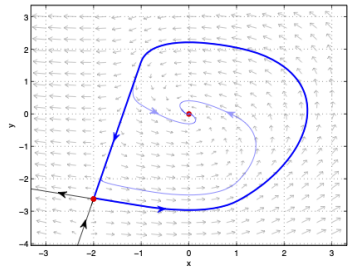

$(\alpha, t_c) = (0, -1.38)$

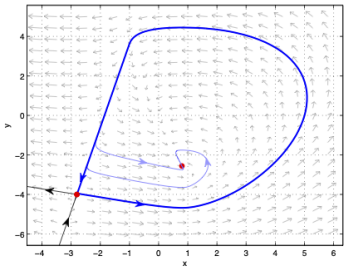

$(\alpha, t_c) = (0.8, -3.2)$

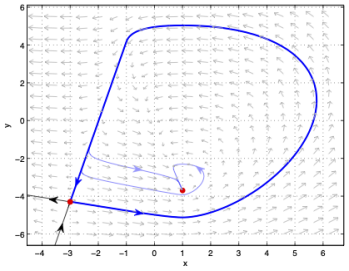

$(\alpha, t_c) = (1, -3.7)$

FIGURE 21. Numerical phase portraits of Theorem 2.4 with $(t_r, t_l, d_r, d_c, d_l) = (1, 4, 1, 1, -1) \in \mathcal{G}_{11}$

[18] Z. Feng; Duffing-van der pol-type oscillator systems, *Discrete Contin. Dyn. Syst. Ser. S*, **7** (2014), 1231-1257.
[19] E. Freire, E. Ponce, F. Rodrigo, F. Torres; Bifurcation sets of continuous piecewise linear systems with two zones, *Int. J. Bifurcation and Chaos*, **8** (1998), 2073–2097.
[20] E. Freire, E. Ponce, F. Rodrigo, F. Torres; Bifurcation sets of symmetrical continuous piecewise linear systems with three zones, *Int. J. Bifurcation and Chaos*, **12** (2002), 1675–1702.
[21] M. Jia, Y. Su, H. Chen; Global studies on a continuous planar piecewise linear differential system with three zones, *Nonlinear Dyn.*, (2022), https://doi.org/10.1007/s11071-022-08005-1.
[22] M. Han; Global behavior of limit cycles in rotated vector fields, *J. Differential Equations*, **151** (1999), 20–35.
[23] M. Itoh, L. O. Chua; Memristor oscillator, *Int. J. Bifurcation and Chaos*, **18** (2008), 3183–3206.
[24] S. Li, J. Llibre; Phase portraits of piecewise linear continuous differential systems with two zones separated by a straight line, *J. Differential Equations*, **266** (2019), 8094–8109.
[25] J. Llibre, M. Ordóñez, E. Ponce; On the exisentence and uniquness of limit cycles in planar continuous piecewise linear systems without symmetry, *Nonlinear Anal. Real World Appl.*, **14** (2013), 2002–2012.
[26] J. Llibre, E. Ponce, C. Valls; Uniqueness and non-uniqueness of limit cycles for piecewise linear differential systems with three zones and no symmetry, *J. Nonlinear Sci.*, **25** (2015), 861–887.
[27] J. Llibre, E. Ponce, C. Valls; Two limit cycles in Liénard piecewise linear differential systems, *J. Nonlinear Sci.*, **29** (2019), 1499–1522.
[28] J. Llibre, J. Sotomayor; Phase portraits of planar control systems, *Nonlinear Anal.*, **27** (1996), 1177–1197.
[29] J. Llibre, A. E. Teruel; *Introduction to the Qualitative Theory of Differential Systems: Planar, Symmetric and Continuous Piecewise Linear Systems*, Birkhäuser Advanced Texts, Berlin, 2014.
[30] H. P. McKean; Nagumo's equation, *Adv. Math.*, **4** (1970), 209–223.
[31] H. P. McKean; Stabilization of solutions of a caricature of the Fitzhugh-Nagumo equation, *Comm. Pure. Appl. Math.*, **36** (1983), 291–324.
[32] L. P. Peng, Z. Feng; Limit cycles from a cubic reversible system via the third-order averaging method, *Electron. J. Differential Equations*, **2015** (2015), no. 111, 1-27.
[33] E. Ponce, J. Ros, E. Vela; Limit cycle and boundary equilibrium bifurcations in continuous planar piecewise linear systems, *Int. J. Bifurcation and Chaos*, **25** (2015), 1530008.
[34] E. Ponce, J. Ros, E. Vela; The boundary focus-saddle bifurcation in planar piecewise linear systems. Application to the analysis of memristor oscillators, *Nonlinear Anal. Real World Appl.*, **43** (2018), 495–514.
[35] J. Rinzel; Repetitive activity and Hopf bifurcation under point-Stimulation for a simple FitzHugh-Nagumo nerve conduction model, *J. Math. Biology*, **5** (1978), 363–382.
[36] D. B. Strukov, G. S. Snider, D. R. Stewart, R. S. Williams; The missing memristor found, *Nature*, **453** (2008), 80–83.
[37] P. Yao, H. Wu, B. Gao, J. Tang, Q. Zhang, W. Zhang, J.J. Yang, H. Qian; Fully hardware-implemented memristor convolutional neural network, *Nature*, **577** (2020), 641–646.
[38] Z. Zhang, T. Ding, W. Huang, Z. Dong; *Qualitative Theory of Differential Equations*, Transl. Math. Monogr., Amer. Math. Soc., Providence, RI, 1992.

Man Jia
School of Mathematics and Statistics, HNP-LAMA, Central South University, Changsha, Hunan 410083, China.
School of Mathematics and Statistics, Fuzhou University, Fuzhou, Fujian 350116, China
Email address: jiaman9305@163.com

Youfeng Su
College of Computer and Data Science, Fuzhou University, Fuzhou, Fujian 350116, China
Email address: yfsu@fzu.edu.cn

Hebai Chen (corresponding author)
School of Mathematics and Statistics, HNP-LAMA, Central South University, Changsha, Hunan 410083, China
Email address: chen_hebai@csu.edu.cn